

# “Establishing the interaction between the CC chemokine ligand 5 and the receptors CCR1 and CCR5“

Von der Fakultät für Mathematik, Informatik und Naturwissenschaften der RWTH Aachen  
University zur Erlangung des akademischen Grades einer Doktorin der Naturwissenschaften  
genehmigte Dissertation

vorgelegt von  
Diplom-Biologin  
Birgit Kramp

aus  
Eschweiler

Berichter: Privatdozent Dr. Rory R. Koenen  
Universitätsprofessor Dr. rer.nat. Jürgen Bernhagen

Tag der mündlichen Prüfung: 04.12.2013

Diese Dissertation ist auf den Internetseiten der Hochschulbibliothek online verfügbar.



The following manuscripts and/or publications are based on the work in this thesis:

**Birgit K. Kramp**, Remco T. A. Megens, Alisina Sarabi, Sabine Winkler, Delia Projahn, Christian Weber, Rory R. Koenen, Philipp von Hundelshausen (2013). Exchange of extra-cellular domains of CCR1 and CCR5 reveals confined functions in CCL5-mediated cell recruitment. Thromb. Haemost. **110**(4):795-806.

Yvonne Döring, Heidi Noels, **Birgit K. Kramp**, Manuela Mandl, Dirk Lievens, Maik Drechsler, Pathricia Tilstam, Marcella Langer, Helene Hartwig, Markus Sperandio, Oliver Soehnlein, Christian Weber (2014). Sialyltransferase ST3Gal-IV deficiency reduces Ccl5-mediated phagocyte accumulation in atherosclerosis. Circ. Res., accepted for publication.

Rory R. Koenen, Philipp von Hundelshausen, Irina V. Nesmelova, Alma Zerneck, Elisa A. Liehn, Alisina Sarabi, **Birgit K. Kramp**, Anna M. Piccinini, Søren R. Paludan, M. Anna Kowalska, Andreas J. Kungl, Tilman M. Hackeng, Kevin H. Mayo, Christian Weber (2009). Disrupting functional interactions between platelet chemokines inhibits atherosclerosis in hyperlipidemic mice. Nat. Med. **15**(1): 97-103.

**TABLE OF CONTENTS**

Table of Contents.....	iiiv
Abbreviations.....	viii
I. Introduction.....	1
I.1. The immune system.....	1
I.2. Chemokines .....	2
I.3. Chemokine receptors .....	5
I.4. 'Crossing borders': from chemokine to chemotaxis.....	7
I.5. Mechanisms that regulate chemokine activity - 'a ménage à plusieurs' .....	9
I.5.1. Posttranslational modifications.....	10
I.5.2. Cooperative interactions between chemokines and chemokine receptors..	12
I.6. The chemokines CCL5 and CXCL4 in immune cell function .....	17
I.7. The chemokine receptors CCR1 and CCR5 .....	19
I.8. Aims of the study.....	22
II. Material and Methods .....	23
II.1. General equipment.....	23
II.2. Antibodies.....	24
II.2.1. Primary Antibodies .....	24
II.2.2. Isotype controls .....	25
II.2.3. Secondary antibodies.....	25
II.3. Mice .....	26
II.4. Molecular biology.....	26
II.4.1. General work with E. coli .....	26
II.4.2. Bacterial strains .....	27
II.4.3. Plasmids .....	28
II.4.4. Polymerase chain reaction.....	29
II.4.5. Small-scale purification of plasmid DNA .....	30

## Table of Contents

---

II.4.6.	Large-scale purification of plasmid DNA .....	30
II.4.7.	Digestion, ligation and precipitation of DNA .....	30
II.4.8.	Agarose gel electrophoresis and DNA purification .....	31
II.4.9.	Quantification of DNA.....	31
II.4.10.	Sequencing of DNA .....	32
II.4.11.	Cloning of Met-CCL5 .....	32
II.4.12.	Cloning of the CCR1 and CCR5 chimeras.....	32
II.5.	Protein analysis.....	33
II.5.1.	Protein concentration assay.....	33
II.5.2.	SDS-polyacrylamide gel electrophoresis (PAGE).....	33
II.5.3.	Coomassie blue staining.....	34
II.5.4.	Silver staining.....	35
II.5.5.	Western blot analysis .....	35
II.5.6.	Dot blot.....	36
II.5.7.	Flow cytometry .....	36
II.6.	Protein expression and purification .....	37
II.6.1.	Purification of recombinant CCL5 and CCL5 variants.....	37
II.6.2.	Protocol using gel filtration to purify CCL5 (A).....	38
II.6.3.	Protocol using Ion exchange chromatography to purify CCL5, Met-CCL5, CCL5_40s and CCL5_E66A (B).....	40
II.7.	Biochemical analysis of the CCL5-CXCL4 heterodimer.....	44
	<i>15N-1H heteronuclear single quantum coherence (HSQC) nuclear magnetic resonance spectroscopy.</i> ....	44
	<i>Molecular dynamics simulations</i> .....	44
	<i>Differential Scanning Calorimetry</i> .....	45
II.8.	Functional analysis of MKEY in comparison to Met-CCL5.....	45
II.9.	Cell culture .....	45
II.9.1.	General .....	45

---

II.9.2.	Cell lines.....	46
II.9.3.	Culturing of adherent cell monolayers.....	46
II.9.4.	Culturing of cells in suspension.....	46
II.9.5.	Freezing and thawing of cells.....	47
II.9.6.	Transfection of eukaryotic cells.....	47
	<i>Transient transfection of HEK-293 cells.....</i>	<i>47</i>
	<i>Stable transfection of L1.2 and HEK-293 cells.....</i>	<i>47</i>
II.9.7.	Isolation of PBMC.....	48
II.9.8.	Isolation of neutrophils and monocytes from mouse bone marrow.....	48
II.10.	Functional assays.....	49
II.10.1.	Transmigration assay.....	49
II.10.2.	Parallel plate flow chamber adhesion assay.....	49
II.10.3.	Immunofluorescence.....	50
II.10.4.	Co-Immunoprecipitation.....	51
II.10.5.	Calcium mobilization assay.....	51
II.10.6.	Binding assay.....	52
II.11.	Data illustration and statistical analysis.....	52
III.	Results.....	53
III.1.	Protein expression and purification.....	54
III.1.1.	Expression and purification of recombinant CCL5, protocol A.....	56
III.1.2.	Expression and purification of recombinant CCL5 and CCL5 variants, protocol B.....	58
III.2.	NMR chemical shift mapping of CCL5-CXCL4 heterodimer.....	62
III.3.	Functional activity of MKEY in comparison to Met-CCL5.....	64
III.4.	Establishing the role of the extracellular domains of CCR1 and CCR5 in CCL5 mediated cell recruitment.....	66
III.4.1.	Design and characterization of the chemokine receptor chimeras.....	66

## Table of Contents

---

III.4.2.	Functional role of the extracellular domains in CCL5-induced arrest under flow .....	68
III.4.3.	CCR1 Extracellular domain 3 is involved in enhanced arrest induced by CCL5 and CXCL4.....	70
III.4.4.	Role of extracellular domains in CCR1 and CCR5 heterodimerization ..	72
III.4.5.	Monocytic CCR1 is required to mediate CCL5-CXCL4-induced arrest.	73
III.5.	Functional role of ST3Gal-IV in CCL5 mediated cell recruitment.....	75
IV.	Discussion .....	78
IV.1.	Two different strategies to purify CCL5 and the CCL5 variants .....	78
IV.2.	The CXCL4/CCL5 heterodimer mediates cell recruitment function via CCR1 and/or CCR5 .....	79
IV.3.	Exchange of extracellular domains of CCR1 and CCR5 reveals confined functions in CCL5-mediated cell recruitment .....	80
IV.4.	ST3Gal-IV deficiency reduces Ccl5 mediated leukocyte transmigration .....	84
V	Summary .....	86
V.1.	Summary.....	86
V.2.	Zusammenfassung .....	88
VI.	Acknowledgement .....	90
VII.	References .....	92
VIII.	Supplement.....	106
IX.	Curriculum Vitae .....	107

**ABBREVIATIONS**

7TM	seven-transmembrane
aa	amino acid
Ab	antibody
APC	activated protein C
APS	ammonium persulfate
C(X)CL/R	C(X)C-chemokine ligand/receptor
CD	cluster of differentiation
CI	chemotactic index
CALDAG	calcium- and diacylglycerol-regulated GEF
DAG	diacylglycerol
DDT	dithiothreitol
DMSO	dimethylsulphoxide
E. coli	Escherichia coli
ER	endoplasmatic reticulum
EtOH	ethanol
FCS	fetal calf serum
FPLC	fast protein liquid chromatography
GAG	glycosaminoglycan
GDP	guanosine diphosphate
GEF	guanine-nucleotide-exchange factor
Gnd-HCl	guanidine-HCl
GPCR	G-protein-coupled receptors
GDP/GTP	guanosine di- or triphosphate
GEF	guanine nucleotide exchange factor
HEPES	4-2-hydroxyethyl-1-piperazineethanesulfonic acid



## Abbreviations

---

HF	hydrofluoric acid
HPLC	high pressure liquid chromatography
HRP	horseradish peroxidase
HSA	human serum albumin
HSQC	heteronuclear single quantum coherence
SVEC	human umbilical vein endothelial cell
IFN- $\gamma$	interferon-gamma
IL	interleukin
IP3	inositol-1,4,5 triphosphate
IPTG	isopropyl- $\beta$ -D-thiogalactopyranoside
kDa	kilo Dalton
LB	Lauria-Bertani broth
MCP	monocyte chemoattractant protein
MD	molecular dynamics simulations
MIP	macrophage inflammatory protein
MM6	mono mac 6
NaEDTA	sodium ethylenediaminetetraacetic acid
NaAc	sodium acetate
NMR	nuclear magnetic resonance
o.n.	overnight
PAMPs	pathogen associated molecular patterns
PBS	phosphate buffered saline
PBMC	peripheral blood mononuclear cell
PF4	platelet factor 4
PI3K	phosphoinositide-3 kinase
PIP3	phosphatidylinositol-3,4,5-trisphosphate
PKA	protein kinase A

PKC	protein kinase C
PLC	phospholipases C
PMN	polymorphonuclear cells
PRR	pattern recognition receptors
RANTES	regulated on activation, normal T-cell expressed and secreted
RNA	ribonucleic acid
rt	room temperature
SDF	stromal cell-derived factor
SDS-PAGE	sodium dodecyl sulfate-polyacrylamide gel electrophoresis
SR-PSOX	scavenger receptor for phosphatidylserine-containing oxidized lipids
ST3Gal-IV	$\alpha$ 2-3 sialyltransferase IV
Sts	sialyltransferases
TBS	tris buffered saline
TEMED	N,N,N',N'-tetramethylethylenediamine
TFA	trifluoroacetic acid
TNF- $\alpha$	tumor necrosis factor-alpha
TSS	transformation and storage solution

## I. INTRODUCTION

### I.1. THE IMMUNE SYSTEM

During evolution the human body evolved an ingenious system to defend against intruders. This so called immune system is a highly adaptable and variable system composed of a million of cells, molecules, mechanisms and organs within an organism, which protect it against pathogens like e.g. viruses, microorganisms, parasites or foreign molecules. Already simple multi-cellular organisms have a system that is activated through molecular patterns of pathogens or dying cells. Higher organisms still depend on this “innate immune system” as the first line of defense. These protective mechanisms range from the barrier functions of the epithelia over soluble factors, such as cytokines, which act as intercellular mediators in the generation of immune response to diverse cellular components including polymorphonuclear leukocytes (PMN or granulocytes) (basophils, eosinophils and neutrophils), mast cells, macrophages, dendritic cells and natural killer cells. A second more specific branch of the immune system has evolved later and was termed the adaptive immune response. It is activated mainly by the cells of the innate immune system days after the infection. This immune response is more specific and leads to the generation of various memory cells, to mount a stronger immune reaction each time the pathogen is encountered. Adaptive immunity comprises antibodies, B cells, and T lymphocytes. Immunological defense against invading pathogens starts with an important immune reaction called inflammation (Latin, *inflammatio*, to set on fire). Within the first hours, the defense is mediated by different cell, including macrophages or endothelial cells, which release inflammatory mediators that lead to an accumulation of cellular and humoral components at the site of infection, causing the characteristic symptoms redness, swelling, heat, and pain. Molecules involved in the inflammatory reactions are soluble cytokines, like several interleukins (IL), interferons (IFN) that increase the permeability of blood vessels, allowing fluid and proteins to pass into the tissues. Cytokines such as interleukin-1 (IL-1) and tumor necrosis factor (TNF) also alter the activation state of endothelial cell layer lining the blood vessels, allowing the leukocytes to adhere and transmigrate into the surrounding tissue. The recruitment of leukocytes from the blood flow to the site of infection by chemotactic cytokines is a vital step during inflammation [1, 2].

## I.2. CHEMOKINES

The coordinated leukocyte movement is fundamental for the immune function during embryonic development as well as during organogenesis. A basic requirement allowing a coordinated cell movement are chemoattractants that signal through seven-transmembrane receptors (7TM-receptors). It is well established, that the most important cellular guidance system in mammals is a class of chemoattractant cytokines – named chemokines. Apart from their eponymous attribute and their prominent role in innate and adaptive immune response, chemokines are involved in a number of physiological processes, like angiogenesis/angiostasis, organization and maintenance of lymphoid organ structure, organogenesis and tissue repair [3]. Of great importance is further their involvement in pathophysiological processes, like cancer, autoimmune diseases and other inflammatory diseases [4-7]. Nearly 50 chemokines have been identified in humans to date. They were classified into four subfamilies according to a characteristic cysteine motif in their amino acid sequence followed by a number that corresponds to the gene number, as depict in Fig.I.1. [8-10].

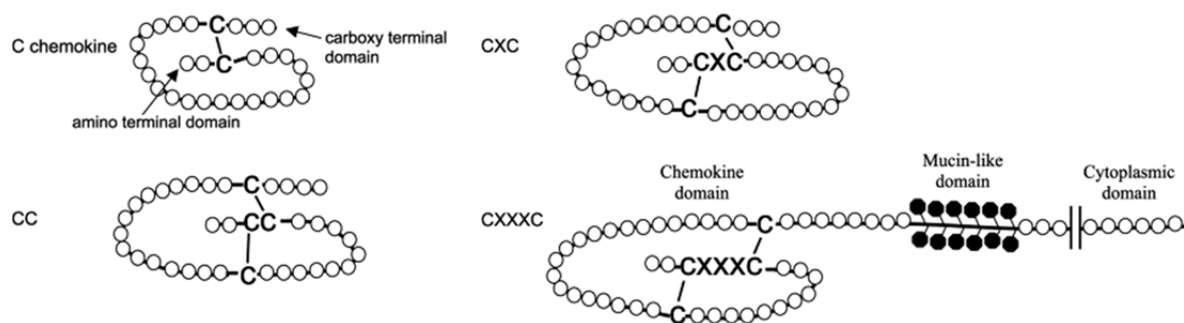


**Fig.I.1.: Schematic representation of the four chemokine subfamilies.**

Chemokines are classified into four groups depending on the location of the first or the first two N-terminal cysteine residues, namely the XC-, CC-, CXC- or the CX<sub>3</sub>C-chemokines. The CC- chemokines are the largest family followed by the CXC chemokines, the C chemokine sub-family consist of only two members. Fractalkine (CX<sub>3</sub>C) chemokine is the only member of this sub-family and is a transmembrane expressed chemokines, characterized by a transmembrane region and an intracellular cytoplasmic domain.

The CC-, or the beta-family, consists of 28 chemokines and is identified by two directly neighboring cysteine residues near to the N-terminus. Members of this family are e.g. the monocyte chemoattractant protein-1 (MCP-1, CCL2) or RANTES (regulated on activation normal T cell expressed, CCL5) [11, 12]. If the two cysteins are interrupted by a single random amino acid, they are subsumed as CXC- or alpha-chemokines. Approximately 17 members have been described, e.g. CXCL4 (platelet factor 4, PF4),

which was the first chemokine described at all [13]. The CXC family can be further subdivided according to their ability to mediate the chemotaxis of endothelial cells and thereby to promote the formation of new vessels [14]. The absence or presence of a specific structural domain, named “ELR motif” (in detail glutamate-leucine-arginine) determines their angiogenic potential. CXC chemokines containing the ELR motif were found to be potent angiogenic factors, inducing the formation of new vessels, e.g. CXCL8 (IL-8). In contrast, CXC chemokines lacking the ELR motif, like CXCL4 fail to induce neo-vascularization but were found to be potent angiostatic factors. [15-17]. The third C or gamma sub-family, only has two members XCL1 (lymphotactin- $\alpha$ ) and XCL2 (lymphotactin- $\beta$ ), they lack two of the four cysteines, but shares homology at its carboxyl terminus with the C-C chemokines [18]. The fourth group, CX<sub>3</sub>C or delta group, consists of only one chemokine, CX<sub>3</sub>CL1 (fractalkine) and is characterized through three random amino acids flanked by one cysteine residue on both sides. Furthermore, it has been the only known chemokine that was found to be membrane bound [19] till recently another membrane bound chemokine, the CXC chemokine 16 or SR-PSOX, was identified in platelets [20]. Chemokines can be broadly divided into homeostatic and inflammatory categories based on their expression pattern and function in the immune system [4, 21]. The pro-inflammatory chemokines are expressed by circulating leukocytes and other cells only upon activation by pro-inflammatory stimuli, whereas homeostatic chemokines are constitutively expressed and are involved in homeostatic lymphocyte and dendritic cell (DC) trafficking and lymphoid tissue organogenesis [3]. However, some chemokines are classified into both categories depending on the biological context or pathological state. Inducible chemokines normally act on monocytes, granulocytes and T-cells in order to recruit cells to areas of inflammation or infection. In contrast, constitutive chemokines normally act on leukocytes in hematopoiesis in order to regulate the trafficking of these leukocytes to primary (bone marrow and thymus) and secondary (lymph nodes and peyer’s patches) lymphatic organs [22, 23]. Most of the chemokine genes that code for the CC chemokines are located in two clusters on chromosome 17, the monocyte chemotactic protein (MCP) and the macrophage inflammatory protein (MIP) clusters [24]. Chemokine proteins that are encoded in one cluster have a higher amino acid sequence identity compared with chemokines that originate from different gene clusters. The same is true for the CXC chemokines, most of the ELR positive CXC chemokine are clustered on chromosome 4, a second cluster contains the ELR negative members. Nevertheless, chemokines even if they are categorized into different subfamilies and

despite their low level of sequence homology share the same three dimensional structure [21, 25, 26]. Each monomer has a flexible N-terminal domain, followed by an N-terminal loop, a three-stranded antiparallel  $\beta$ -sheet region overlaid by a prominent C-terminal  $\alpha$ -helix [27]. *In vitro* and *in vivo* data indicate that monomeric chemokines are sufficient to bind and activate the cognate receptor [28-30] but nevertheless at sites of inflammation, where high amounts of chemokines are released, they were shown to form homo- and heteromers or even higher order oligomers, which can modulate the cellular response [18, 31, 32]. A number of higher order oligomeric structures have been observed in crystal structures. Given the tendency of most CC chemokines to form similar “CC-like dimers” and CXC chemokines to form “CXC-like dimers”, there is a surprising number of different higher order oligomerization topologies, where small sequence variations seem to have consequences on the form of higher order oligomers. Oligomeric structures varying from more globular tetrameric forms [33, 34] to more extended decameric forms have been observed [35-37]. The functional aspect of heterophilic chemokine interaction will be discussed more detailed in section I.5 “Mechanisms that regulate the chemokine activity – a ‘ménage à plusieurs’”.

Furthermore oligomerisation of chemokines seems to be an important feature for proper receptor binding and activation. Glycosaminoglycans (GAG) that are present on the cell surface may facilitate oligomerization of chemokines to enhance the luminal presentation, since particular mutated variants unable to bind to GAGs fail to induce transmigration *in vivo*, whereas they do induce chemotaxis *in vitro* [38-41]. The immobilization of chemokines on GAG is believed to be a mechanism for localization and concentration of secreted chemokines in a specific tissue compartment, thereby forming a 2D haptotactic gradient and preventing their rapid diffusion into the blood stream. A tissue defined repertoire of GAGs with specific binding affinities to chemokines [42, 43] together with a striking preference of chemokines for specific GAG types (shown by studies employing synthetic GAG) contribute to the locally defined presentation [43]. A common heparin-binding motif for several chemokines has been identified; the basic BBXB motif (the B represents a basic amino acid residue) is located for example in the 40s loop of CCL5, CCL3 and CCL4 [22] or the 50s loop of CXCL11 [44] and the 20s loop of CXCL12 [41]. Other processes may also involve GAG, such as the transport of chemokines through the cell, protection from proteolytic degradation, co-receptor or even signaling functions [13, 42, 43, 45].

### I.3. CHEMOKINE RECEPTORS

Chemokines signal through specific cell surface-expressed G-protein coupled receptors (GPCR). They are part of the largest family of membrane proteins which mediates most cellular responses to hormones and neurotransmitters, as well as being responsible for vision, olfaction and taste. At the most basic level, the structure of all GPCR is characterized by seven membrane spanning  $\alpha$ -helical segments separated by alternating intracellular and extracellular loop regions [46]. This wide range of chemical signals is transduced into intracellular responses through the coupling of the receptor protein to heterotrimeric guanosine triphosphate (GTP) binding proteins (G proteins). The interaction of a ligand with a G protein coupled membrane receptor results in the exchange of guanosine diphosphate (GDP) bound to the G protein  $\alpha$  subunit for GTP, which causes the subsequent dissociation of the heterotrimer into the  $\alpha$  and  $\beta\gamma$  subunits, resulting in the activation of several downstream effectors. The nomenclature of the chemokine receptors is based on the ligands they bind to, extended by an 'R' for receptor. Accordingly, they are also divided into four groups, CXCR, CCR, XCR and CX<sub>3</sub>CR. Currently, 20 chemokine receptors and about 50 chemokines are known and the unequal ligand receptor ratio already indicates that one chemokine ligand can bind to more than one receptor, this complexity is increased even further by the ability of chemokines to bind several receptors [21, 47]. Thus the chemokine network was formerly suggested as redundant, but in present days it is accepted that a chemokine can mediate distinct functions through different receptors and that the engagement of the same receptor by different chemokines ligands not necessarily leads to the same cellular responses. This is known as the concept of 'functional selectivity' [5]. Sequence and length of the chemokine receptors are very similar, the length varies from 320 to 370 amino acids and sequence identity ranges from 25 to 80%. So far, 18 genes encoding the 'classical' chemokine receptors have been identified in the human genome: 6 CXCR genes, 10 CCR genes, 1 XCR gene and 1 CX<sub>3</sub>CR gene. Furthermore, 5 genes encoding atypical (non-signaling) chemokine receptors have been described [48]. The 'classic' chemotactic receptors are characterized by a typical motif in the second intracellular loop, the DRYLAIVHA motif, which is supposed to be essential for the G protein coupling. The atypical chemokine receptors have a sequence which deviates from the DRYLAIVHA motif, suspected to be causal for the inability to lead to a normal cellular response. These atypical receptors are also named 'silent' or 'decoy' receptors since they bind

chemokines, but do not elicit standard chemotactic responses instead they are rather considered to act as scavengers that remove excess chemokines. Currently four interceptors (internalizing receptors) have been described, namely DARC (Duffy Antigen Receptor for Chemokines), CCX-CKR1, D6 and CXCR7 [49]. Quite recently their ability to internalize and degrade chemokines has been extended by the capability of transporting chemokines from the basal to the apical side of endothelial cells, thus modifying gradients and creating functional chemokine patterns in tissues [50].

For decades, the structural biology of the GPCR family remains a relatively blind spot, to obtain the crystal structure of GPCRs is extremely challenging because they are unstable outside of an intact membrane system and known to adopt many conformational states. In 2000, the first structure was solved, the bovine rhodopsin receptor and it took another ten years to be able to reveal the crystal structure of a chemokine receptor. CXCR4 was the first chemokine receptor to be crystallized. The main fold of CXCR4 consists of the same bundle of seven trans-membrane helices. Compared with previous GPCR structures, the shape of the ligand binding pocket is larger and more open which may be consistent with the ability to bind more than one ligand [51, 52] (Fig.1.2.). Last year then Park *et. al.* were able to clarify the structure of the native fully active chemokine receptor CXCR1 reconstructed in a phospholipid bilayer [53]. The receptor protein was recombinant expressed in *E.coli*, purified and refolded in an artificial lipid bilayer. The structure was investigated by a method based on nuclear magnetic resonance spectroscopy, which offers the first time the opportunity to obtain the native structure of a chemokine receptor without modification in the amino acid sequence. Structure comparison of CXCR4 with CXCR1 confirmed the finding that the ligand binding cavity is larger, more open and closer to the cell surface which may be a common feature of the “multiple-ligand binding nature” of the chemokine receptors [53]. Less is known about the mode of ligand binding and receptor activation by the natural ligand, since crystal structures of the receptors were determined when the receptor molecule was bound to small peptide antagonist with dimensions significantly below the size of chemokines. The ligand binding regions have been defined by employing mutated chemokine ligands and receptors. The putative ligand-receptor interaction model was proposed as a general two-site mechanism. In this model, the receptor N-terminus is involved in the initial recognition of the chemokine through binding to the chemokine N-loop (site I). This initial binding facilitates the correct chemokine orientation, promoting the binding of the chemokine N-loop to the extracellular loops and transmembrane regions of the receptor (site II) leading to receptor



activation [54, 55]. An emerging body of data proposes a more complex scenario in which site I binding and site II binding are far from independent, that site I binding results in conformational changes in the receptor, triggering downstream interactions and/or changes that are essential for site II binding of N-terminal chemokine residues to the receptors' extracellular domain [56-58] or site I binding triggers structural/dynamic changes throughout the chemokine ligand for optimal binding to the receptor residues [59].

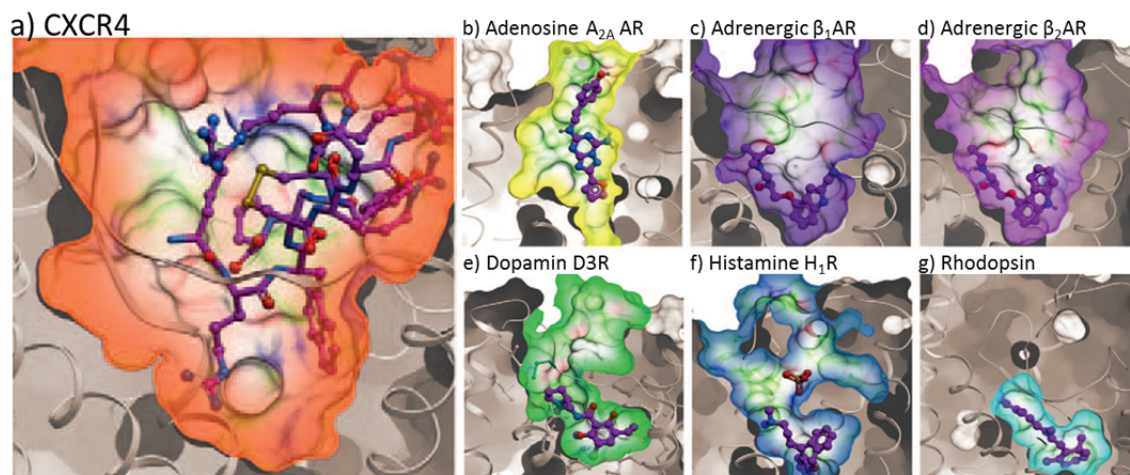


**Fig.I.2. Diversity of the ligand-binding pocket shape and properties in GPCR crystal structures.** Structural diversity, including large backbone deviations of ECLs and TM helices, results in dramatic variations in size, shape and binding properties of GPCR pockets. CXCR4 has compared to the others (b-g) a large and open pocket able to bind larger proteins. Adapted from Katritch *et. al.* 2012 [52].

### I.4. 'CROSSING BORDERS': FROM CHEMOKINE TO CHEMOTAXIS

The binding of a chemokine to its cognate receptor leads to ligand-adapted modification of the tertiary structure of the receptor protein and in turn to the activation of heterotrimeric G-proteins. The activated G-proteins exchange guanosine diphosphate (GDP) for guanosine triphosphate (GTP) and dissociate into  $\alpha$  and  $\beta$  subunits, which in turn activate several downstream signaling pathways. The G proteins are classified by their  $\alpha$ -subunit, into at least four classes  $\alpha_i$ ,  $\alpha_s$ ,  $\alpha_q$  and  $\alpha_{12/13}$  [60]. The typical chemokine receptors are supposed to be coupled to  $G\alpha_i$ , because most of the mediated responses could be inhibited by pertussis toxin (PTx), a bacterial toxin that catalyzes the ADP-ribosylation of the  $G\alpha_i$  subunit [61]. Since PTx was unable to block all chemokine induced responses completely, it was assumed that chemokine receptors can be coupled to more than one G-protein class and actually it was reported

that chemokine receptors can be associated with other PTx insensitive G-proteins like  $G_{q/11}$  [62].

Leukocyte recruitment to sites of injury or infection has been described as a multi-step process, as depicted in Fig.I.3. The process starts with the capture of leukocytes by binding to selectin-molecules on the inner blood vessel wall with marginal affinity. Thereby, these leukocytes slow down and start rolling. At once, chemokines released by activated cells, e.g. endothelial cells or macrophages, and presented on the endothelium cause changes in the integrin structure from low to a high affinity conformation. In the activated state, integrins bind tightly to complementary glycosylated ligands expressed on endothelial cells, with high affinity, leading to tight adhesion. Followed by the crawling (chemotaxis along a haptotactic gradient) of leukocytes on the luminal endothelial surface. Finally, the leukocytes transmigrate across the endothelial cell layer, a step which is regulated by several molecules of the tight junctions. This series of events can be observed for neutrophils, lymphocytes and monocytes, although the molecules involved are different among the leukocyte subpopulations [63-65].

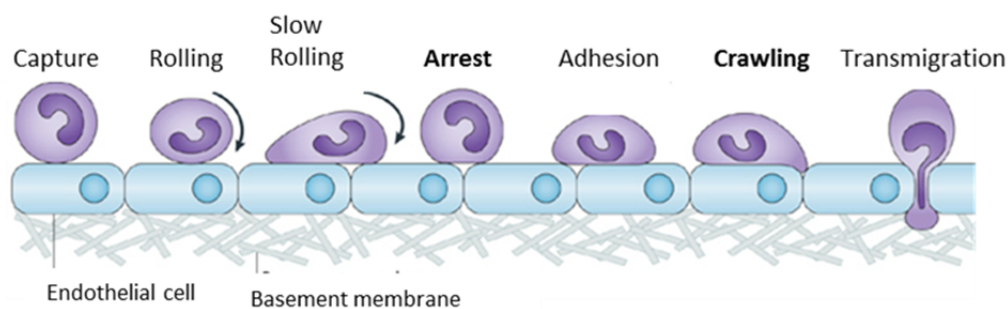


**Fig.I.3.: Leukocyte extravasation from the blood flow into inflamed tissue.**

A multistep cascade leads to the activation of integrins and their ligands by chemokines. The steps involved in this process are capture, rolling, slow rolling, integrin activation, firm adhesion and crawling, finally transmigration across the endothelial layer. Figure modified from [63].

Two steps depend mainly on chemokine mediated signaling (which are highlighted in bold in Fig.I.3.); first the integrin activation, secondly the migration along the endothelial surface. The intracellular signaling pathways involved in rapid integrin activation and chemotaxis seem to engage different downstream signaling molecules. The  $\beta\gamma$  subunit released from the  $G\alpha_i$  protein activates the phospholipase C (PLC), which then mobilizes inositol-1,4,5 triphosphate ( $IP_3$ ) and diacylglycerol (DAG) which in turn triggers the release of calcium from the endoplasmatic reticulum (ER) stores. Subsequently, leading to the activation of the RAP1 guanine nucleotide exchange factor (GEF) CalDAG-GEFI,

RAP1-GFP in turn mediates rapid integrin activation [66, 67]. During crawling, cell polarization is a prerequisite for efficient migration, meaning that the molecular processes at the leading edge and the trailing edge (uropod) of a moving cell are different. Referred to leukocyte recruitment, this means that signaling molecules, including PI3K, phospholipase C (PLC) and members of the Rho GTPase family, such as Rac, accumulate with the highest concentration at the region of the cell membrane associated with the highest amount of G-protein activity. This provides amplification of the polarizing signal, which promotes remodeling of the actin cytoskeleton, e.g. polymerization of F-actin at the leading edge of leukocytes and furthermore activation of adhesion molecules and inactivation at the opposite region. The asymmetric distribution of the PI3K product phosphatidylinositol (3,4,5)-triphosphate at the front of the cell is a hallmark of cell polarization in neutrophils [68, 69]. The detailed molecular mechanisms underlying leukocyte adhesion and migration still need to be clarified. In fact, it is still not known why and if at all arrest-mediating chemokines exclusively use  $G\alpha_i$ . Indeed, some chemokine receptors lack to trigger chemotaxis or to mobilize calcium in response to their ligand depending on the cell in which they are expressed [70, 71]. Furthermore research indicates  $G\alpha_i$  independent signaling in immune cell function, e.g. during T cell stimulation by antigen-presenting cells, T cell chemokine receptors coupled to the  $G_q$  and/or  $G_{11}$  protein were recruited to the immunological synapse by a  $G_i$ -independent mechanism [72] or  $G_q$  deficient neutrophils and dendritic cells (DCs) showed defective chemotactic response upon stimulation in contrast to  $G_q$ -deficient T-cells, which respond normally. This suggests that this alternative chemokine receptor pathway controls the migration of only distinct subsets of cells [73]. Additionally some cases of chemokine receptor-independent signal transduction, via GAGs such as heparan sulfate and chondroitin sulfate, have been reported. For instance, in HeLa-CD4 cells completely devoid of GPCRs high concentrations of CCL5 induce rapid tyrosine phosphorylation of multiple proteins, but fail to induce the phosphotyrosine kinase in GAG-deficient cells [74]. This GPCR-independent signal was mediated by glycosaminoglycan chains of CD44 [32].

### **I.5. MECHANISMS THAT REGULATE CHEMOKINE ACTIVITY - 'A MÉNAGE À PLUSIEURS'**

Fast and coordinated recruitment of leukocytes as a response to tissue damage or infection is of vital importance, therefore a direct and confined up-regulation of

inflammatory chemokines and chemokine receptors is necessary for a rapid influx. On the other hand it is indispensable that the inflammatory response is terminated after the infection is resolved to prevent a prolonged inflammatory response that can lead to chronic inflammation or tissue damage. Therefore, an exact regulation of chemokine activity is required. The cellular response to chemokines can be modulated by mechanisms affecting the chemokine or the receptor. These regulative mechanisms act on multiple levels, ranging from the differential expression pattern of chemokines and their receptors, over posttranslational modifications to the availability of active receptors on cell surface and cooperative interactions between chemokines, receptors and signaling pathways. The availability of chemokines and chemokine receptors is dependent on the temporal and spatial expression, mRNA stability and protein degradation. This is particularly evident for the inflammatory chemokines and their cognate receptors, which are only expressed upon activation by e.g. highly conserved microbial pathogen associated molecular patterns (PAMPs), like the bacterial cell-surface lipopolysaccharides (LPS), or by endogenous cell molecules that are released upon tissue injury or stress, like double stranded ribonucleic acid (RNA). These ‘danger’ signals are recognized by pattern recognition receptors (PRRs), e.g. the toll-like receptors. The activation of the PRRs induces the transcription of genes encoding for inflammatory chemokines [75].

### **I.5.1. POSTTRANSLATIONAL MODIFICATIONS**

These processes are too slow to be solely responsible for the fast and local restricted modulation of chemokine function during inflammation. The next level of fine-tuning is more direct, *inter alia* through post-translational modifications like glycosylation or proteolytic processing, which can alter the affinity and the mode of interaction between receptor and chemokine. Indeed, the isolation of chemokines from natural sources did reveal posttranslational modifications, i.e. glycosylation and proteolytic processing [76, 77]. Most inflammatory chemokines are substrates of proteases expressed on the cell surface (e.g. dipeptidyl peptidase IV (CD26) or aminopeptidase N (CD13)), in intracellular granules (matrix metalloproteases, MMPs) or are even abundant in body fluids (e.g. plasmin or thrombin) [78, 79]. For the granulocyte chemotactic protein CXCL8 (IL8) a heterogeneous mixture of six natural occurring N-terminal truncated variants has been described, ranging from 79 to 70 amino acid length. Comparative studies revealed that the shorter variants (7,8 and 9-77) are more potent in inducing neutrophil chemotaxis than the 6-77 and 1-77 variants [79]. For example, CXCL7

requires N-terminal truncation in order to become chemotactically active [80]. The proteolytic modification can also alter the receptor specificity, like it was shown for CC chemokine ligand 5 (CCL5), where N-terminal truncation (3-68) weakens the binding and activation capacity to the CC chemokine receptors 1 (CCR1) and 3 (CCR3) but in return strengthens the affinity towards CCR5. Furthermore, CCL5 (3-68) inhibited infection of mononuclear cells by an M-tropic HIV-1 strain more efficiently than unmodified CCL5. Thus, proteolytic processing of CCL5 may also constitute an important regulatory mechanism during antiviral responses [81, 82]. During later stages of inflammation, proteolytically processed variants arise that retain their binding capacity but fail to activate the cognate receptor, providing natural antagonists. Finally, further cleavage results in totally inactive variants that may contribute to terminate the inflammation.

Besides proteolytic cleavage, other posttranslational modifications like glycosylation were found, e.g. for CCL2, 5, 11 and 14 as well as for XCL1 and CX<sub>3</sub>CL1. Until today, the functional role *in vivo* remain unknown [76]. In contrast to the lack of knowledge concerning the *in vivo* role of the addition of sugar moieties to chemokines, a little more is known about the *in vivo* role of these modifications on chemokine receptor function. Like for other transmembrane receptors, chemokine receptors may be modified by the addition of sugar moieties to the amid group of asparagin residues (N-glycosylation) or to hydroxyl groups of serin or threonine residues (O-glycosylation). These modifications occur mainly in the Golgi and are catalyzed by glycotransferases and glycosidases. Experimental data on chemokine receptor glycosylation are still rare. A few receptors were shown to carry N-linked or O-linked carbohydrate moieties, e.g. CCR2B, CXCR2, CXCR4, DARC and CCR5 [83-88]. The exact role of glycosylation of chemokine receptors remains unclear, but similar to other GPCRs it may increase the flexibility or directly participate in the ligand binding. Depending on their nature, glycosylation may provide additional negatively charged moieties for the electrostatic interactions with the positively charged chemokines. One group of glycotransferases are the sialyltransferases (Sts), which transfer sialic acid, a family of negatively charged monosaccharides, to the terminal portions of the N- or O-linked sugar chains of glycoproteins or glycolipids [89]. STs are preferentially localized to the Golgi apparatus within the cell; however some data indicate that STs may also be expressed on the cell surface. These cell surface STs have been found on platelets, lymphoblastoid cells, B lymphocytes, early-activated CD8 T cells and polymorphonuclear leukocyte (PMN) [90]. Twenty human sialyltransferases have been identified and are classified into four groups according to the type of linkage

formed and the nature of the sugar acceptor. These include six beta-galactoside  $\alpha$ 2–3 sialyltransferases (ST3Gal I-VI) [89]. Recently, sialylation by the  $\alpha$ 2-3 sialyltransferase ST3Gal-IV was shown to influence the chemokine induced firm adhesion of leukocytes. The function of CXCR2, a chemokine receptor involved in leukocyte adhesion and transmigration, was shown to strongly depend on posttranslational sialylation mediated by ST3Gal-IV. In mice deficient for ST3Gal-IV, an impaired adhesion of leukocytes to inflamed microvessels, upon injection of the CXCR2 ligands, CXCL8 and CXCL1 was observed. Additionally the binding of CXCL8 and CXCL1 to neutrophils isolated from these ST3Gal-IV<sup>-/-</sup> mice was impaired, indicating an important role of ST3Gal-IV on CXCR2 mediated leukocyte adhesion [91]. Furthermore, an *in vitro* study employing CCR5 mutants, in which the putative sialylation sites were exchanged, revealed that CCL3 and CCL4 receptor binding and activation depend on the addition of sialic acid moieties to the receptor [88].

## **I.5.2. COOPERATIVE INTERACTIONS BETWEEN CHEMOKINES AND CHEMOKINE RECEPTORS**

### ***Chemokine-chemokine interaction***

At chemokine rich sites during the initial stages of an inflammatory response, the concentration of specific chemokine can be suboptimal to induce sufficient cellular response, therefore leukocytes may require further stimuli to be fully activated. An interesting mode of cooperative action to reach maximal migration is synergy between chemokines. This synergistic effect can be based on 'dual receptor-mediated synergy' (compare Fig.I.4.), where the chemokine binds its cognate receptor and the cooperation of the signal occurs downstream of the receptor. In addition, heterophilic interaction between chemokines, involving a single chemokine receptor that is activated by its ligand heteromerized to a second chemokine (Fig.I.4.), can influence the cellular response.

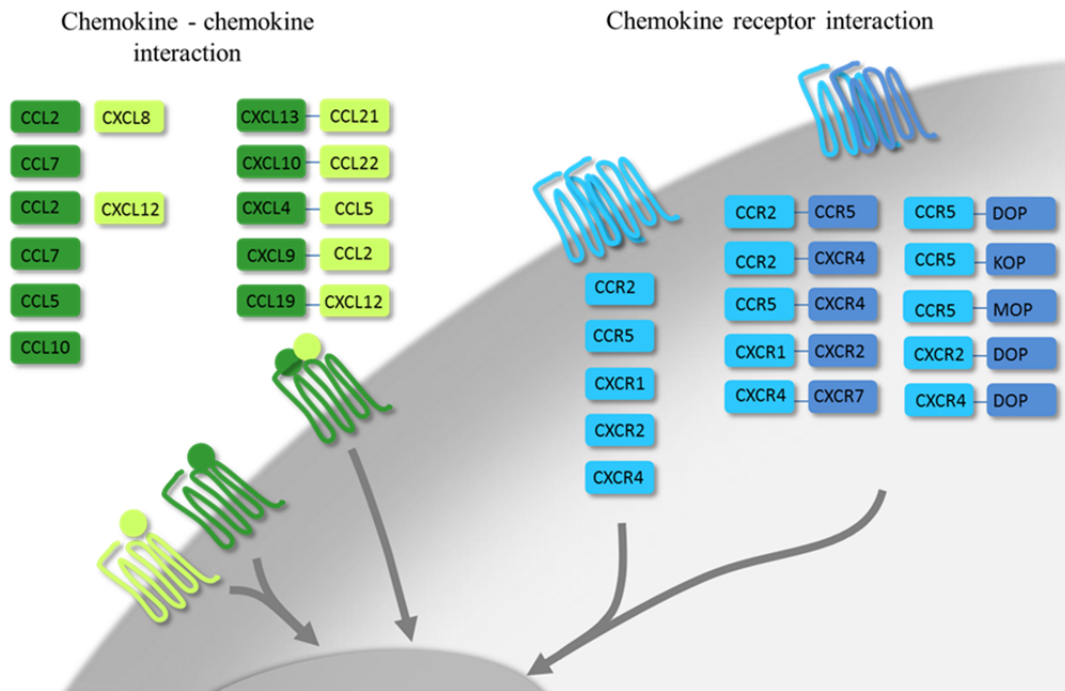


**Fig.I.4.: Overview of the possible cooperative interactions between chemokines and chemokine receptors.** Cooperativity between chemokines can be based on (a) 'dual receptor mediated synergy' or the (b) formation of chemokine heterocomplexes which in turn can enhance or dampen the primordial function of the single chemokine (chemokine-chemokine interaction is shown in shades of green). Like chemokine ligands, the receptors form (c) homo and (d) hetero-oligomers that modulate the cellular response (chemokine receptor interaction is shown in shades of blue).

So far, data concerning dual receptor mediated synergy demonstrate that the presence and activity of the corresponding GPCR for each chemokine is required to accelerate leukocyte recruitment. Chemotactic response of neutrophils to low doses of CXCL6 or CXCL8 was significantly enhanced due to the presence of constitutive plasma chemokines like CCL2, CCL7 as well as the CXC chemokine 12 [92, 93]. The observation of synergy between the CC chemokines 2, 5 and 7 and CXCL8 or CXCL12 inducing monocytes chemotaxis was found to depend on the expression of their corresponding receptors, because the synergy was inhibited in the presence of a blocking antibody or an antagonist against one of the participating receptors [71, 94]. The molecular mechanisms are still unknown, but so far the results indicate that the dual receptor mediated synergy is probably based on a interplay of signaling pathways. In contrast to the exclusive synergistic influence on chemokine responses described above, the formation of chemokine heterodimers can enhance (indicated in table I.1 as positive) or dampen (indicated in table I.1 as negative) the primordial function. However, many studies describing chemokine heterodimerization lack to define a possible impact on the cellular response or immune cell function, because they are solely based on methods

revealing the physical interaction like co-immunoprecipitation, surface plasmon resonance- or mass spectrometry and nuclear magnetic resonance spectroscopy [31, 95].

**Table I.1. Overview of the chemokine heterodimers.**

Heteromer	Functional consequences	References
CXCL4–CXCL8	positive or negative	[18, 96, 97]
CCL5–CXCL4	positive	[18, 98]
CCL19–CCL22	positive	[31, 99]
CCL19–CXCL13	positive	[31]
CCL21–CXCL13	positive	[31]
CXCL10–CCL22	positive	[99]
CCL22–CCL19	positive	[99]
CXCL9–CXCL12	positive	[100]
CCL7–CCL19	positive	[101]
CCL7–CCL21	positive	[101]
CCL3–CCL4	ND	[31]
CCL2–CCL8	ND	[95]
CCL2–CCL13	ND	[95]
CCL2–CCL11	ND	[95]
CCL8–CCL13	ND	[95]
CCL8–CCL11	ND	[95]

Until now, a negative cooperative interaction was described only for CXCL4 on CXCL8 mediated hematopoiesis, where CXCL4 blocks the CXCL8 mediated activation of hematopoietic progenitor cells [102]. The CXCL4/CXCL8 heterodimer formation on the other hand accelerates the original response, it enhances the chemotactic capacity on cells transfected with CXCR1 and CXCR2. Furthermore the CXCL4 heteromer formation with CCL5 leads to an increased adhesion of monocytes on the activated endothelium [18]. The synergism of CXCL13 with CCL19 or CCL21, at suboptimal concentrations of the individual chemokines on the activation of the CC chemokine receptor 7, was also shown to be based on their heteromerization [31]. Such a synergistic effect was further observed for CCL22-induced lymphocyte migration together with CXCL10, which was independent of the presence of the corresponding receptor for CXCL10 (CXCR3) [99].



Another study demonstrated that the homeostatic chemokines CCL19 and CCL21 enhance CCL7-induced migration of monocytes [101]. The CXC chemokines 9 and 12 were also shown to form heterocomplexes that might be responsible for the increased recruitment of CXCR4 expressing T cells and malignant B-cells to the tumor vasculature [100]. Positively charged and/or polar residues in the first  $\beta$ -strand of the synergistic chemokines have been reported to be crucial for the heteromer formation and for the potential to induce synergistic leukocyte migration [99, 101]. Even if some data indicate that heteromerization influences the receptor binding properties, there is still a great lack of knowledge.

### *Chemokine receptor interaction*

Similar to the chemokine ligands, chemokine receptors were shown to form homo and hetero-oligomers. The first milestone in the acceptance of this hypothesis was the finding that gamma-amino-butyric acid (GABA) B receptors R1 and R2 exist as obligatory heterodimers [103]. A first conclusive result that receptor oligomers exist in native membranes was adduced by atomic force microscopy images of rhodopsin in mouse rod outer-segment disc membranes [104, 105]. However, although GPCRs may activate G proteins as monomers [13, 106, 107], nowadays it is widely established that chemokine receptors homo- and heterodimerize or even form higher order oligomers. Interestingly, chemokine receptors even interact with GPCR from other classes such as CXCR2 with the  $\delta$ -opioid receptor (DOP) [108] and CCR5 with the opioid receptor of the  $\delta$ -,  $\mu$ -, and  $\kappa$ - types (DOP, MOP, KOP) [109, 110]. There are many challenges in studying the occurrence and functional effects of chemokine receptor oligomerization, thus there is still a limited understanding of these variations on the classic imagination that one GPCR activates one G protein per ligand binding event. The first observations revealing a functional relevance were made following the discovery of a natural genetic mutation of the CCR5 receptor named CCR5- $\Delta$ 32, which confers resistance to human immunodeficiency virus (HIV)-1 infection when individuals are homozygous for this allele [111]. Interestingly, heterozygous individuals show a retarded progression of HIV-1 infection. This has been hypothesized to result from dimerization of CCR5- $\Delta$ 32 with wild type CCR5 molecules, thereby causing retention of the complex in the endoplasmic reticulum (ER) and preventing transport of normal CCR5 to the cell surface. This finding gave rise to the notion that CCR5 naturally occurs as a functional

homodimer [112]. During recent years, the results of several groups support the hypothesis of a functional diversity between heteromers and homomers. One can conclude, based on the previous findings that chemokine receptor heteromerization can modulate the cellular response. And in fact, several studies reveal different consequences following receptor hetero-oligomerization. Cooperativity in ligand binding, either positive or negative, is one generally observed mechanism following receptor heteromerization. For example, a negative cooperativity in ligand binding and subsequent receptor activation between heteromers of CCR2, CCR5 and CXCR4 has been demonstrated *in vitro* and *in vivo* [113-115]. In another finding CXCR7, which is normally supposed to act as silent chemokine receptor [116], was able to modulate specialized signaling functions of CXCR4 through heteromerization with CXCR4 and enhanced CXCL12-mediated signaling [117]. The functional consequences of chemokine receptor heteromerization are summarized in table I.2. Nevertheless here, the underlying mechanisms responsible for the modulation of the cellular response still need to be understood.

**Table I.2. Chemokine receptors known to form heteromers and the functional consequences.**

		Functional consequences	References
CCR2	CCR5	Negative cooperativity in ligand binding	[114, 118]
CCR2	CCR5	Positive cooperativity in ligand binding	[62]
CCR5	CXCR4	Positive cooperativity in T cell activation	[104]
CCR2/5	CXCR4	Negative cooperativity in leukocyte migration <i>in vivo</i>	[118]
CCR7	CXCR4	Positive cooperativity in CXCR4 signaling	[117]
CCR5	MOP	Cross-desensitization	[119, 120]
CXCR4	MOP	Cross-desensitization	[121]
	DOP		
CXCR2	DOP	CXCR2 antagonism enhanced DOP function	[108]

## I.6. THE CHEMOKINES CCL5 AND CXCL4 IN IMMUNE CELL FUNCTION

One of the first chemokines described was platelet factor 4 (PF4) or CXCL4 [122]. The CXCL4 expression and storage was solely believed to occur in megakaryocytes and in platelets  $\alpha$ -granules, today expression has been detected in different cell types including monocytes, T cells, neutrophils and smooth muscle cells [123]. The human CXCL4 gene encodes a protein of 70 amino acids that is located in the CRO cluster on chromosome 4q13.3 [11]. Although CXCL4 was the first chemokine isolated, yet little is known about its role in inflammation, since it seems to lack most significant chemotactic properties on immune cells. In contrast to other CXC-chemokines, the N-terminal Glu-Leu-Arg (ELR) motif is missing in CXCL4, which was shown to be critical for receptor activation [15]. Due to the weak chemotactic potency, CXCL4 concentrations are several orders of magnitude higher than those required for other CXC chemokines, like CXCL8, to induce a normal cellular response [124]. Thus, its role in monocyte recruitment might be rather supportive or modulating than autonomous. Indeed, this suggestion is supported by the findings that CXCL4 accelerates the CCL5 mediated leukocyte arrest [18] and that heteromerization of CXCL4 with CXCL8 enhances the anti-proliferative effect of CXCL4 on endothelial cells in culture, as well as the CXCL8-induced migration of CXCR2-transfected cells [97]. Furthermore, CXCL4 blocks the CXCL8-mediated activation of hematopoietic progenitor cells [102]. Yet, there is still doubt about the corresponding receptor, some studies showed binding and activation of a CXCR3 splice variant named CXCR3B [125-127]. CXCR3B is 52 amino acid residues longer at its N-terminus compared with the previously described CXCR3, now termed CXCR3A. The CXC chemokines 9, 10, and 11 bind to CXCR3A and CXCR3B whereas CXCL4 binds exclusively to CXCR3B, with an affinity ( $K_d$  4 nM) comparable to the other ligands. Additionally it was shown that the engagement of CXCR3B by CXCL4 leads to the activation of the  $G\alpha_s$  subunit in contrast to the other ligands that employed the pertussis toxin-sensitive  $G\alpha_i$ . More recent reports even doubt the existence of the CXCR3B splice variant, since blast searches failed to identify a matching cDNA clone [128]. Moreover, the authors critically discussed, if the spliced human CXCR3-B mRNA would be



**Fig.I.4. Structure representation of a CXCL4 tetramer.**

In solution CXCL4 mainly exists as a tetramer.

translated and, if so, whether the efficiency would be high enough to have an actual influence. Besides the interaction with other chemokines CXCL4 is known to interact strongly with the anionic heparin ( $K_d$  4.4 nM) [129], which is based on highly specific interactions of positively charged amino acid residues in the C-terminus of CXCL4 with the negatively charged sulfate group of the heparin polymer. It has been shown that CXCL4 mediates signaling via binding to the GAG chondroitin sulfate [130]. CXCL4 was found mainly as a tetramer [131], the homodimerization was described to be thermodynamically unfavorable in solution, whereas in a tetramer formation these amino acids do not repel each other.

The CC-chemokine ligand 5 (CCL5) was named RANTES after it was initially identified

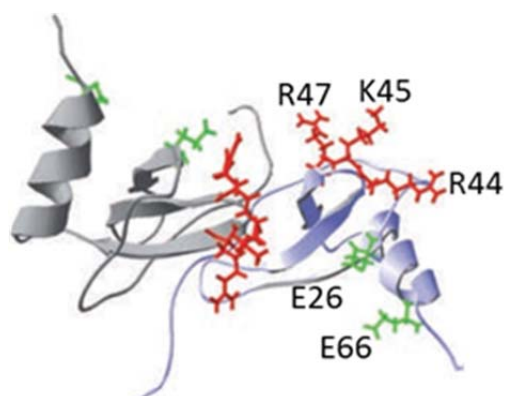


**Fig.I.5. Ribbon representations of a CCL5 dimer.** Amino-acid residues Arg44, Lys45 and Arg47, which are primarily responsible for interaction with glycosaminoglycans, are shown in red and the aa Glu26 and Glu66, which are involved in the oligomer formation, are shown in green.

to be expressed by T-lymphocytes. Further, CCL5 recruits T cells, eosinophils and macrophages to sites of inflammation [132, 133]. At once, a protein with chemotactic activity present in the supernatant of thrombin-stimulated platelets was discovered, which was subsequently characterized as CCL5 [134]. Additionally, it could be identified in the  $\alpha$ -granules of human platelets by immunocytochemistry [135]. Since then it was detected in many other cell types, such as fibroblasts, epithelial cells, and mesangial

cells, upon stimulation with proinflammatory cytokines e.g. IFN- $\gamma$  and TNF- $\alpha$ . CCL5 is assigned to the proinflammatory chemokines as it is a potent chemoattractant for monocytes, T cells and eosinophilic granulocytes [132]. Likewise most others, CCL5 is a circa 8 kDa molecular weight  $\beta$ -family member chemokine, sharing the quaternary structure typical for the CC-chemokines, where the dimer formation occurs mainly at the mobile N-terminal regions [97]. The CCL5 coding gene is located in the MIP cluster on chromosome 17q12 [11]. An important feature for CCL5 function is the ability to form higher-order oligomers and the binding to GAGs, which has been shown to be particularly important for triggering flow-resistant cell arrest [38, 136, 137]. The structural requirements for the oligomerization of CCL5 and also for its binding to heparin-like glycosaminoglycans (GAGs) have been extensively characterized [26, 39,

136]. Mutation of acidic residues E26 and E66 into neutral amino acids lead to variants reduced to the level of tetramers and dimers [26], which failed to induce *in vivo* cell recruitment. A biophysical study provided a model of the oligomeric CCL5, where E66 and E26 contribute to the dimer interface through the formation of salt bridges and an additional mechanism where GAG binding may promote oligomer formation was suggested [37]. Alanine scanning of two positively charged basic clusters located in the 40s and 50s region, in detail <sup>44</sup>RKNR<sup>47</sup> and <sup>55</sup>KKWVR<sup>59</sup>, revealed their involvement in binding to the negatively charged sulfate groups of heparin [39, 136]. Indeed, mutation of the 40s motif in CCL5 resulted in a variant with strongly reduced GAG-binding and an 80-fold reduction in affinity selectively for CCR1 but a normal binding to CCR5 [39]. Chemokines and chemokine receptors appear to play a role in the pathogenesis of multiple sclerosis. In an experimental autoimmune encephalomyelitis (EAE) model, the CCL5-40s variant inhibited the development in mice and rodents [138-140]. As already described above (I.5.1.), the N-terminus of chemokines is important for proper chemokine receptor activation and N-terminal modifications, like truncation, provide a strong mechanism to control chemokine function *in vivo*. When the mature sequence of CCL5 was primarily recombinant expressed in a prokaryotic system, the initiating methionine was found to be retained, resulting in a CCL5 variant, named Met-CCL5 [141]. Since then it was found that Met-CCL5 is a strong CCR1 and CCR5 receptor antagonist [141], which has been applied in several studies. Blocking CCL5 via administration of Met-CCL5 in rodent and monkey arthritis models resulted in a markedly reduced inflammatory response [142-145]. Furthermore Met-CCL5 reduces the progression of atherosclerosis in *Ldlr*<sup>-/-</sup> mice [146] and *in vivo* administration of Met-CCL5 greatly ameliorated liver fibrosis in mice and was able to accelerate fibrosis regression [147].

### **I.7. THE CHEMOKINE RECEPTORS CCR1 AND CCR5**

The CC-chemokine receptors CCR1 and CCR5, together with other chemokine receptor genes, including CCR2, CCRL2, CCR3, and CXCR1, are found to form a gene cluster on chromosome 3p<sup>1</sup>. The first CC chemokine receptor cloned was named CCR1 [148] and is expressed on neutrophils, eosinophils, basophils, monocytes and macrophages as well as on immature DCs, memory T cells, B cells, NK cells and mast cells. CCR5 was shown on monocytes and macrophages, DCs, T helper 1 cells, regulatory T cells, B cells, NK cells,

---

<sup>1</sup> <http://www.ncbi.nlm.nih.gov/gene?term=gene>

neutrophils and thymocytes [5, 149, 150]. CCL5 binds with high affinity to both receptors. In addition to CCL5, CCR5 binds seven other chemokines [151] that not essentially bind to CCR1 such as CCL4.

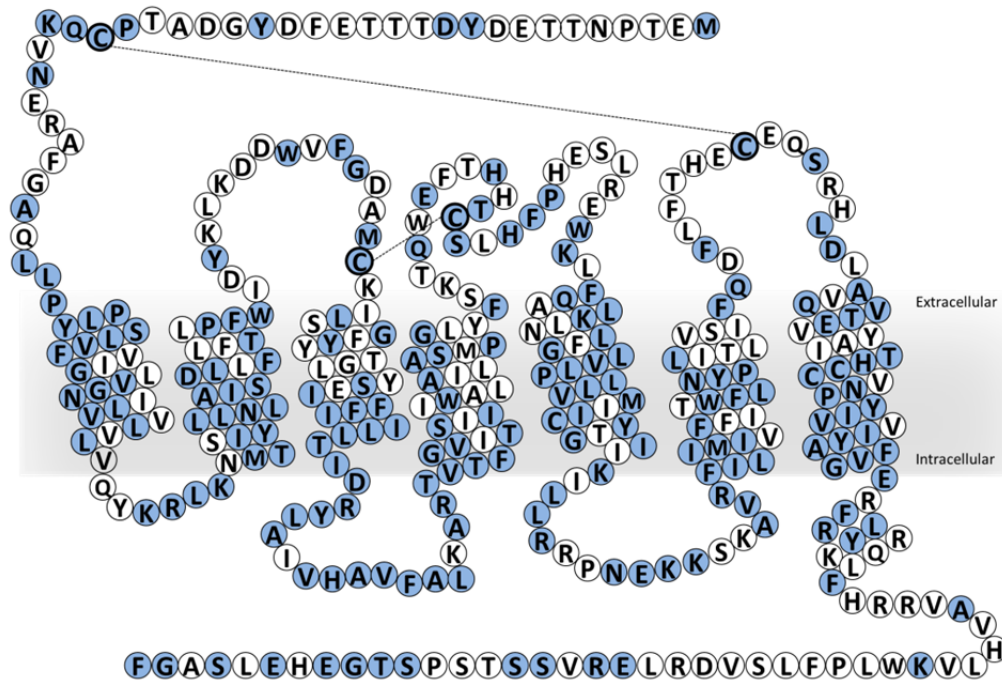


**Fig.I.6: Schematic presentation of an alignment of the CCR1 amino acid sequence with CCR5.**

Topographic blot based on the CCR1 amino acid sequence; blue circles denote identical residues in CCR5 through CCR1 with annotated disulfide bonds (dotted lines).

For CCR5, constitutive dimerization could also be evidenced through bioluminescence when transiting through the endoplasmic reticulum (ER) [152] and by the aforementioned observation that the presence of the CCR5- $\Delta$ 32 variant prevents transport of normal CCR5 from the ER to the cell surface [112]. In addition, synthetic peptides that were designed to disrupt CCR5 dimerization reduced the function of CCR5 *in vitro* and *in vivo* [153]. Concerning a possible dimerization of CCR1, no data exist up to now. In addition to the identical secondary structure that all rhodopsin class G protein coupled receptors share, CCR1 and CCR5 have a very high sequence homology. The overall identity is about 66% [154], which is mainly located in the transmembrane and cytoplasmatic parts of the receptors (cf. Fig.I.6.). Besides this high homology previous studies have suggested specialized roles for CCR1 and CCR5 in leukocyte recruitment [137, 155]. CCR1 was found to be predominantly required for the initial adhesion of human monocytes and T cells to endothelial cells, whereas CCR5 appeared to mediate in the first line the spreading on endothelial cells preceding transendothelial migration [155]. Another feature

supporting the functional specification of CCR1 and CCR5 are differences in the phenotype of mice deficient for one of the receptors. CCR5 deficiency in *Ldlr*<sup>-/-</sup> mice showed a decrease in inflammation and improved plaque stability. Contradictory, in the same mouse model CCR1 deficiency enhanced inflammation and atherosclerotic lesion development [156-158]. Additionally selective blocking of CCR5 and not CCR1, using the antagonist TAK-779 attenuates atherosclerotic lesion formation by blocking T cell migration into lesions as shown in *Ldlr*<sup>-/-</sup> mice [142, 159]. Furthermore, CCL5 engagement of CCR1 and CCR5 induced a similar pattern of receptor down-modulation but the patterns of receptor recycling that are induced are very different. Specifically, CCR5 recycles to the cell surface [160] and CCR1 was found to not recycle at all [161].

## I.8. AIMS OF THE STUDY

The regulation of chemokine function is multidimensional, affecting the chemokine or the chemokine receptor. This includes the heterophilic interaction between chemokines that can modulate the primordial function. CXCL4 was shown to accelerate the CCL5 mediated cell arrest [18]. First to reveal this interaction, metabolically <sup>15</sup>N-labeled CCL5 was expressed in *E. coli* and subsequently purified employing FPLC and HPLC methods. Within the scope of this study, small antagonists, preventing the CCL5–CXCL4 heterodimer formation, were constructed. The *in vivo* functionality was investigated in comparison to the CCL5 antagonist Met-CCL5. Thus Met-CCL5, for administration into a mouse model, was cloned, expressed in normal LB and purified. Previous studies have suggested specialized roles for CCR1 and CCR5 in leukocyte recruitment [155, 162]. CCR1 was found to be predominantly required for the initial adhesion of human monocytes and T cells to endothelial cells, whereas CCR5 appeared to mediate in the first line the spreading on endothelial cells preceding transendothelial migration [155]. Since chemokines are believed to predominantly interact with the extracellular loops [51, 163]. The extracellular regions of CCR1 and CCR5 are the most heterogeneous domains. To identify the possible role of the extracellular loops for receptor specification, chimeric receptor constructs were generated by exchanging the respective extracellular loops of CCR1 and CCR5. To be able to map the interaction surface between CCL5 and CCR1 and CCR5 different CCL5 and CCL5 mutants were used in cell adhesion assay and chemotaxis. Therefore CCL5-40s and CCL5-E66A are also expressed and purified. Furthermore, a recent study suggest that posttranslational modifications of chemokines receptors, precisely the addition of sialic acid to the terminal portions of the N- or O-linked sugar chains of glycoproteins or glycolipids, influence the interaction with the ligand [91]. In vitro data also suggest a role of sialic acid moieties for CCR5 function, thus the binding of CCL5 to leukocytes isolated from mice deficient for the sialyltransferase was determined. Finally the ability of isolated cells to induce calcium flux upon stimulation with CCL5 and to adhere to activated mouse endothelial cells (SVEC).



## II. Material and Methods

All solutions were prepared with Millipore water (Milli-Q Plus ultrapure purification, Millipore, Billerica, USA). Protocols were adapted from standard protocols [96] if not stated otherwise. All reagents were of analytical grade and purchased from major chemical suppliers such as Sigma-Aldrich (Steinheim, Germany), Carl Roth (Karlsruhe, Germany), Merck (Darmstadt, Germany) and Fluka (Buchs, Switzerland) unless otherwise stated in the text.

### II.1. GENERAL EQUIPMENT

autoclave	Systec 2540EL (Systec, Wettenberg, Germany)
balance	Analytical Plus, (Ohaus, Pine Brook, USA)
centrifuges	Eppendorf 5417C (Eppendorf, Hamburg, Germany), Heraeus Labofuge 400 and Heraeus Multifuge 3 S-R (Heraeus, Osterode, Germany), Beckman Avanti J 30 I (Beckman Coulter, Krefeld, Germany)
electroporator	Amaxa II Nucleofector™ System
fermenter	Minifor Bioreactor (LAMBDA Laboratory Instruments, Brno, Czech Republic)
fluorescence	LS 55 Fluorescence Spectrometer (PerkinElmer, USA)
FPLC system	Äkta FPLC ( Amersham/GE Healthcare, Uppsala, Sweden)
Flow cytometers	FACSCantoII, FACSCalibur, FACSAria (BD Biosciences, San Jose, CA, USA)
gel electrophoresis	Mini-sub cell GT (Bio-Rad, Hercules, USA)
HPLC system	Spectra System SCM (Thermo Electron Corp., Thermo Scientific, Waltham, USA), Varion Prostar HPLC System (Varian Inc., Palo Alto, USA), Waters Delta Prep 3000

	HPLC System (Warers Corp., Milford, USA)
image reader	LAS 3000 (Fujifilm, Düsseldorf, Germany)
incubator	Innova 4230 (New Brunswick Scientific, USA)
laminar flow hood	Herasafe (Heraeus, Osterode, Germany)
lyophilisator	Alpha 2-4 LD plus (Christ, Osterode , Germany)
microscopes	Olympus IX71, IX50, IX51 (Olympus Optical, Hamburg, Germany)
Two photon microscope	Leica SP5II MP, Mannheim, Germany
PCR thermocyclers	MyCycler (Bio-Rad, Hercules, USA)
pH-meter	InoLab level 1 (WTW, Weilheim, Germany)
sonicator	Branson S-250 D Digital Sonifier (Branson, Danbury, USA)
spectrophotometer	GeneQuant (Amersham/GE Healthcare, Uppsala, Sweden), NanoDrop 1000 (PeqLab, Erlangen, Germany)
Western blot transfer	iBlot® 7-Minute Blotting System (Life Technologies, Darmstadt, Germany)

## **II.2. ANTIBODIES**

### **II.2.1. PRIMARY ANTIBODIES**

CCL5	mouse Anti-Human Rantes VL1, RANT100 (Caltag, Burlingame, USA)
biotinylated $\alpha$ -human CCL5 (BAF278)	R&D Systems (Wiesbaden, Germany).
$\alpha$ -HA, Alexa Fluor® 594 conjugate	Invitrogen (Karlsruhe, Germany)

## Material and Methods

---

$\alpha$ -myc-FITC	Invitrogen (Karlsruhe, Germany)
$\alpha$ -hCCR1-phycoerythrin	R&D Systems (Wiesbaden, Germany).
$\alpha$ -hCCR5-allophycocyanin	R&D Systems (Wiesbaden, Germany).
HA -Tag (C29F4) (monoclonal, rabbit)	Cell signaling (Danvers, MA, USA)
Myc-Tag (71D10) (monoclonal, rabbit)	Cell signaling (Danvers, MA, USA)
Myc-Tag (9B11) HRP (monoclonal, mouse)	Cell signaling (Danvers, MA, USA)
HA-Tag (6E2)HRP (monoclonal, mouse)	Cell signaling (Danvers, MA, USA)
CD45-APC-Cy7(clone 30-F11)	BD Biosciences (New Jersey, USA)
CD115-PE (clone AFS98)	eBioscience/BD (San Diego, CA, USA)
Gr1-PerCp (clone RB6-8C5)	eBioscience/BD (San Diego, CA, USA)
CD11b-eFluor 450 (clone M1/70)	eBioscience/BD (San Diego, CA, USA)
Ly6G-FITC (clone 1A8)	BioLegend (San Diego, CA, USA)
anti-RANTES-biotin (ab83135)	Abcam (Cambridge, UK)

### II.2.2. ISOTYPE CONTROLS

IgG1-allophycocyanin	R&D Systems (Wiesbaden, Germany).
IgG2b-phycoerythrin	R&D Systems (Wiesbaden, Germany).

### II.2.3. SECONDARY ANTIBODIES

goat-anti-mouse-IgG-HRP	horseradish peroxidase (HRP)-conjugated, sc-2031 (Santa Cruz Biotech, Santa Cruz, USA)
Streptavidine-HRP	horseradish peroxidase (HRP)-conjugated, 016-030-084 (Jackson ImmunoResearch, West Grove, USA)

Streptavidin-PE-Cy7      BD Pharmingen

### II.3. MICE

Wild-type (wt) C57BL/6 and Apolipoprotein E deficient (*ApoE*<sup>-/-</sup>) mice were obtained from the local animal breeding facility (University Hospital, Aachen). *ApoE*<sup>-/-</sup> and mice are established mouse models to study the development and disease progression of atherosclerosis. The  $\alpha$ 2–3 sialyltransferase IV *knock out* mice (ST3Gal-IV<sup>-/-</sup>) were obtained from the local animal breeding facility (Ludwig Maximilian University, Munich). All studies with mice were approved by local authorities and complied with German animal protection law.

### II.4. MOLECULAR BIOLOGY

#### II.4.1. GENERAL WORK WITH E. COLI

*E. coli* strains were cultured in LB medium at 37°C with vigorous shaking. For growth on solid media, a bacteria suspension was spread on an LB agar plate or a single bacteria colony was inoculated to achieve single colony growth. The LB plates were incubated inverted overnight at 37°C. For culturing of bacteria transformed with a plasmid conferring antibiotic resistance, growth medium was supplemented with the appropriate antibiotic. For long-term storage of bacteria at -80°C, LB medium containing the corresponding antibiotics was supplemented with glycerol to a final concentration of 25% (v/v). All solutions used for bacteria work were autoclaved or filter-sterilized.

#### ***Bacteria growth media***

Bacteria growth medium was autoclaved for 20 min at 121°C. LB agar medium was allowed to cool to 50°C before addition of antibiotics.

LB medium:                      0.5% (w/v) yeast extract

   1% (w/v) peptone

   1% (w/v) NaCl

LB agar medium:              LB medium with 1.5% (w/v) agar

LB-agar plates for blue      LB-agar medium

white screening                50  $\mu$ l of 40 mg/ml X-gal dimethylformamide-solution

### ***Preparation of heat-shock competent E. coli***

*E. coli* cells were inoculated in 5 mL LB medium and incubated overnight at 37°C with vigorous shaking. Then 100 mL LB medium were inoculated with 1 ml of the overnight culture and incubated at 37°C until the optical density at 600 nm (OD<sub>600</sub>) of approximately 0.4 was reached, indicating the early exponential growth phase. OD<sub>600</sub> was measured in a spectrophotometer with pure medium as reference. The culture was centrifuged (10 min/ 3000 g/ 4°C), and the pellet was resuspended in 10 mL ice-cold TSS buffer. 500 µL aliquots were frozen immediately in liquid nitrogen and stored at -80°C.

TSS buffer:                    10% (w/v) polyethyleneglycol (PEG) 8000 (Promega)  
                                      5% (v/v) DMSO  
                                      20 mM MgCl<sub>2</sub>  
                                      in 1x LB medium (II.2.1)

### ***Heat-shock transformation of competent E. coli***

100 µl thawed competent *E. coli* were gently mixed with 1-10 ng of plasmid DNA (see II.4.3.), and incubated for 30 min on ice. The bacteria were heat-shock treated for 45 sec in a 42°C water bath, and then incubated for 2 min on ice. After addition of 500 µL LB medium, the bacteria were incubated for 1 h at 37°C with gently shaking. The bacteria were spread on selective LB agar plates and incubated overnight at 37°C.

## **II.4.2. BACTERIAL STRAINS**

DH5α	Invitrogen (Karlsruhe, Germany)
<i>E. coli</i> TOP10	Life Technologies, (Darmstadt, Germany)
Rosetta (DE3) pLysS	Novagen/Merck Bioscience (Darmstadt, Germany)

### II.4.3. PLASMIDS

pET-26b(+)	expression vector containing pelB signal sequence for secretion of the recombinant protein into periplasma (Novagen/Merck Bioscience, Darmstadt, Germany)
pET-26b(+) Met-CCL5	Met-CCL5 expression vector
pET-26b(+) CCL5	CCL5 expression vector
pET-32b(+) CCL5	CCL5 expression vector containing a thioredoxin tag fused with the recombinant protein (Novagen/Merck, Darmstadt, Germany)
pET-24a CCL5_40s	CCL5-40s expression vector, designed in house and supplied by (GenScript USA Inc., Piscataway, USA),
pET-24a CCL5_E66A	CCL5-E66A expression vector, designed in house and supplied by GenScript
pCR-2.1-Topo	Bacterial expression vector conjugated with a Topoisomerase, Life Technologies, (Darmstadt, Germany)
pCR-2.1-Topo-Met-CCL5	Subcloning of the Met-CCL5 PCR product for further cloning into the pET-26d+ vector.
pcDNA3.1	Mammalian expression vector, Life Technologies, (Darmstadt, Germany)
pcDNA4.A	Mammalian expression vector, Life Technologies, (Darmstadt, Germany)

pcDNA3.1_CCR1	Missouri S&T cDNA Resource Center (Rolla, MO)
pcDNA3.1_CCR5	Missouri S&T cDNA Resource Center (Rolla, MO)
pcDNA3.1_CCR5_1N1, _1E1, _1E2, _1E3,	were designed in house and supplied by GenScript in pUC57 and subcloned into pcDNA3.1
pcDNA3.1_CCR1_5N1, _5E3	were designed in house and supplied by GenScript in pUC57 and subcloned into pcDNA3.1
pcDNA3.1_CCR5-HA and CCR5_1E3 -HA	were designed in house and supplied by GenScript in pUC57 and subcloned into pcDNA3.1
pcDNA4.A _CCR1-Myc and CCR1_5E3 -Myc	were designed in house and supplied by GenScript in pUC57 and subcloned into pcDNA4A

### II.4.4. POLYMERASE CHAIN REACTION

Polymerase chain reaction (PCR) was used to amplify specific DNA sequences [164]. Additionally, this method allows the deletion, insertion or exchange of sequences in order to generate new DNA constructs. The specific Oligonucleotides were obtained from MWG (Eurofins MWG, Ebersberg, Germany). PCR fragments were amplified using the *PfuUltra* High Fidelity DNA polymerase (Agilent technologies) or Go *Taq*<sup>®</sup> Flexi (Promega, Madison, USA). The Annealing temperature was calculated based on the primer melting temperature.

PCR reaction: 50-200 ng template DNA  
1x PCR reaction buffer  
0.5  $\mu$ M forward primer  
0.5  $\mu$ M reverse primer

200  $\mu$ M each of dNTPs (dATP, dCTP, dGTP, dTTP)

1.3 U *PfuUltra* High Fidelity DNA polymerase (Agilent technologies) or Go *Taq*<sup>®</sup> Flexi (Promega, Madison, USA)

H<sub>2</sub>O to final volume of 50  $\mu$ l

PCR program	Initial denaturation	95°C, 1 min	} 25-30 cycles for normal PCR } 18 cycles for mutagenesis PCR
	Denaturation	95°C, 30 sec	
	Annealing	55-65°C, 30 sec	
	Extension	72°C 1-6 min	
	Final extension	72°C 5 min	

#### II.4.5. SMALL-SCALE PURIFICATION OF PLASMID DNA

Small-scale purification of plasmid DNA from bacteria on culture was performed using the Qiagen Plasmid Mini Kit<sup>™</sup> (Qiagen, Hilden, Germany) according to the manufacturer's instructions.

#### II.4.6. LARGE-SCALE PURIFICATION OF PLASMID DNA

Large-scale purification of plasmid DNA from bacteria on culture was performed using the Qiagen Plasmid Midi or Maxi Kit<sup>™</sup> (Qiagen, Hilden, Germany) according to the manufacturer's instructions.

#### II.4.7. DIGESTION, LIGATION AND PRECIPITATION OF DNA

Digestion of DNA was performed using restriction endonucleases (NEB, Massachusetts, USA) according to the manufactures instructions. In brief 50-200 ng DNA for analytical purpose or 1-2  $\mu$ g DNA for preparative use were digested in the appropriate enzyme buffer with 5-10 U or 20-50 U of enzyme in a 10 or 50  $\mu$ l reactions. The digested DNA was seperated by agarose gel electrophoresis (II.4.8) and visualized or extracted and purified for further cloning steps (II.4.8.). The ligation reaction was carried out either at room temperature for 3 h or overnight at 4°C in 1x ligation buffer. Exactly 200 U T4 DNA ligase was added to a final volume of 10  $\mu$ l. The vector/insert ratio was approximately 1 to 3.



#### **II.4.8. AGAROSE GEL ELECTROPHORESIS AND DNA PURIFICATION**

Digested DNA fragments were separated by agarose gel electrophoresis. The negatively charged DNA fragments migrate towards the anode in an electric field with a rate correlated to the size. DNA samples were mixed with DNA loading buffer and loaded on a agarose gel (1-2% (w/v) agarose dissolved in TAE electrophoresis buffer containing 0.1  $\mu\text{g}/\text{mL}$  ethidium bromide). After electrophoresis at 120 V, the DNA was visualized on a UV light transilluminator and photographed for documentation.

DNA loading buffer (6x):                      30% (v/v) glycerol  
  
    6 mM EDTA  
  
    0.25% (w/v) bromophenol blue  
  
    0.25% (w/v) xylene cyanol

TAE electrophoresis buffer (1x):        40 mM Tris-acetate  
  
    1 mM EDTA

If necessary, the DNA of interest was excised from the gel using a scalpel blade and was then purified using the QIAquick Gel Extraction Kit (Qiagen, Hilden, Germany) according to manufacturer's instructions. Briefly, the gel slice was incubated at 50°C for 10 min in three volumes of solubilisation buffer (QG), after addition of one gel slice volume of isopropanol the mixture was applied to a column and centrifuged for 1 min at 10,000 g. The column was washed twice and finally, the DNA was eluted in appropriate volume (25-50  $\mu\text{l}$ ) of ultra pure  $\text{H}_2\text{O}$ .

#### **II.4.9. QUANTIFICATION OF DNA**

DNA concentration was determined by measuring the absorbance at 260 nm ( $A_{260}$ ) using a NanoDrop ND-1000. For double-stranded DNA an  $A_{260} = 1$  corresponds to 50  $\mu\text{g}$  DNA/mL. The absorbance at 280 nm was also measured to estimate DNA purity. Pure DNA has an  $A_{260}/A_{280}$  ratio of 1.8-2.0 at pH 7.0.

#### II.4.10. SEQUENCING OF DNA

The sequencing reactions were performed by MWG Biotech AG using primers binding the T7 promotor and BGH reserve priming sites within the pcDNA3.1(+) vector or primers binding the M13 forward or reverse priming sites within the pCR<sup>®</sup>2.1-TOPO<sup>®</sup> vector.

#### II.4.11. CLONING OF MET-CCL5

The coding region of CCL5 in pET-26b(+), fused to the hexapeptide leader sequence MKKKWPR. The CCL5 sequence was amplified by PCR using the following specific primers: forward primer 5' ATCATATGTCCCCATATTCCTCGGACACCAC 3', together with the reverse primer 5' ACGGATCCRAGCTCATCTCCAAAGAGTTG 3'. Thereby the amino acids KKKWPR from the MKKKWPR leader were deleted (II.4.4.). The PCR fragment was controlled by agarose gel electrophoresis (II.4.8.) and subsequently cloned into the pCR-2.1<sup>®</sup>-TOPO according to the TOPO TA Cloning<sup>®</sup> protocol (Invitrogen). Positive clones were verified by analytical digestion and sequencing. The pCR-2.1-Met-CCL5 vector and the pET-26b(+) (Merck Biosciences, Darmstadt, Germany) expression vector were both digested (II.4.7.), thereby the pelB leader sequence of the pET-26b(+) was deleted. The DNA fragments were then separated by agarose gel electrophoresis and subsequently isolated (II.4.8.). Following ligation (II.4.7.) and transfection, positive clones were verified. Finally pET-26b(+) $\Delta$ pelB-Met-CCL5 was transfected into *E. coli* Rosetta (DE3) pLysS.

#### II.4.12. CLONING OF THE CCR1 AND CCR5 CHIMERAS

The CCR1 sequence was aligned against the CCR5 sequence [165] using the BLOSUM62 matrix. Sequences were aligned using CLUSTAL-W [166]. The length of the extracellular loops (ECL) was determined according to the UniProtKB/Swiss-Prot database, considering a minimum length of 18 residues in the core of the lipid double membrane and criteria from sequence analysis. All chimeric constructs of CCR5 and CCR1 were designed in house and purchased from Genescript (GenScript USA Inc., Piscataway, USA), in pUC57 and subsequently cloned, employing restriction endonucleases (II.4.7.), agarose gel electrophoresis (II.4.8) and the T4 ligase (II.4.7) into the mammalian expression vectors pcDNA3.1 and pcDNA4.A (II.4.3). In the same manner CCR1, CCR5 and CCR1-5N1 or CCR1-5E3 containing a synthetic C-terminally

Myc-tag or a hemagglutinin (HA) tag were constructed. The nomenclature and detailed information of the mutant constructs is summarized in the Table.III.4.12. or in the alignment of the wt receptor sequences with the chimeric constructs in the supplement. All constructs were stably transfected into *HEK-293* and *LI.2* mouse pre B cells.

construct name	description	exchanged amino acids
CCR5_1N1	hCCR5 containing the N-terminus of hCCR1	CCR5 M1R30 to CCR1 M1Q35
CCR5_1E1	hCCR5 containing the first ECL of hCCR1	CCR5 H92Q107 to CCR1 D92K107
CCR5_1E2	hCCR5 containing the second ECL of hCCR1	CCR5 T172I203 to CCR1 S172L203
CCR5_1E3	hCCR5 containing the third ECL of hCCR1	CCR5 Q266Q282 to CCR1 Q266L282
CCR1_5N1	hCCR1 containing the N-terminus of hCCR5	CCR1 M1A34 to CCR5 M1A30
CCR1_5E3	hCCR5 containing the third ECL of hCCR1	CCR1 Q266Q282 to CCR5 Q266Q282

**Table.II.4.12. Summary of the CCR1/CCR5 chimeric receptor constructs.**

## **II.5. PROTEIN ANALYSIS**

### **II.5.1. PROTEIN CONCENTRATION ASSAY**

The concentration of protein solutions was determined via the DC Protein Assay (BioRad, Hercules, USA). This method is similar to the Lowry Assay [167] and is based on the reaction of proteins with an alkaline copper tartrate solution and folin reagent. The measurement was done according to manufacturer's instruction. Briefly, 5  $\mu$ L of the fractions and BSA as standard were mixed with 25  $\mu$ L copper tartrate solution and 200  $\mu$ L folin reagent. The complexation of the protein with copper tartrate and the following reduction of the folin reagent by the complex were measured at 750nm.

### **II.5.2. SDS-POLYACRYLAMIDE GEL ELECTROPHORESIS (PAGE)**

During protein purification or for analyzing co-precipitated receptor molecules, the proteins were at first separated by SDS-PAGE (Sodiumdocecylsulfate-polyacrylamide-gel electrophoresis) [168]. SDS binds to polypeptides resulting in a negative charge directly proportional to protein size. Protein samples accumulate in a stacking gel before migrating simultaneously into the resolving gel. Electrophoresis was carried out in a Mini-PROTEAN® 3 cell system (Bio-Rad, Hercules, USA) at 120 V until the

bromphenol blue dye front reached the bottom of the gel. The separated protein in the resolving gel were then analysed either by coomassie blue, silver staining or western blotting (II.5.3-5)

Resolving gel	10-15% (w/v) acrylamide/Bis
	375 mM Tris-HCl, pH 8.8
	0.1% (w/v) SDS
	0.1% (w/v) ammonium persulfate
	0.1% (v/v) TEMED
Stacking gel:	5% (w/v) acrylamide/Bis
	125 mM Tris-HCl, pH 6.8
	0.1% (w/v) SDS (sodium-dodecylsulfate)
	0.1% (w/v) ammonium persulfate
	0.1% (v/v) TEMED
Electrophoresis buffer:	250 mM Tris base
	1.92 M glycine
	1% (w/v) SDS

### II.5.3. COOMASSIE BLUE STAINING

The coomassie blue staining of the gels was carried out with PageBlue Protein Staining Solution (MBI Fermentas, Ontario, Canada). They were subsequently destained with a 12.5% (v/v) isopropanol, 30% (v/v) EtOH.

#### **II.5.4. SILVER STAINING**

Silver gel staining was adapted from Blum [169], First the proteins are fixed in the gel with solution A at least for 1 h. Second, washed 3 x 20 sec with solution B the gel was sensitized for 1 min (solution C). Followed by staining with solution D containing AgNO<sub>3</sub> for 20 min. To visualize the protein the gel was incubated with the developing solution E. Finally the reduction reaction was stopped using solution F.

Solution A	50% methanol 12% acetic acid 0.05% formalin
Solution B	50% methanol
Solution C	0.02% (w/v) Na <sub>2</sub> S <sub>2</sub> O <sub>3</sub> x 5 H <sub>2</sub> O
Solution D	0.02% AgNO <sub>3</sub> 0.076% formalin
Solution E	6% Na <sub>2</sub> CO <sub>3</sub> 0.0004% Na <sub>2</sub> S <sub>2</sub> O <sub>3</sub> x 5 H <sub>2</sub> O 0.05% formalin
Solution F	50% methanol 12% acetic acid

#### **II.5.5. WESTERN BLOT ANALYSIS**

Separated proteins from a SDS-PAGE (II.5.2) were transferred to a nitrocellulose membrane and detected using specific primary antibodies either directly conjugated with HRP or further incubated HRP-conjugated secondary antibodies. The proteins were transferred from the gel to either the nitrocellulose Hybond membrane (Amersham/GE Healthcare, Uppsala, Sweden) using the wet/tank method at 90 V for 1 hour in ice-cold blotting buffer or employing the iBlot semidry transfer system (Life Technologies, Darmstadt, Germany). Nonspecific binding sites on the membrane were blocked with 5% (w/v) nonfat milk in TBS for 30-60 min at rt. Thereafter, the membrane was incubated with a primary antibodies diluted in blocking buffer for 1 hour at rt or overnight at 4°C. After 3 times washing with TBS/0.05% (v/v) Tween, if the primary antibody was not directly conjugated to HRP, the membrane was incubated with a HRP-conjugated secondary antibody diluted in TBS for 1 hour at rt or overnight at 4°C. In the presence of hydrogen peroxide (H<sub>2</sub>O<sub>2</sub>) the protein-bound HRP converts luminol to an excited

intermediate dianion, which emits light on return to its ground state. This light can be captured by a detector (LAS 3000 Image Reader, Fujifilm, Düsseldorf, Germany).

Blotting buffer (1x)	25 mM Tris base
	192 mM glycine
	10% (v/v) methanol
	0.005% (w/v) SDS
TBS (1x)	25 mM Tris-HCl, pH 7.4
	2.7 mM KCl
	137 mM NaCl

### **II.5.6. DOT BLOT**

This technique was used to identify the presence of the proteins in the fractions purified by FPLC in a more rapid approach compared to western blot. Fractions were spotted on a nitrocellulose membrane and after drying it was further proceed like for a western blot after the transfer of the protein to the nitrocellulose membrane (II.5.5).

### **II.5.7. FLOW CYTOMETRY**

Flow cytometry can be used to just analyze cells by their size, granularity and protein expression (by e.g. fluorescence-conjugated detection Abs) or to sort cell populations (FACS Fluorescent activated cell sorting). In a buffer stream, one cell at a time passes by an argon laser, which excites fluorescently labeled cells. Measurements of the size (forward scatter) and granularity (sideward scatter) are independent from the fluorescence signal. Measurement of fluorescence intensity using fluorescence labeled Abs was done to examine the expression of chemokine receptors on the cell surface. The results were displayed as histograms showing the logarithmic distribution of the fluorescence intensity or as diagrams demonstrating the change in mean fluorescence intensity (MFI). For receptor expression determination,  $1 \times 10^5$  cells were resuspended in PBS with specific Ab or IgG isotype control (10  $\mu$ l/test) and incubated for 30 min on ice. If necessary, the cells were further incubated, after washing, with a fluorescence conjugated detection

antibodies and analyzed immediately in a FACS CantoII (BD Biosciences) and evaluated with FlowJo Software (Treestar, Inc, Ashland, OR, USA).

## II.6. PROTEIN EXPRESSION AND PURIFICATION

### II.6.1. PURIFICATION OF RECOMBINANT CCL5 AND CCL5 VARIANTS

Two different protocols have been used to purify CCL5 and the mutant variants Met-CCL5, CCL5\_40s and CCL5\_E66A. All variants were expressed using the pET vector system where the CCL5 gene was cloned under the control of a strong bacteriophage T7 promoter. When transformed into an *E. coli* expression strain containing a chromosomal copy of the T7 RNA polymerase gene under *lacUV5* control the expression can be induced by the addition of IPTG (isopropyl- $\beta$ -D-thiogalactopyranoside) to the bacterial culture. Here the *E. coli* host strain Rosetta (DE3)-pLysS was employed using either the pET-32a(+) or the pET-26b(+) vector (Novagen/ Merck Bioscience, Darmstadt, Germany) or the pET-24a vector (GenScript). Rosetta strains additionally supply tRNAs on a compatible chloramphenicol resistant plasmid, providing enhanced expression of target genes otherwise limited by the codon usage of *E. coli*. The use of the pET-32a(+) enables the expression of the protein of interest fused to thioredoxin which is supposed to increase the amount of soluble protein in the cytoplasm [170], but at least 50% of the protein still form inclusion bodies. This expression vector is further called pET-32a(+)-CCL5. The other CCL5 expression vectors are based on either pET-26b(+) for CCL5 and Met-CCL5 or pET-24a for CCL5\_40s and CCL5\_E66A. These constructs, except Met-CCL5, are additionally N-terminal fused to the hexapeptide leader sequence MKKKWPR, hereinafter referred to as pET-26b(+)-CCL5, pET-26b(+)-Met-CCL5, pET-24a-CCL5\_40s and pET-24a-CCL5\_E66A. The CCL5\_40s variant is based on the finding that CCL5 contains a basic amino acid clusters, in detail <sup>44</sup>RKNR<sup>47</sup>, located in the 40s loop region, that is involved in the binding to GAGs [39]. And CCL5\_E66A is a CCL5 variant that is deficient to form higher order oligomers, it is reduced to a tetramer [26]. Of note, pET-24a-CCL5\_40s and pET-24a-CCL5\_E66A were codon optimized (supplied from Genescript). CCL5 and Met-CCL5 that were expressed using pET-26d(+), a vector normally carrying an N-terminal *pelB* sequence for periplasmic localization of the protein. These constructs were also expressed as inclusion bodies because the *pelB* leader was deleted (as described in section II.4.11.). A short summary of the different expression constructs, which highlights the differences already described in the text is given below.

pET-32a(+)-CCL5

**M.** **.DDDDK** SPYSSDTTP CCFAYIARPL PRAHIKEYFY TSGKCSNPAV VFVTRKNRQV  
CANPEKKWVR EYINSLEMS **Stop**

pET-26d(+)-CCL5

**MKKKWPR** SPYSSDTTP CCFAYIARPL PRAHIKEYFY TSGKCSNPAV VFVTRKNRQV CANPEKKWVR  
EYINSLEMS **Stop**

pET-24a(+)-CCL5 40s

**MKKKWPR** SPYSSDTTP CCFAYIARPL PRAHIKEYFY TSGKCSNPAV VFVT**AANA**QV CANPEKKWVR  
EYINSLEMS **Stop**

pET-24a(+)-CCL5 E66A

**MKKKWPR** SPYSSDTTP CCFAYIARPL PRAHIKEYFY TSGKCSNPAV VFVTRKNRQV CANPEKKWVR  
EYINSL**AMS** **Stop**

pET-26d(+)-Met-CCL5

**M** SPYSSDTTP CCFAYIARPL PRAHIKEYFY TSGKCSNPAV VFVTRKNRQV CANPEKKWVR  
EYINSLEMS **Stop**

**II.6.2. PROTOCOL USING GEL FILTRATION TO PURIFY CCL5 (A)***Cultivation, Cell breakage and inclusion body extraction*

The purification described below is depicted in the flow chart (A) in Figure III.1., employing the gelfiltration chromatography as an initial step. The bacteria transfected with pET-32a(+)-CCL5 were grown either in LB or in Spectra-9N medium (Cambridge Isotope Labs, New Jersey, USA) containing <sup>15</sup>N-enriched isotope for metabolic labeling. In detail, the bacteria were transferred from an overnight plate to 2x 1L prewarmed medium (LB or Spectra-9N) containing 100 µg/mL carbenicillin and 40µg/mL chloramphenicol. The bacteria were cultivated on an orbital shaker at 37°C. As soon as an OD<sub>600</sub> about 0.6 was reached the CCL5 expression was induced by addition of 1mM IPTG and further incubated overnight. The cells were harvested by centrifugation at 5000 rpm for 10 min. The pellet was subsequently frozen in liquid nitrogen to facilitate the cell lysis. Immediately after thawing, the pellet was resuspended in 5 ml per g wet cell weight BugBuster<sup>®</sup> Protein Extraction Reagent (Novagen/Merck Biosciences, Darmstadt, Germany) supplemented with Benzonase<sup>®</sup> nuclease. To obtain a homogenous lysate the mixture was additionally sonicated and filtered over a 40 µm cell strainer to remove DNA clumps. The aggregated proteins were pelleted by centrifugation (30 min, 25,000 g) afterwards washed 2x with PBS (PAA, Pasching, Austria) to remove detergents. The pre-cleaned inclusion bodies were solubilized in 6 M guanidine hydrochloride (Gnd-HCl) containing 1 mM DTT for about 1 h at 60°C or overnight at room temperature. Then the solution was centrifuged to remove remaining aggregates and was transferred to gel



filtration chromatography using the ÄKTA FPLC System (fast protein liquid chromatography).

### *Gel filtration using the Sephacryl S-100HR column*

The denatured fusion proteins were loaded onto the Sephacryl S-100HR column (Amersham/GE Healthcare, Uppsala, Sweden). and separated according to their masses in 6 M Gnd-HCl, 50 mM Tris pH 8, 1 mM DTT, 2,5 ml fractions were collected. The fractions containing the CCL5/thioredoxin fusion protein were identified by dot blotting and thereafter combined and subsequently processed to renaturation.

### *Protein renaturation*

The fusion protein was folded by drop-wise 6-fold dilution in 50 mM Tris pH 8 supplemented with a redox system of 1 mM cysteine (final concentration) and 8 mM cystine gently stirred overnight at 4°C. To remove remaining protein contaminants, the refolded fusion-protein was additionally purified by affinity chromatography.

### *Affinity chromatography using HiTrap chelating HP column*

The HiTrap chelating HP (Amersham/GE Healthcare, Uppsala, Sweden) column was first loaded with Ni<sup>2+</sup>, according to the manufacturer's instruction. Prior to chromatography precipitations and other non-soluble particles were removed by centrifugation (20.000g 30 min) and filtration (0.22 µm, Millipore, Billerica, USA). The protein was loaded onto the column with binding buffer composed of 20 mM Tris pH 8 and 2 M Urea with a flow rate of 2 mL/min. The CCL5/thioredoxin fusion protein was eluted with a linear 0-100 % gradient imidazole. 2-3 mL fractions were collected, the protein containing samples were then pooled for the enterokinase digestion.

### *Cleavage of the tioredoxin tag*

Before digestion Urea and Imididazol were removed by dialysis against 20 mM Tris pH 8. The thioredoxin tag was removed from CCL5 by digestion with 1 U enterokinase per 50 µg fusion protein (Novagen/ Merck Bioscience, Darmstadt, Germany) overnight at rt. During digestion CCL5 forms insoluble aggregates with remaining CCL5/thioredoxin fusion protein, which were pelleted by centrifugation.

### *Ion exchange chromatography using the MonoS™ 5/50 GL column*

The CCL5 CCL5/thioredoxin aggregates were dissolved in 20 mM Tris pH 8 and 8 M urea, the pH of the solution was adjusted to less than 5.5. CCL5 was separated from the

thioredoxin tag by the strong cationic exchange chromatography. The sample was loaded onto the MonoS™ 5/50 GL column (Amersham/ GE Healthcare, Uppsala, Sweden) with 50 mM NaAc pH 5.5 and 6 M Urea. The CCL5 was eluted at 1 mL/min using a linear gradient from 0-50% 2 M NaCl and 0.5 mL fractions were collected. The correct size was verified by SDS-PAGE and western blots.

*Polishing by reverse phase HPLC using the Grace Vydac C-8 column*

CCL5 was finally polished by reverse phase chromatography using the high performance liquid chromatography (HPLC) using a preparative Grace Vydac C-8 column (250 x 10 mm, 5 µm, Grace Davison Discovery Sciences, Deerfield, USA). The protein is separated based on the strength of the hydrophobic interaction with the C8 octyl group immobilized to the stationary phase of the column. The protein adsorbs to the hydrophobic surface of the column and desorb as soon as the binary polar eluent, acetonitril (ACN), reaches a critical concentration. The purified protein was recovered from the column employing a linear gradient elution from 0-67% acetonitril in 35 min.

Binding buffer	0.1% TFA (trifluoroacetic acid)
Elution buffer	0.1% TFA (trifluoroacetic acid) 90% acetonitrile

The collected fractions were pooled, dialysed first against 1% acetic acid then against 0.1% TFA then frozen in liquid nitrogen and subsequently lyophilized. The protein was again controlled by SDS-PAGE and western blot or mass spectrometry.

**II.6.3. PROTOCOL USING ION EXCHANGE CHROMATOGRAPHY TO PURIFY CCL5, MET-CCL5, CCL5\_40S AND CCL5\_E66A (B)**

*Cultivation, Cell breakage and inclusion body extraction*

The flow chart of the protocol employed to purify CCL5, CCL5\_40s, CCL5-E66A and Met\_CCL5 is depicted in Figure III.1.B and proceeded with the purified and de- and re-naturated inclusion bodies directly to the ion exchange chromatography. The bacteria transfected with either pET-26b(+)-CCL5 or pET-26b(+)-Met-CCL5 or pET-24a(+)-CCL5\_E66A or pET-24a(+)-CCL5\_40s were transferred from overnight plates to 2x1L or a 4 L fermenter prewarmed LB medium containing 50µg/ml kanamycin and 40 µg/mL chloramphenicol. At OD<sub>600</sub> > 0.6 the expression of the proteins were induced by addition

## Material and Methods

---

of 1mM IPTG and cultivated over night at 37°C on an orbital shaker or in the Minifor Bioreactor (LAMBDA Laboratory Instruments, Brno, Czech Republic) continuously stirred, vented and pH adjusted. The next day cells were harvested by centrifugation for 30 min at 5000 rpm. The cell pellet was subsequently resuspended completely in 13 ml suspension buffer per liter culture volume. To facilitate the resuspension the solution is additionally sonicated. Cell lysis was then initiated by the addition of 0.4 mg lysozyme and 2  $\mu\text{mol}$   $\text{MgCl}_2$ . To digest the DNA 20  $\mu\text{g}$  DNaseI per ml cell suspension or alternatively 5  $\mu\text{l}$  Benzonase<sup>®</sup> nuclease (Novagen/Merck Biosciences, Darmstadt, Germany) per g wet cell pellet weight were added. The solution was diluted with 13 ml lysing buffer per liter culture volume and then incubated for 1 h at rt, slightly rotating. To further support the cell lysis the solution was frozen in liquid nitrogen and left to defrost at rt. After thawing 3.5  $\mu\text{mol/ml}$  solution  $\text{MgCl}_2$  were added and the solution was further incubated at rt until the viscosity significantly decreased. The protein containing inclusion bodies were then pelleted by centrifugation at 11,000g, 4°C for 20 min. The pellet was resuspended in the washing buffer containing TritonX100, sonicated and again pelleted, minimum two times. Afterwards the detergent was removed by washing the pellet with the buffer without TritonX100 at least two times. The pre-cleaned inclusion bodies were then dissolved in 2 ml/g wet cell weight in 6 M Gnd-HCl, 50 mM Tris pH 8, 1 mM DTT at 60°C for 30 min or overnight at rt under continuous stirring. Precipitations and other non-soluble particles were removed by centrifugation (11,000g 20 min, 4°C) before dialysis against 1% acetic acid overnight at 4°C. The precipitated contaminants, like proteins (e.g. proteases) that adsorbed onto the hydrophobic inclusion bodies, were separated by centrifugation.

Solution buffer	50 mM Tris pH 8
	1 mM NaEDTA
	10 mM DTT
	25% Sucrose
Lysis buffer	50 mM Tris pH 8
	1% TritonX100
	1% desoxycholate

	100 mM NaCl
	10 mM DTT
Wash buffer with TritonX100	50 mM Tris pH 8
	1% TritonX100
	1mM NaEDTA
	100 mM NaCl
	1mM DTT
Wash buffer without TritonX100	50 mM Tris pH 8
	1mM NaEDTA
	100 mM NaCl
	1mM DTT

#### *Protein renaturation*

The CCL5 and CCL5 variants were recovered in the supernatant that was following to lyophilization again dissolved in 6 M Gnd-HCl and then renatured. Hence the CCL5 containing solution was drop wise 10x diluted in 50 mM Tris pH8 supplemented with the redox additives 0.01 mM oxidized glutathion and 0.1 mM reduced glutathion following gently stirring overnight at 4°C.

#### *Ion exchange chromatography using the HiTrap SP FF™ column*

After centrifugation the conductivity was adjusted to less than 20 mS and the pH to less than 5, remaining aggregates and impurities were removed by centrifugation and filtration prior to Ion exchange chromatography. The sample was loaded onto the HiTrap SP Sepharose FF column (Amersham/ GE Healthcare, Uppsala, Sweden) with 50 mM NaAc pH 5.5. The CCL5 proteins were eluted at 1 mL/min using a linear gradient from 0-100% 2 M NaCl and 1 mL fractions were collected. Met-CCL5 was directly processed to the polishing step, before the correct size was verified by SDS-PAGE and western blots or dot blot. The protein containing fractions were pooled, dialysed against 1% acetic acid and 0.1% TFA and lyophilized. For CCL5-40s, E66A and the wild type CCL5 followed by the cleavage of the MKKKWPR fusion construct.

### *Cleavage of the MKKKWPR leader*

First the Protein concentration was estimated then the protein solution was adjusted to a concentration of 1 mg/ml in 100 mM Tris-HCL (pH 8). Trypsin was added to the solution in a ratio of 1:250 enzyme to substrate, in detail 40 µg trypsin were added to 10 ml of the 1mg/ml protein solution. The digestion mixture was incubated for 3 h at 37°C. The reaction was then stopped by inhibition of the trypsin with 1 mM PMSF for further 30 min at 37°C. The cleaved product was separated by ion exchange chromatography.

### *Ion exchange chromatography using the HiTrap SP FF™ column*

First the conductivity was adjusted to less than 20 mS and the pH to less than 5, remaining aggregates and impurities were removed by centrifugation and filtration. The sample was loaded onto the HiTrap SP Sepharose FF column with 50 mM NaAc pH 5.5 and 6 M Urea. The CCL5 proteins were eluted at a flow rate of 1 mL/min using a linear gradient from 0-100% 2 M NaCl and 1 mL fractions were collected. The correct size was verified by SDS-PAGE and western blots or dot blot. The protein containing fractions were pooled, dialysed against 1% acetic acid and 0.1% TFA and lyophilized.

### *Polishing by reverse phase HPLC using the Grace Vydac C-8 column*

The reverse phase HPLC was performed in the same way as already described in section II.6.1. Additionally the correct mass was verified by electrospray ionization mass spectrometry (ESI-MS). The activity was finally determined by chemotaxis assay with freshly isolated PBMCs as described in II.10.1.

### *Activity control by transmigration assay*

If necessary, for the *in vitro* and *in vivo* assays like flow adhesion assay or chemotaxis or application into a mouse model, the activity was estimated by chemotaxis assay (II.10.1.) with freshly isolated PBMC from human peripheral blood (II.8.7).

## II.7. BIOCHEMICAL ANALYSIS OF THE CCL5-CXCL4 HETERODIMER

The biochemical analysis described in section II.7 were performed in the lab of Dr. Kevin Mayo (Department of Biochemistry, University of Minnesota) and Prof Dr. Andreas Kungl (Department of Pharmaceutical Chemistry, University of Graz).

### *15N-1H HETERONUCLEAR SINGLE QUANTUM COHERENCE (HSQC) NUCLEAR MAGNETIC RESONANCE SPECTROSCOPY.*

In brief, the heterodimerization was characterized by the  $^{15}\text{N}$ - $^1\text{H}$  heteronuclear single quantum coherence (HSQC) nuclear magnetic resonance (NMR) spectroscopy.  $^{15}\text{N}$  labeled CCL5 was dissolved at a concentration of 0.3 mM in 50 mM sodium phosphate buffer (95%  $\text{H}_2\text{O}$  and 5%  $\text{D}_2\text{O}$  pH 3.4.). Then CXC chemokine ligand 4 was added to the CCL5 solution the following NMR experiments were carried out at 40 °C on a Varian Unity Inova 600-MHz spectrometer equipped with an H/C/N triple-resonance probe and  $x/y/z$  triple-axis pulse field gradient unit. A gradient sensitivity-enhanced version of two-dimensional  $^1\text{H}$ - $^{15}\text{N}$  HSQC was applied with 256 ( $t_1$ )  $\times$  2048 ( $t_2$ ) complex data points in nitrogen and proton dimensions, respectively. Raw data were converted, processed and analyzed by using NMRPipe and NMRview. The chemical-shift differences were averaged according to equation 1 and assignments were made based on those reported for CCL5 [171, 172]:  $\delta\text{NH} = ((\Delta\delta(1\text{H}))^2 + 0.25(\Delta\delta(15\text{N}))^2)^{1/2}$ .

### *MOLECULAR DYNAMICS SIMULATIONS*

The NMR or x-ray structures of CCL5 and CXCL4 were taken from the Protein Data Bank, (1RTO for CCL5 and 1RHP for CXCL4). Heterodimers were built manually by replacing one monomer subunit in a homodimer with a monomer subunit from another homodimer using Insight-II software (Biosym Technologies Inc., San Diego, CA). Molecular dynamics simulations were performed for homodimers of CCL5, CXCL4 and CC-type and CXC type heterodimers of CCL5/CXCL4 using the c29b2 version of CHARMM33. A one nanosecond trajectory was simulated for each hetero- and homodimer. All dimers were simulated in a 74 x 68 x 63 Å<sup>3</sup> explicitly solvated periodic box. To make the box neutral, Cl<sup>-</sup> ions were added. Simulations were carried out using the version 22 all-hydrogen force field with a dielectric constant of 1.0. Each simulation was initialized with 2000 steps of steepest descent minimization, followed by gradual heating to 300 K and 5000 steps of system equilibration. The temperature during simulations was maintained at 300 K.

### ***DIFFERENTIAL SCANNING CALORIMETRY***

A high-sensitivity differential scanning calorimeter MicroCal VP-DSC (MicroCal, Inc., Northampton, USA) was used at a heating rate of 60 °C h<sup>-1</sup>. Cells were pressurized to about 28 psi to prevent loss of solvent by evaporation and the appearance of bubbles upon heating. Solvent buffer (PBS) was used to fill the reference cell and to obtain the instrumental baseline. Excess heat-capacity functions were obtained after baseline adjustment and normalization to protein concentration (CCL5-CXCL4 0.5 mg each). The heat capacity profiles were fitted applying a non-two-state model using MicroCal's Origin software resulting in calorimetric ( $\Delta H_{cal}$ ) and van't Hoff ( $\Delta H_v$ ) enthalpy values. Temperature of protein unfolding ( $T_{unfold}$ ) is taken as temperature of maximum heat capacity. Subsequent cooling and heating scans at 60°C h<sup>-1</sup> were performed to gain information on the reversibility of protein unfolding.

### **II.8. FUNCTIONAL ANALYSIS OF MKEY IN COMPARISON TO MET-CCL5**

The following experiment was performed by Dr. Alma Zerneck.

Apolipoprotein E deficient (ApoE<sup>-/-</sup>) mice were fed a high fat diet for 12 weeks. Additionally sMKEY, MKEY or Met-RANTES (50 mg each) was injected intraperitoneally 48 and 3 h before the assay. The adhesion of circulating monocytes labeled with rhodamine-6G in carotid arteries was then visualized and quantified in multiple high-power fields (at least six fields, 200x magnification) using epifluorescence microscopy (Zeiss Axiovert).

### **II.9. CELL CULTURE**

#### **II.9.1. GENERAL**

Cells were maintained in exponential growth in TS-25, TS-75 or TS-175 (Greiner Bio-one, Frickenhausen, Germany) in a humidified 5% CO<sub>2</sub> atmosphere incubator at 37°C. All media and solutions used for cell culture were from Gibco (Gibco/Invitrogen, Karlsruhe, Germany) or PAA (Pasching, Austria) if not stated otherwise and purchased sterile or sterilized through a 0.22 µm filter. The PCR mycoplasma detection Kit (TAKARA, Otsu, Japan) was regularly used for detection of contamination of the cell lines with mycoplasma.

### II.9.2. CELL LINES

Primary cells	Origin	Source	Medium
HAoEC	Human aortic endothelial cells	PromoCell (Heidelberg, Germany)	Endothelial Growth medium MV
THP-1 cells	Human leukemia monocytic cells	American Type Culture Collection (ATCC® TIB202)	RPMI1640 Medium + 10%, 2mM glutamine 50 µM β-mercaptoethanol
L1.2 cells	Murine pre-B lymphoma cells	a kind gift from Dr. M. Locati (University of Milano Italy)	RPMI 1640 + 10% FCS, 1 mM pyruvate, 50 µM β-mercaptoethanol, 10 mM HEPES
HEK293	human embryonic kidney cells	ATCC CRL 1573, (Manassas, USA)	DMEM + 10% FCS
SVEC	Simian virus transduced mouse endothelial cells	ATCC CRL-2181 (Manassas, USA)	DMEM + 10% FCS or DMEM + 5% FCS

### II.9.3. CULTURING OF ADHERENT CELL MONOLAYERS

Adherent cell lines were grown until confluence and then passaged by using the cell detachment solution Accutase™. The monolayer was first washed with phosphate buffered saline (PBS) (PAA, Pasching, Austria) and then incubated 5-10 min with 0.25% (v/v) Accutase™ at 37°C. After detachment of the monolayer, Accutase™ was inactivated by the addition of medium. For subculturing, cells were harvested by centrifugation (5 min, 200 g, at room temperature) and then split with a ratio of 1:3.

### II.9.4. CULTURING OF CELLS IN SUSPENSION

Cells growing in suspension were cultured at a density of  $10^5$  -  $10^6$  cells/mL. Cells were harvested by centrifugation (5 min, 200 g, rt) and passaged with a ratio of 1:3-1:5.



### **II.9.5. FREEZING AND THAWING OF CELLS**

Freeze stocks of cell lines were stored in 1.8 mL cryovials in liquid nitrogen. Cells were first harvested and then resuspended at a concentration of  $10^6$  -  $10^7$  cells/mL in complete medium containing 10% (v/v) dimethylsulfoxide (DMSO). The cryovials were placed overnight (o.n.) at  $-80^{\circ}\text{C}$  in a cryocontainer to assure slow cooling and then transferred to liquid nitrogen for long-term storage. For thawing of cells, cryovials were rapidly thawed in a  $37^{\circ}\text{C}$  water bath. 5 mL warm corresponding growth were slowly added to the cells medium, centrifuged and resuspended again in growth medium.

### **II.9.6. TRANSFECTION OF EUKARYOTIC CELLS**

#### ***TRANSIENT TRANSFECTION OF HEK-293 CELLS***

*HEK-293* cells were transiently transfected with hCCR1-Myc, hCCR5-HA or hCCR1\_5E3-Myc or hCCR5\_1E3-HA. Cells were grown until the cells reached 50-80% confluence, depending on the subsequent application. Serum free medium (OptiMEM, Life technologies) was mixed with the DNA, then the investigated amount of FugeneHD was carefully added, after 5 min incubation at rt the mixture was added to the cells in a drop wise manner. The optimal ratio of transfection reagent to DNA calculated was 3:1. After 24h the medium was carefully exchanged.

#### ***STABLE TRANSFECTION OF LI.2 AND HEK-293 CELLS***

*HEK-293* cells were stably transfected with liposomes (FugeneHD, Promega) to express hCCR1, hCCR5 and the CCR1/CCR5 chimeras described in Table.III.4.12. and more precisely in the supplement (V.III.). The same procedure as the transient transfection was applied with the difference that the cells were grown until they reached 80% confluence. After 48h the normal medium was exchanged against normal medium supplemented with 800  $\mu\text{g/ml}$  G418 sulfate for the selection of transfected cells. The selection medium was changed every two days for 2-3 weeks. After this period the cells were rinsed off with accutase, transferred to a 96 well plate in a dilution of approximately one cell per well and grown until the cells reached a visible density.

Murine pre-B lymphoma *LI.2* cells were transfected by nucleofection using the Amaxa Nucleofector<sup>TM</sup> kit V and an Amaxa II Nucleofector<sup>TM</sup> System (Lonza AG, Visp, Switzerland). Briefly,  $2 \times 10^6$  cells were resuspended in 100  $\mu\text{l}$  of nucleofection solution,

and after addition of 2 µg of the indicated expression vector, the cells were immediately pulsed using the U-15 program. 48h after transfection the cells were transferred into the selection medium, normal medium supplemented with 600 µg/ml neomycin (G481) and cultivated like described above for the *HEK293 cells*. Afterwards the transfected cells were diluted to a 96well round bottom plate with about one cell per well (compare HEK-293 cells above). Furthermore, the expression was enhanced by the addition of sodium butyrate (sigma-aldrich) for 12h directly after transfection or to re-induce the expression weeks after the transfection. Finally cell selection according to the highest surface expression, for *L1.2* and *HEK-293* cells, was determined by flow cytometry II.5.7.

### **II.9.7.ISOLATION OF PBMC**

Human peripheral blood was supplied by healthy donors from the lab. PBMC were isolated from venous blood of healthy donors by Ficoll-hypaque density gradient centrifugation. After dextran sedimentation, the plasma supernatant was carefully overlaid on Biocoll separating solution, density 1.077 g/ml (Biochrom, Berlin, Germany) and centrifuged (20 min, 450 g, RT, without brake). The PBMC interface layer was harvested, diluted in PBS and centrifuged (5 min, 400 g, RT). The mononuclear cells were washed twice with PBS, and the number of viable cells was determined by trypan blue exclusion.

### **II.9.8.ISOLATION OF NEUTROPHILS AND MONOCYTES FROM MOUSE BONE MARROW**

Primary monocytes and neutrophils of *ST3G4<sup>+/+</sup>* and *ST3G4<sup>-/-</sup>* mice were isolated with cell separation kits from Miltenyi Biotec according to the manufacture's protocol. For monocytes we used the 'CD115 MicroBead Kit', for neutrophils the 'Neutrophil Isolation Kit, mouse'. Both cells types were isolated from mouse bone marrow and further processed for flow chamber adhesion assays.

## II.10. FUNCTIONAL ASSAYS

### II.10.1. TRANSMIGRATION ASSAY

#### *Chemotaxis of HEK-293 cells stably expressing CCR1, CCR5 or CCR1/CCR5 chimeras*

The Costar Transwell™ system (5.0- $\mu$ m pore size) (Corning Glass, Corning, NY) was used to quantify the migration of *HEK-293* cells stably expressing CCR1, CCR5 or CCR1/CCR5 chimeras towards CCL5 and the CCL5\_40s and CCL5\_50s mutants (100 ng/ml). After 4 h, the inserts were removed and the number of migrated cells in the lower well was counted for 1 min using the high throughput loader on a Becton Dickinson FACSCantoII (BD Biosciences, San Jose, CA, USA) with the gates set to acquire the cells of interest.

#### *Chemotaxis using PMBC, to control the activity of the purified CCL5*

To control the activity of the purified CCL5 and the variants used in functional assays, the number of freshly isolated PMBCs (II.9.7) migrated towards the purified proteins, in the case of CCL5 towards different concentrations (50, 100 and 150 ng/ml) and for Met-CCL5 a comparison to CCL5 and application together with CCL5, was estimated also employing a Costar Transwell™ system (5.0- $\mu$ m pore size).

### II.10.2. PARALLEL PLATE FLOW CHAMBER ADHESION ASSAY

#### *Adhesion of CCR1-, CCR5- and chimera-transfected L1.2 cells*

Adhesion of stably transfected *L1.2* cells, labeled with calcein (Life technologies) to a mouse tumor necrosis factor (TNF)  $\alpha$ -activated (10 ng/mL, 4 hours) monolayer of SV40-immortalized mouse endothelial cells (SVEC, ATCC CRL-2181) was analyzed in a parallel wall chamber under laminar flow conditions (0.1 ml/min, 1.5 dynes/cm<sup>2</sup>).

The *L1.2* transfectants were activated with H<sub>2</sub>O (control), CCL5 and mutants (500 ng/ml) or/and CXCL4 (500 ng/ml) at 37 °C 10 min prior to perfusion. During perfusion, stably adherent cells were counted in at least ten random microscopic fields using microscopic video imaging [173].

#### *Adhesion of THP-1 cells to TNF $\alpha$ activated HAoEC*

Adhesion of human acute monocytic leukemia cell line (THP-1, ATCC TIB-202) to Human Aortic Endothelial Cells (HAoEC) activated with human TNF $\alpha$  (10 ng/mL, 4

hours) directly stimulated with CCL5 (500 ng/ml) or/and CXCL4 (500 ng/ml) was determined under the same conditions as used above. THP cells were pretreated with pertussis toxin (PTX, 100 ng/ml, 30min, 37°C, Sigma-Aldrich) or left untreated. Stable cell arrest was assessed in the presence or absence of either the CCR5 antagonist DAPTA (10 nM) or J113863 antagonizing CCR1/CCR3 (10 nM) or SB297006 a selective CCR3 (80 nM) antagonist (Tocris Bioscience Bristol, UK).

#### *Adhesion of neutrophils and monocytes isolated from ST3Gal-IV<sup>-/-</sup> and ST3Gal-IV<sup>+/+</sup>*

Monocytes and neutrophils isolated from ST3Gal-IV<sup>+/+</sup> and ST3Gal-IV<sup>-/-</sup> mice (II.9.8) (stained with calcein, vide supra) were perfused over TNF activated (20 ng, 4 h) SVEC monolayers. The number of stably adherent cells was determined in at least ten random microscopic fields. Ccl5 (5 µg) was either deposited on the endothelial cell monolayer 10 min prior to perfusion or the leukocytes were pre-treated with the murine Ccl5 (5µg, 10 min) in suspension.

#### **II.10.3. IMMUNOFLUORESCENCE**

The wild type HEK293 cells were seeded on round glass cover slides coated with polylysine the day before transfection with pcDNA3.1-CCR1-Myc, pcDNA3.1-CCR5-HA or pcDNA4-CCR1\_5E3-Myc or pcDNA3.1-CCR5\_1E3-HA. Liposomal transfection was carried out after cells reached 60-70% confluence, subsequently the cells were incubated for 48h at 37° and 5% CO<sub>2</sub> (II.9.6). All following steps were carried out at room temperature. Cells were fixed in 2% (w/v) paraformaldehyde-PBS for 15 min and then permeabilized in 0.2% (v/v) saponin diluted in PBS for 25 min. After blockage with 1% BSA (v/v) in PBS the cells were sequentially stained with 20 µg/ml anti-Myc-fluorescein isothiocyanate (II.2.1.) and anti-HA Alexa Fluor<sup>®</sup> 594-conjugated mAb (II.2.1.) at a concentration of 50 µg/ml. Finally the cells were counterstained with 4',6-Diamidino-2-phenylindol (DAPI) (Life Technologies). The cover slides were then mounted on a microscope slide. The cell proteins were visualized using a two-photon microscope (Leica SP5II MP, Mannheim, Germany) set to confocal mode as previously described [174].

#### II.10.4. CO-IMMUNOPRECIPITATION

HEK293 cells were transiently transfected with pcDNA4.1-CCR1-Myc, pcDNA3.1-CCR5-HA or pcDNA4-CCR1\_5E3-Myc or pcDNA3.1-CCR5\_1E3-HA 48h before the experiment (II.9.6). For pull down of the CCR1/CCR5 receptor complexes the transfected as well as untransfected HEK cells were lysed in non-denaturing lysis buffer to a final concentration of  $5 \times 10^6$  cells/ml o.n. at 4°C. At the same time, the 10µg of the appropriate antibodies, αHA -Tag (C29F4) or respectively αMyc-Tag (71D10) (II.2.1.) were bound to Dynabeads<sup>®</sup> protein G beads (life technologies, Darmstadt, Germany), incubated for 10 min at rt gently shaking. Supernatants were then incubated with the antibody coated protein G beads for 60 min at rt. Proteins were analyzed by western blot using antibodies to the Myc-Tag and the HA-Tag directly conjugated to HRP (II.2.1.).

Non-denaturing lysis buffer:	1% (w/v)	Triton X-100
	1% (w/v)	(CHAPSO) (Calbiochem)
	50 mM	Tris-HCl (pH 7.4)
	100 mM	NaCl
	15 mM	EGTA
		supplemented with a proteinase inhibitor cocktail (Complete Mini, Roche, Mannheim, Germany)

#### II.10.5. CALCIUM MOBILIZATION ASSAY

The activation of cells due chemokine/GPCR interaction causes a rapid influx of  $\text{Ca}^{2+}$  and the release of  $\text{Ca}^{2+}$  from the endoplasmic reticulum. This calcium mobilization can be visualized by the fluorophore Fura-2. Fura-2 AM (Molecular Probes, Eugene, OR, USA) is a calcium indicator, which can be loaded into cells. Upon binding to cytosolic  $\text{Ca}^{2+}$  the extinction maximum shifts from 380 nm for the calcium free Fura-2 to 340 nm. The calcium signal is given as the  $\Delta F_{340 \text{ nm}}/F_{380 \text{ nm}}$ . Briefly, neutrophils isolated from the ST3Gal-IV<sup>-/-</sup> mice were suspended at a concentration of  $5 \times 10^5$  cells per ml in RPMI without indicator (PAA) supplemented with 0.5 % BSA. Then cells were loaded with 2 µg/ml Fura-2 AM for 15 min at 37°C, washed carefully with prewarmed RPMI + BSA and stored until the measurement at 37°C. Calcium measurement was performed using a LS 55 Fluorescence Spectrometer (PerkinElmer, USA).

### **II.10.6. BINDING ASSAY**

Whole blood obtained from the retro-orbital plexus of either ST3Gal-IV<sup>-/-</sup> or ST3Gal-IV<sup>+/+</sup> mice was EDTA-buffered and subjected to red-blood-cell lysis (Pharmlyse BD Biosciences) were incubated with an antibody cocktail containing CD45-APC-Cy7, CD115-PE, Gr1-PerCp, CD11b-eFluor 450 and Ly6G-FITC. After washing, 0.5 µg murine Ccl5 (Peprotech) was added to each sample ( $5 \times 10^5$  cells) and incubated for 10 min on ice, cells were washed again and stained on ice with an anti-Rantes Biotin-Strep-PE-Cy7 antibody, which had been Streptavidin-PE-Cy7 labeled and washed a priori. Cells incubated with the anti-Rantes Biotin-Strep-PE-Cy7 antibody alone served as a control. The binding of CCL5 was determined by measuring the fluorescence intensity by FACS (II.5.7) with the gate set on the cells of interest and results were analyzed by FlowJo software.

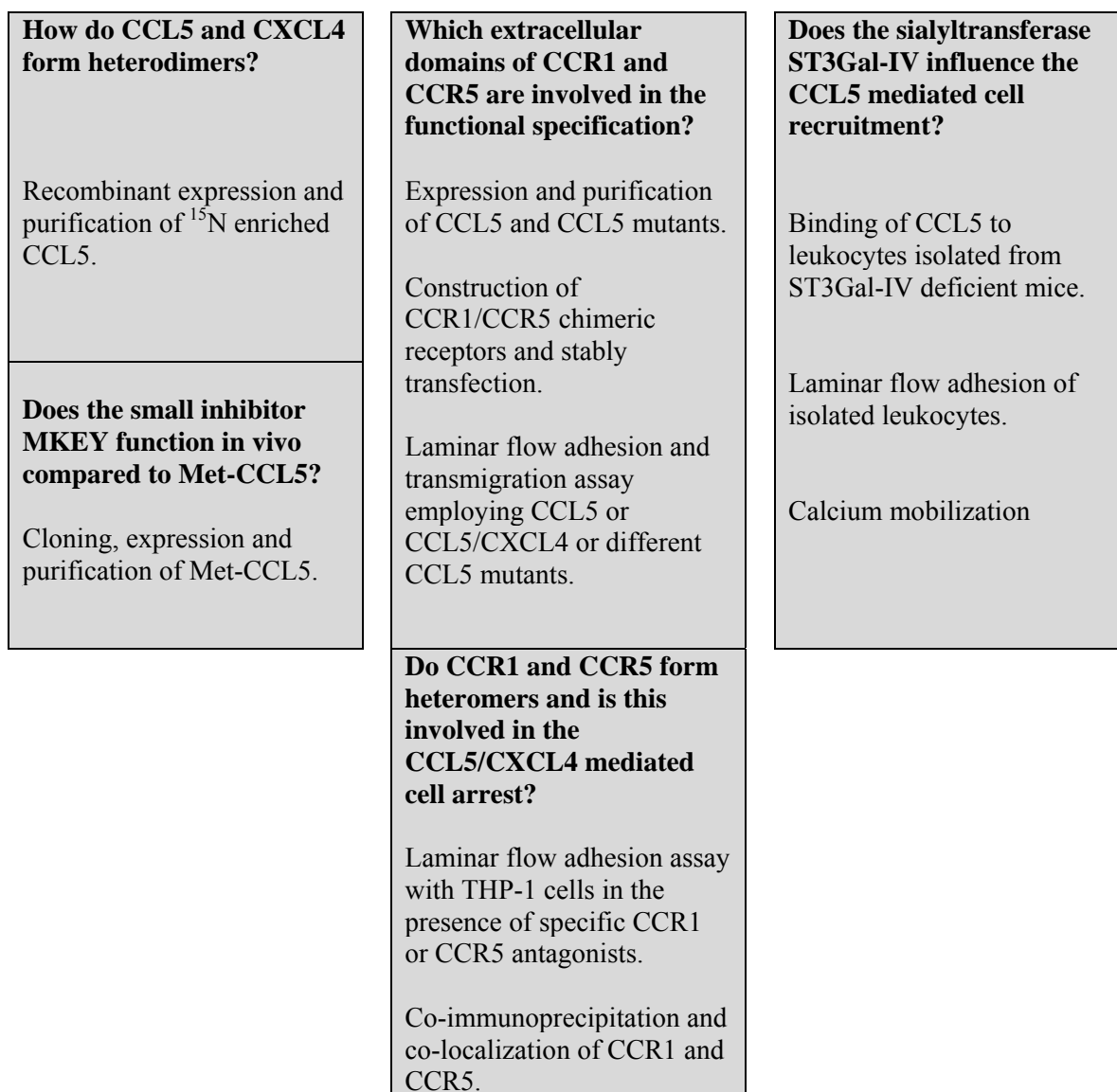
### **II.11. DATA ILLUSTRATION AND STATISTICAL ANALYSIS**

Data in section III.4 “Establishing the role of the extracellular domains of CCR1 and CCR5 in CCL5 mediated cell recruitment.” are expressed as mean  $\pm$  standard error of the mean. The number of independent experiments was 5 or, if deviating, indicated in each figure legend. The differences in the means of the four groups of the functional experiments were calculated by 1- or 2-way ANOVA using GraphPad Prism version 5.04 for Windows (GraphPad Software, La Jolla, CA, [www.graphpad.com](http://www.graphpad.com)). The comparison of all pairs was done by the Newman-Keuls or Bonferroni tests, where applicable. A P-value below 0.05 was considered statistically significant. The data in section III.5. are expressed as mean  $\pm$  SD error of the mean. The number of independent experiments was 5, deviating are indicated in the figure legend. 1-way ANOVA with Tukey's Multiple Comparison test.

### III. RESULTS

In the following section the results obtained throughout this thesis will be displayed and explained. For a better overview of the result section the following flow chart outlines the experimental setup for each project.

**Fig.I.7. Flow scheme, briefly summarizing the contents of this work**



### III.1. PROTEIN EXPRESSION AND PURIFICATION

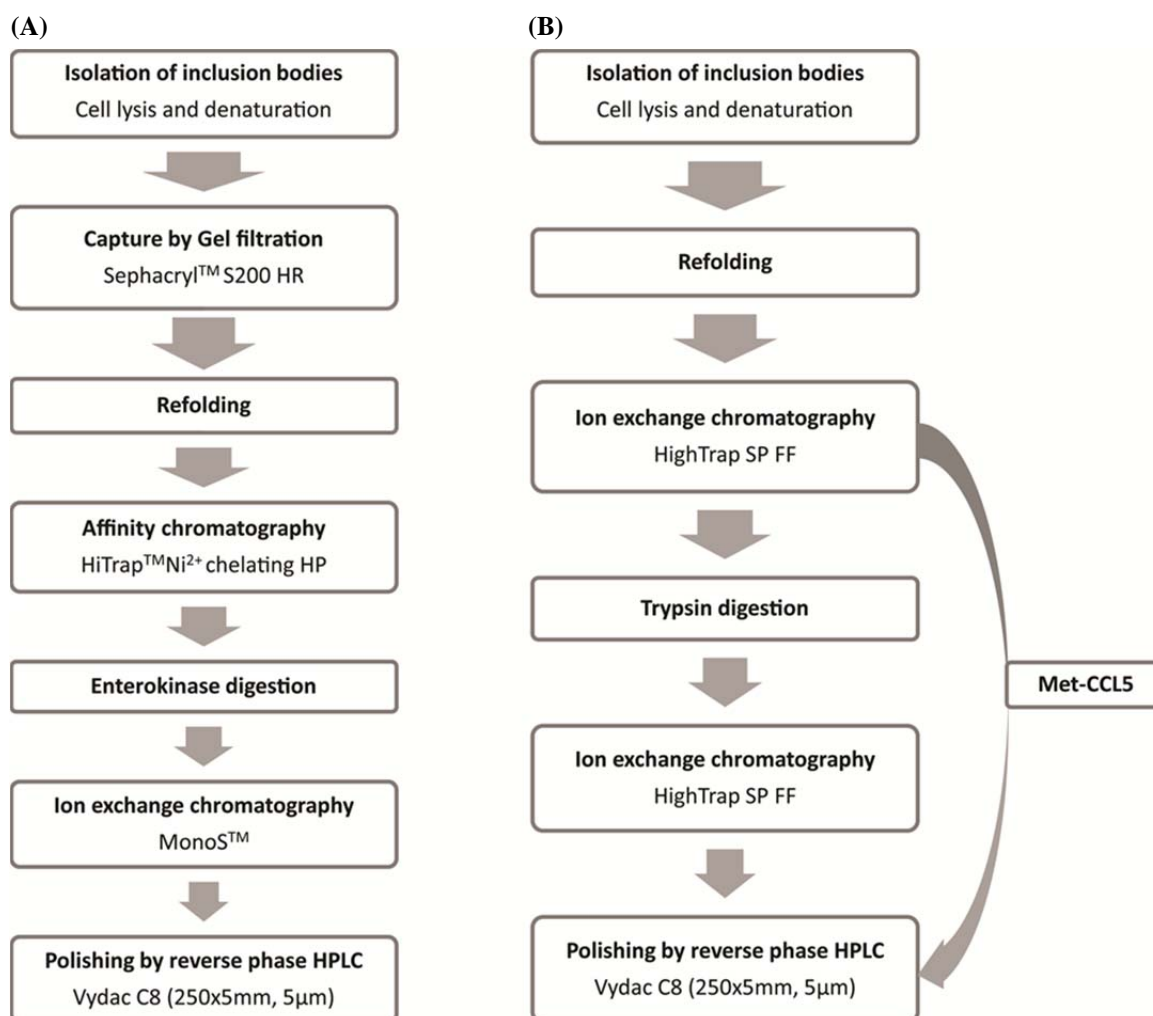


**Fig.III.1.1. Flow chart of CCL5 purification strategies.**

(A) procedure using gel-filtration, affinity chromatography and ion exchange chromatography for CCL5 purification (B) procedure using exclusively ion exchange chromatography to purify CCL5, Met-CCL5, CCL5\_40S and CCL5\_E66A.

In this section the results for the expression and purification of CCL5 along with the three others (Met-CCL5, CCL5-40s and CCL5-E66A) will be displayed and described. Since results obtained here (e.g. chromatograms) are similar, representative images for each step are shown.

To characterize the CXCL4 and CCL5 interaction and to develop a 3-dimensional model by NMR (nuclear magnetic resonance) spectroscopy, CCL5 had to be labeled with the stable isotope <sup>15</sup>N, which considerably increases the resolution and sensitivity of the NMR spectra, hence the cells were grown in <sup>15</sup>N-enriched media. For the use in functional assays, like chemotaxis, parallel flow chamber assay or application into mice CCL5 and the variants Met-CCL5, CCL5-40s and CCL5-E66A were cultivated in normal



LB medium. In many cases and several *E. coli* host systems, recombinant expressed proteins accumulate intracellularly in insoluble aggregates, the so-called inclusion bodies, which are the “starting material” for both purification strategies. In inclusion bodies the proteins are mostly inactive and denatured and in addition dimers or multimers may be present. Beside the resultant necessity to first solubilize and secondly to refold the protein *in vitro* to gain the biological active form, the expression in inclusion bodies can be advantageous: the recombinant protein can make up to 50% or even more of the total cellular protein and the inclusion bodies often contain almost exclusively the overexpressed protein. Furthermore, inclusion bodies protect the protein from proteolytic degradation. Different fusion tags can be used to facilitate the protein purification, N<sup>15</sup> labeled CCL5 was expressed fused to a thioredoxin leader, from a pET-32a(+), which is supposed to increase the amount of soluble active protein accumulating in cytoplasm [170]. This, however, can only be achieved when the expression rate is limited and when using host strains that are permissive for the formation of disulfide bonds in the cytoplasm. Otherwise, like it is the case here, the overexpressed target protein will accumulate in inclusion bodies. The other constructs, based on pET-26b(+) or pET-24a(+), for the expression of CCL5, Met-CCL5, CCL5-40s and CCL5\_E66A are all N-terminal fused to a small hexapeptide leader sequence MKKKWPR, which provide a cleavable basic leader and reduces mRNA secondary structure, improving the expression and facilitating purification. Two slightly different purification protocols have been used, the first one (see flow scheme III.1.1) uses in a first step gel-filtration as an initial purification step (A), to capture the inclusion bodies. The protocol depicted under II.5.1 (B) directly processed the denatured proteins to ion exchange chromatography, the beneficial feature of this protocol is a reduced expenditure of time. The inclusion bodies were purified from the bacterial lysate as described in section II.6.2 for protocol (A). Also for the second protocol (B) the inclusion bodies were purified (III.1.1.) but compared to the first protocol more intensively since the first capture step, where crude impurities are removed, is omitted.

### III.1.1. EXPRESSION AND PURIFICATION OF RECOMBINANT CCL5, PROTOCOL A

Following protocol A, pre-cleaned inclusion bodies were denatured in 50 mM Tris pH 8 containing 6 M guanidine-HCl and 1 mM DTT, the resulting solution was applied in 4-5 sequential steps onto the gel filtration column Sephacryl 200 HR (II.6.2) using a flow rate of 1 mL/min and 2.5 mL fractions were collected (Fig.III.1.2). The first opalescent fractions were discarded, all following fractions were pooled and subsequently processed to the refolding. Therefore the pre-cleaned proteins were at first 6-fold diluted in 50 mM Tris pH 8 buffer supplemented with the redox additives cysteine (1 mM) and cystine (8 mM), the refolding reaction was run over night at 4°C gently stirring.

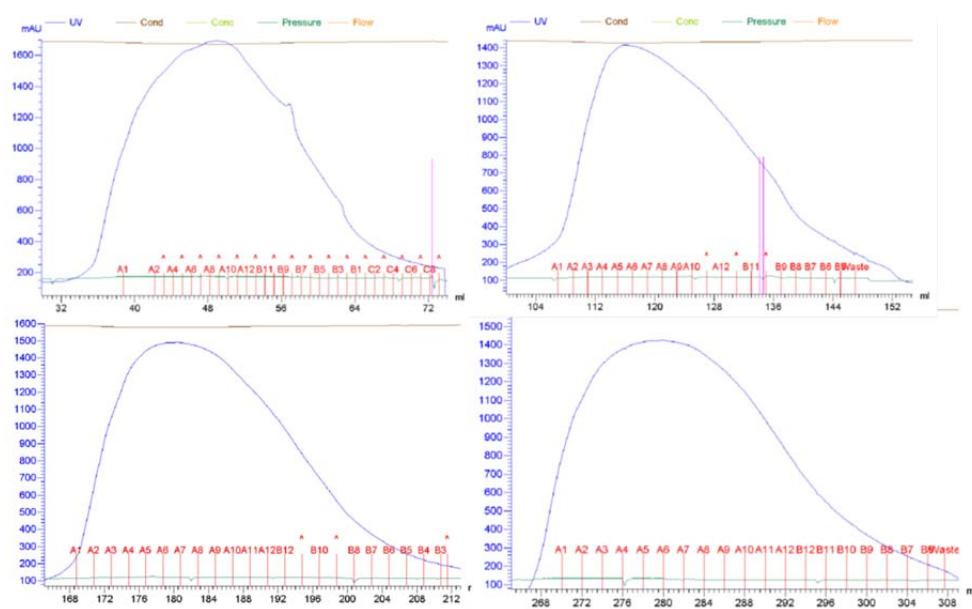


**Fig.III.1.1:** Gel filtration chromatogram of  $^{15}\text{N}$ -CCL5 using a Sephacryl S-200HR column.

The CCL5 fusion protein or Met-CCL5 was loaded in several successively steps with 6 M Guanidine-HCl; 50 mM Tris; pH 8; 1 mM DTT onto the column. 5 mL fractions were collected and processed to the next purification step.

The next purification step is based on the ability of the thioredoxin tag to bind  $\text{Ni}^{2+}$  ions, an immobilized metal affinity chromatography (IMAC) chromatography employing HiTrap  $\text{Ni}^{2+}$  chelating column (Fig. III.1.3), was used here. The refolded fusion protein was again loaded in sequential steps of 2 ml onto the column and eluted with 250 mM imidazole (II.6.2). All protein containing fractions were pooled and dialyzed against 20 mM Tris pH 8 overnight at 4°C.

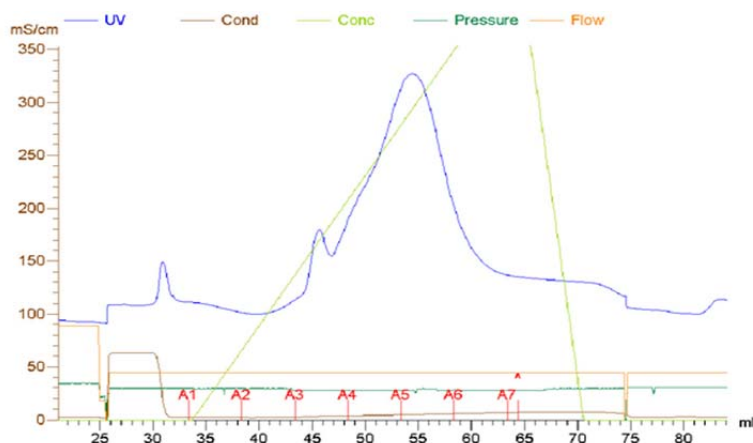


**Fig.III.1.2: Affinity chromatography of the thioredoxin-CCL5 fusion protein using the HiTrap Ni<sup>2+</sup> chelating column.**

As binding buffer 20 mM Tris pH 8; 2 M Urea was used. Bound proteins were eluted with the same buffer supplemented with 250 mM imidazole at 1mL/min. 2 mL fractions were collected and used for further purification.

To prepare the obtained fusion protein for cleavage of the thioredoxin tag, at first the buffer was exchanged by dialysis and then the volume of the solution was decreased using a Macrosep<sup>®</sup> concentration tube. Subsequently the thioredoxin tag was removed by digestion with enterokinase (1 U/ 50  $\mu$ g CCL5) for 16 hours at room temperature. The thioredoxin free <sup>15</sup>N-CCL5 forms an insoluble hetero-aggregate with the <sup>15</sup>N-CCL5-thioredoxin fusionprotein, these aggregates were pelleted for 30 min at 25,000 g and redissolved in a buffer containing 8 M Urea and 20 mM Tris pH 7.5. The remaining thioredoxin CCL5 fusion protein was separated from the cleaved CCL5 employing ion exchange chromatography, using a MonoS<sup>™</sup> column (II.6.2). To prevent aggregation and to facilitate the binding of the cleaved CCL5 to the column resin, the pH was set to 5.5. Meanwhile the column was equilibrated with a buffer composed of 50 mM sodium acetate (pH 5.5) containing 6 M urea. The bound protein was eluted with a linear 0-1 M NaCl gradient (Fig.III.1.3.-A). The fraction containing the cleaved CCL5 were pooled and dialyzed against acetic acid and 0.1% TFA for the final polishing. In case the cleavage was not sufficient, like shown in the chromatogram on the right (Fig.III.1.3.-B), all fractions in the peak area were collected, again dialysed against 20 mM Tris pH 8 overnight at 4°C, concentrated and again digested with enterokinase (*vide supra*).

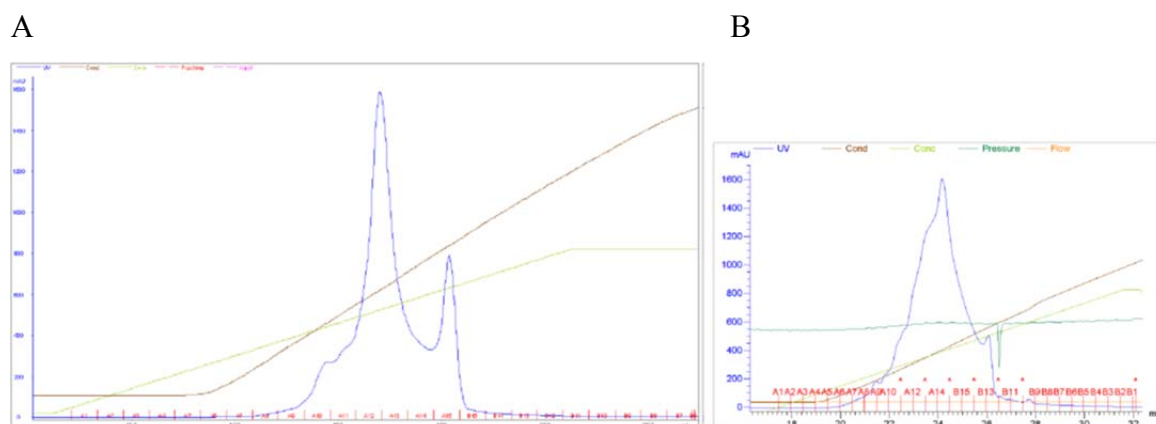


**Fig.III.1.3: FPLC chromatogram using the Mono S™.** To separate the thioredoxin-CCL5 fusion protein, first peak (fraction A10-A13), from the cleaved CCL5 second peak (fraction A14+A15) an ion exchange chromatography was performed, using a Mono S™ column with 50 mM NaAc; pH 5.5, 6 M Urea as binding buffer. CCL5 was eluted through increased ion concentration, by adding NaCl to the binding buffer. The chromatogram on the left site depicts a “good” enterokinase digestion, in contrast to the digestion in the right chromatogram, which was less efficient, only the second peak (B15) contains pure CCL5.

Followed by the final polishing by the reverse phase HPLC, which is able to separate proteins with a very high resolution and therefore capable to remove incorrectly folded proteins or other impurities, like LPS. Since this step is the same for both purification protocols, it is only described once at the end of this section.

### III.1.2. EXPRESSION AND PURIFICATION OF RECOMBINANT CCL5 AND CCL5 VARIANTS, PROTOCOL B

The second protocol (B) is shorter compared to the first protocol but achieved equal yields. The first capture step, as already mentioned, was excluded, therefore the purity of the inclusion bodies was even more important for a satisfactory further purification. Met-CCL5, CCL5, CCL5-40s and CCL5-E66A were all expressed in inclusion bodies. To be able to proceed with the inclusion bodies directly to the ion exchange chromatography intensive washing is required to remove the crude impurities. Then the inclusion bodies were dissolved in 50 mM Tris pH 8 and solubilized by the addition of 6 M Gnd-HCl and 1 mM DTT followed by dialysis against 1% acetic acid overnight at 4°C. Contaminants, like proteins (e.g. proteases) that adsorbed onto the hydrophobic inclusion bodies were precipitated during dialysis. The precipitated contaminants were then separated by centrifugation. To prepare the inclusion bodies for the ion exchange chromatography the supernatant was at first lyophilized then dissolved and at once denaturated in 6 M Gnd-HCl and 1 mM DTT. For renaturation, the protein containing mixture was diluted 10x in 50 mM Tris pH8 supplemented with the redox additives 0.01 mM oxidized glutathion and

## Results

0.1 mM reduced glutathion following stirring o.n. at 4°C. After centrifugation, adjustment of the conductivity to less than 20 mS and to a pH lower than 5 the protein solution was loaded onto the HiTrap SP FF column. CCL5 and the CCL5 variants were eluted by a linear 2 M NaCl gradient from 0-100%, fractions of 1 ml were collected and controlled by dot blot (Fig.III.1.4.).

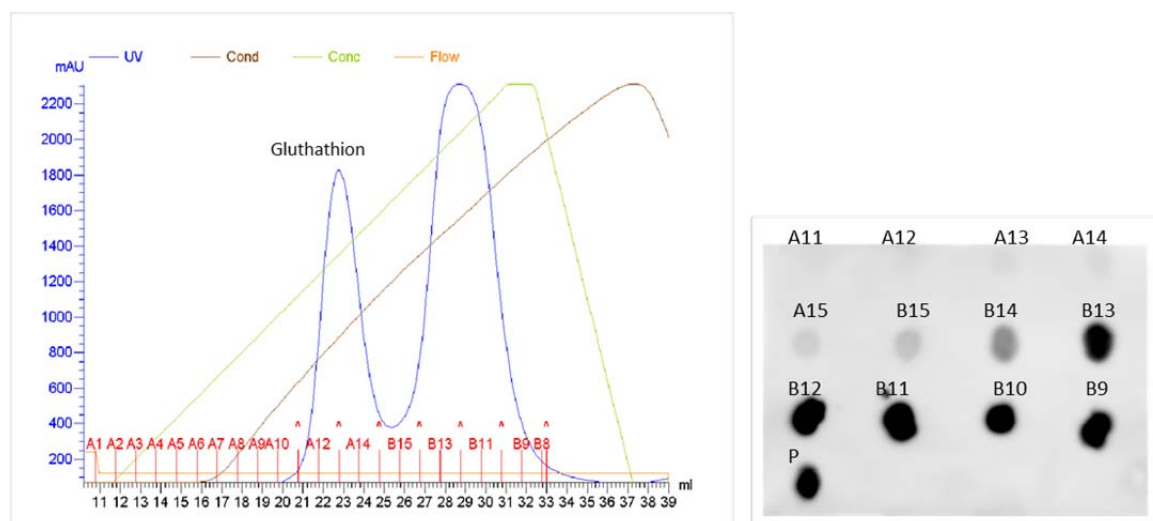


**Fig.III.1.4. Ion exchange chromatography using a HiTrap SP FF column.**

CCL5 and its variants were bound to the column with 50 mM NaAc pH 5.5 and eluted by the addition of 2M NaCl. The positive fractions (B13-B9), as determined by dot blot (II.5.6), were combined for further purification, cleavage of the MKKKWPR leader of CCL5, CCL5-40s and CCL5-E66A and Met-CCL5 polishing by HPLC. The first peak contains mainly glutathion.

Met-CCL5 was now directly processed to the polishing step employing the HPLC. CCL5, CCL5-40s and CCL5-E66A need to be liberated from the MKKKWPR leader. The positive fractions were pooled, extensively dialysed and lyophilized. Afterwards the protein was dissolved again in 50 mM Tris-HCl (pH8), with a concentration set to 1mg/ml. The MKKKWPR leader was cleaved by the addition of trypsin. Since CCL5 contains more than one trypsin cleavage site it is very important to stop the digestion after 3h of incubation at 37°C by the addition of protease inhibitors. The mixture was then prepared as described before (first ion exchange chromatography) and loaded onto the column with a buffer containing 50 mM NaAc pH 5.5 and 6 M Urea. The CCL5 proteins were eluted using a linear NaCl gradient, 1 mL fractions were collected. The collected fractions were controlled by dot blot or as shown here by coomassie blue staining following SDS-PAGE (Fig.III.1.5).

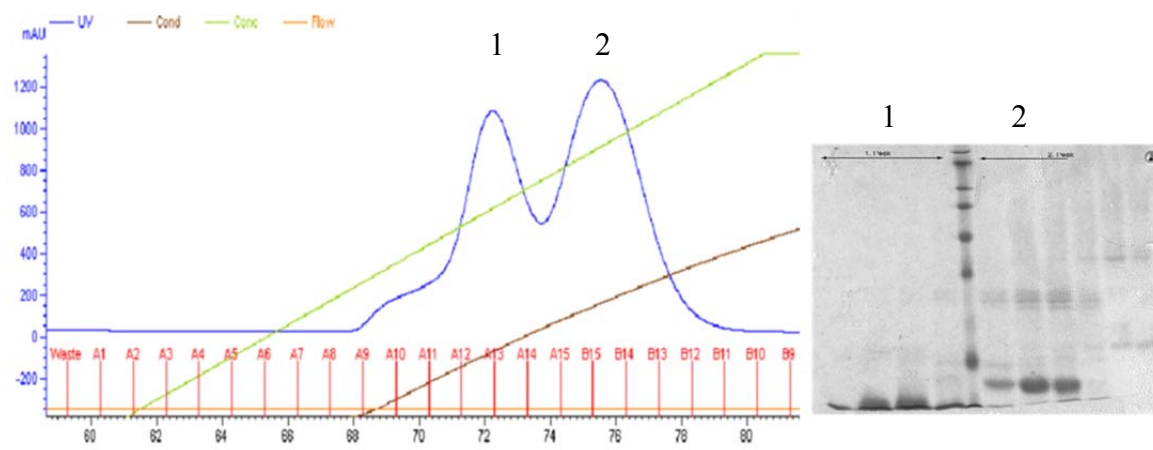


**Fig.III.1.5. Ion exchange chromatography to separate the MKKKWPR leader free CCL5.**

To separate the pure CCL5 from the cleaved leader the reaction mixture was bound to the HiTrap SP FF column in the presence of 50 mM NaAc (pH 5.5) and 6 M Urea. The eluted fractions were collected and controlled by SDS-Page followed by coomassie blue staining. The second peak (A15-B14) contains protein with the appropriate size (8kDa). The positive fractions were collected and prepared for the final polishing step.

The final polishing by reverse phase HPLC is the step with the highest resolution, capable to remove incorrectly folded proteins or other impurities, like LPS. This is in particular important when the purified protein is used in an animal model, because LPS contaminations can trigger an undesirable immune response. After buffer exchange by dialysis against 0.1% TFA, the protein solution was loaded on the column with 1 mL/ min flow rate and recovered with the organic solvent acetonitril (90%) in 0.1% TFA using a 0-67% gradient (II.6.2.- 6.3.)

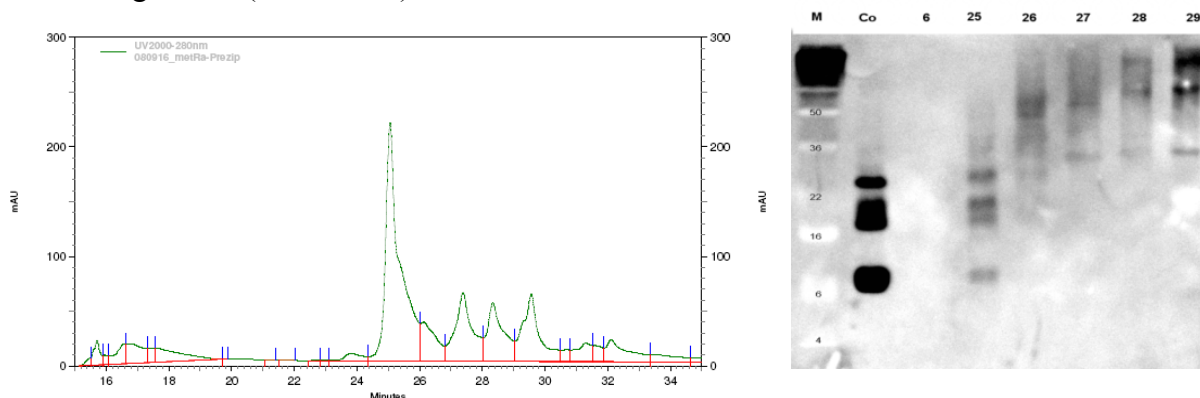


**Fig.III.1.6. Reverse phase chromatography applying the high performance liquid chromatography (HPLC) using a preparative Grace Vydac C-8 column.**

The fractions in the peak area were manually collected and analyzed by western blot following SDS-PAGE. The fraction at a retention time of 25min was first dialyzed to further control purity and functionality.

All peaks obtained from the HPLC run were collected and lyophilized to remove the TFA and acetonitril traces and dissolved in ultra pure H<sub>2</sub>O (Fig.III.1.6.). The purity and correct

## Results

size was further validated by SDS-PAGE followed by silver gel staining and by mass spectrometry (Fig.III.1.7.).

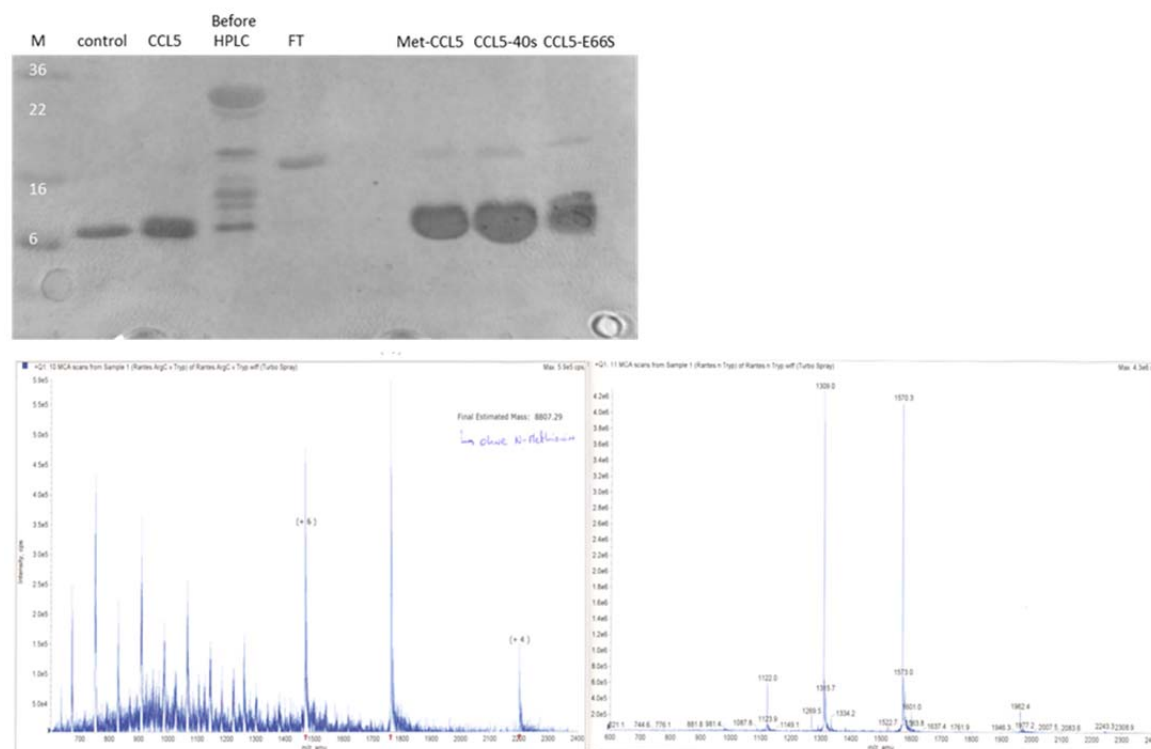


**Fig.III.1.7 Validation of the correct size and purity of Met-CCL5, CCL5 and CCL5-40s and E66A.**

Purity and correct size was controlled by silver gel staining following a SDS-PAGE (II.5.2., II.5.4.). The correct mass was determined by mass spectrometry, electro spray ionization, left panel before Trypsin digestion, right panel after trypsination with an estimated mass of 8807.29.

To absolutely make sure that the purified protein is correctly folded and functional it is indispensable to control the activity, especially important for the use in *in vivo* cell adhesion (II.8.) or *in vitro* recruitment (II.10.1.) or parallel flow chamber assays (II.10.2.). Therefore the chemotactic activity of the purified proteins was measured using freshly isolated PBMCs from human peripheral blood (II.9.7.). Chemotaxis was investigated in Transwell™ migration assays (II.10.1.). For CCL5 different concentrations (50-150 ng/ml) were tested compared to medium control (Fig.III.1.8.-A). For Met-CCL5 the inhibitory effect was determined in comparison to a medium control and to CCL5 or CCL5 together with Met-CCL5 (all 100 ng/ml) (Fig.III.1.8.-B). If not used directly the purified proteins were extensively dialyzed against 1% acetic acid and 0.1% TFA, lyophilized and the protein powder was stored at -20°C or -80°C. The lyophilized CCL5 was always diluted first in water and, if necessary, by the addition of acetic acid to enable the protein to dissolve completely.



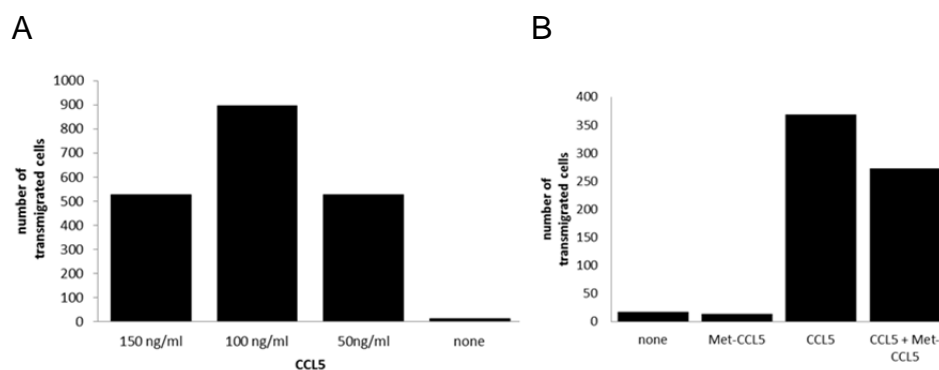


**Fig.III.1.8. Chemotaxis assay to determine the activity of the purified CCL5 and variants.**

PBMCs from human peripheral blood were used in a chemotaxis assay using Costar Transwell™ system (5.0- $\mu$ m pore size) as described in section II.10.1. Cells were counted by FACS with the gate set on the cells of interest.

### III.2. NMR CHEMICAL SHIFT MAPPING OF CCL5-CXCL4 HETERODIMER

Based on the observation that CXCL4 accelerates primordial CCL5-mediated function and since this synergy could be explained by the formation of heterodimers, we wanted to clarify the structural basis of this interaction. The heterodimerization was characterized by the  $^{15}\text{N}$ - $^1\text{H}$  heteronuclear single quantum coherence (HSQC) nuclear magnetic resonance (NMR) technique in the lab of Dr. Kevin Mayo (Department of Biochemistry, University of Minnesota). With this method it is possible to determine chemical shifts of amino acids that are involved in the interaction of CXCL4 with CCL5. Titration of CXCL4 into a uniform  $^{15}\text{N}$ -labeled CCL5 solution caused a chemical-shift change and a decrease in CCL5 monomer signal intensities, coherent with the estimated interaction of CCL5 and CXCL4 (Fig.III.2.1.). The maximal  $^{15}\text{N}$ - $^1\text{H}$  chemical shift changes during heterodimer formation were observed in the N-terminal residues which indicated a CC-type rather than a CXC-type interaction. The latter was further substantiated by only minimal chemical shift changes detected in the residues in the first  $\beta$ -strand of CCL5 known to be involved in the CXC-type dimer formation.



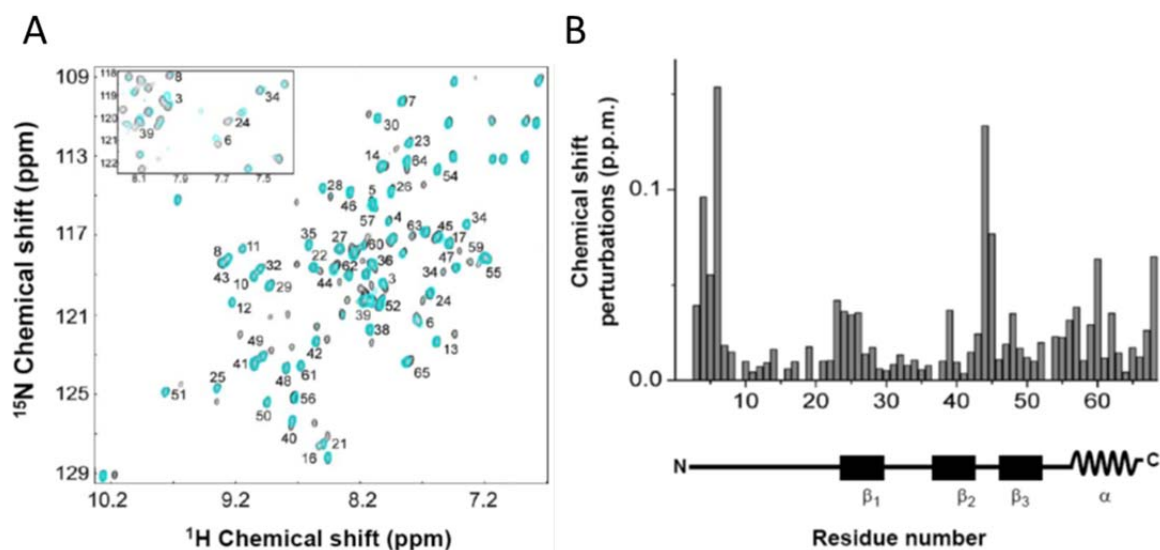


**Fig.III.2.1: Biophysical characterization of CCL5-CXCL4 interaction.** A HSQC spectrum of  $^{15}\text{N}$ -CCL5 in the absence (gray cross-peaks) or presence (blue cross-peaks) of CXCL4 (molar ratio 1:1) with numbers indicating the respective CCL5 aa residues. Inset: Region from the HSQC spectrum of  $^{15}\text{N}$ -CCL5, exemplifying chemical shift changes caused by the addition of CXCL4 at the molar ratio of 1:16 [98]. B. Chemical shift perturbations analysis. Changes in chemical shift of  $^{15}\text{N}$ -CCL5 backbone amides in ppm. caused by the addition of CXCL4 (molar ratio, 1:2). Bottom, schematic representation of the estimated CCL5 secondary structure; black boxes and the wavy line,  $\beta$ -strands and a  $\alpha$ -helix, respectively [98].

The CC-type heterodimerization was confirmed molecular dynamics simulations on docked CC-type and CXC-type CCL5-CXCL4 heterodimers revealed a more thermodynamically favorable CC-type heterodimer conformation, as shown in the Fig.III.2.2 A for the calculated free energies. Based on the molecular dynamics simulation a structure of the CCL5-CXCL4 heteromer could be calculated (Fig.III.2.3 A). The N-terminal residues of CCL5 (3-6 aa) were shown to be in close proximity to the N-terminal residues of CXCL4 (7-10 aa). In the presence of CXCL4 these residues of CCL5 displayed the greatest chemical shift changes, in particular at high concentrations of CXCL4 (Fig.III.2.1 inset). The highly negatively charged residues of the N-terminal domain of CXCL4 were shown to cross the first and second loop of CCL5, characterized by a positive net charge (Fig.III.2.3 A). The chemical shift changes within the first and second loop of CCL5 affect the amino acids 21 to 24 and 44 to 46 (Fig.III.2.2). In line with chemical shift changes observed in residues 60 and 62, the N-terminus of CXCL4 is proximal to the C-terminus helix of CCL5. Differential scanning calorimetry indicated that CCL5-CXCL4 heterodimers are stable at temperatures up to  $65^\circ\text{C}$  (Fig.III.2.3 B).

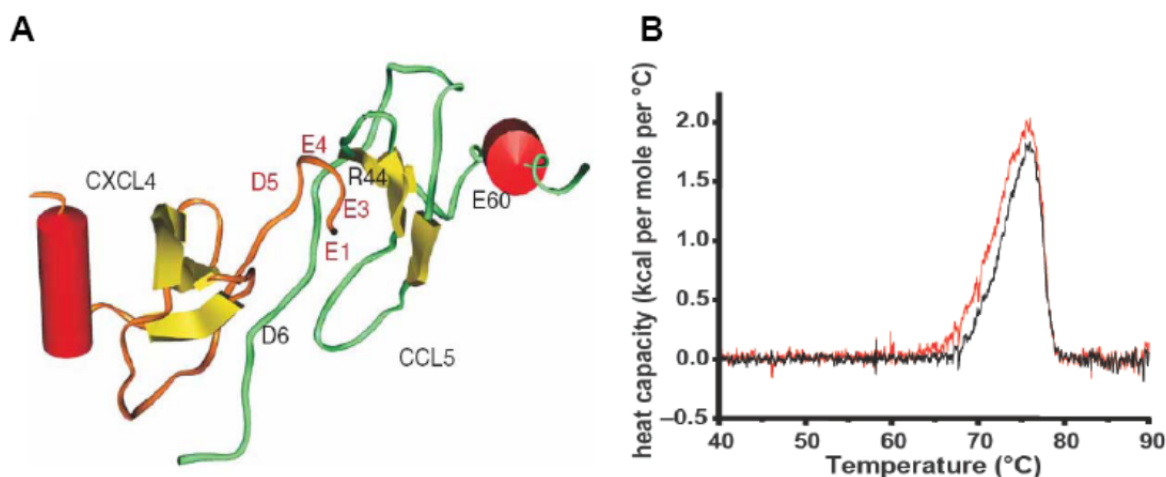
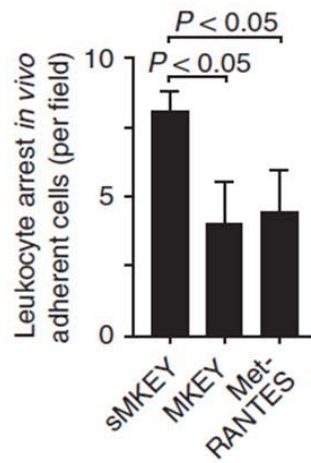


**Fig.III.2.2: Structural model of the CCL5-CXCL4 heterodimer.** (A) The most prominently involved residues are shown in red (CXCL4) and black (CCL5). The negatively charged N-terminus of CXCL4 extends over the net positively charged first and second loops of CCL5. (B) Differential scanning calorimeter analysis of the heteromer. Solvent-normalized heat capacity curves as a function of temperature obtained by heating of CCL5-CXCL4 complex in PBS. Black and red curves represent two separate experiments with calculated melting temperatures of CCL5-CXCL4 of 76 °C [98].

### III.3. FUNCTIONAL ACTIVITY OF MKEY IN COMPARISON TO MET-CCL5

Within the scope of the present study, small peptide antagonists to prevent the CCL5 CXCL4 heterodimer formation have been designed and synthesized. They are termed “CKEY2” and a mouse orthologue “MKEY” and are composed of the aa residues 25–44 found in the 1 and 2  $\beta$ -strands of the native CCL5 and two cysteines at the N- and C-terminus, forming disulfide-bridges to obtain a cyclic structure, generating a  $\beta$ -hairpin-like structure.  $^{15}\text{N}$ - $^1\text{H}$  HSQC chemical-shift mapping revealed that CKEY2 interacts with  $^{15}\text{N}$ -CCL5 in a similar pattern than CXCL4 (data not shown), particularly with the N-terminus of CCL5. Besides the biochemical analysis of the inhibitory potential of CKEY2 on the CCL5-CXCL4 heterodimer formation its pharmacological properties were estimated by intravital microscopy to visualize (II.8.) the recruitment of rhodamine-labeled leukocytes in carotid arteries of high-fat diet-fed hyperlipidemic mice (*Apoe*<sup>-/-</sup>). Compared with scrambled MKEY (sMKEY), pretreatment of mice with MKEY markedly reduced leukocyte arrest on activated endothelium, which is depended on CCL5 receptor ligands, as evidenced by its inhibition with Met-RANTES.



**FigIII.3.1.Disruption of CCL5-CXCL4 reduces leukocyte adhesion to activated endothelium.**

Adhesion of rhodamine-labeled leukocytes to inflamed endothelium in carotid arteries of Apoe<sup>-/-</sup> mice pretreated with sMKEY, MKEY or Met-RANTES (n = 3 each) as assessed by intravital microscopy.

### III.4 ESTABLISHING THE ROLE OF THE EXTRACELLULAR DOMAINS OF CCR1 AND CCR5 IN CCL5 MEDIATED CELL RECRUITMENT

#### III.4.1. DESIGN AND CHARACTERIZATION OF THE CHEMOKINE RECEPTOR CHIMERAS

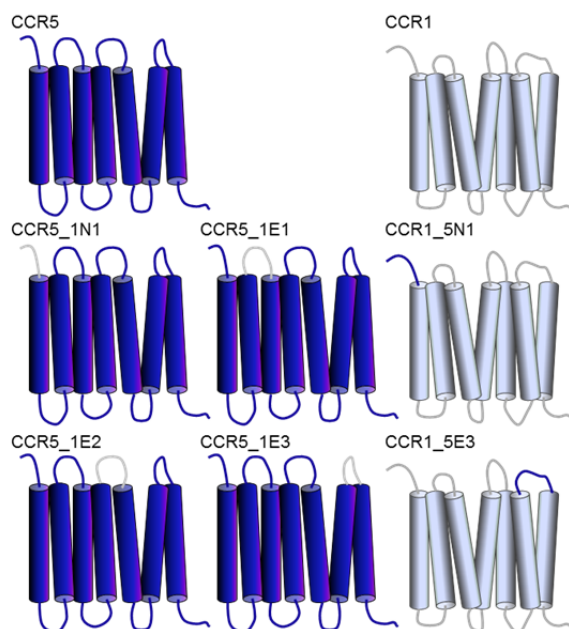


**Fig.III.4.1. Schematic diagram of the different CCR1- CCR5 chimeras.** The CCR5 part of the various chimeras is marked in blue and the CCR1 domains in gray.

Previous reports have revealed a functional specialization of CCR1 and CCR5 in the recruitment of monocytes and T cells, whereby CCR1 was more important in promoting stable arrest on endothelial cells and CCR5 primarily mediated subsequent spreading and transendothelial migration [137, 155]. Yet, the three-dimensional structure of a natural chemokine binding to its receptor has not been solved but it is believed that the extracellular loops predominantly interact with larger ligands such as chemokines or heteromers as opposed to small molecule antagonists that bind deep in the ligand pocket located between the extracellular parts of the transmembrane domains [51, 163]. In contrast to the highly conserved transmembrane regions of CCR1 and CCR5, sequence analysis demonstrates that the extracellular regions are remarkably heterogeneous. In order to identify the role of these extracellular regions for leukocyte arrest and migration, we generated chimeric constructs by exchanging the respective extracellular loops of CCR1 and CCR5. These constructs were stably expressed in *HEK-293* and *LI.2* cells as described in section II.9.6. and clones with similar surface levels, as determined by flow cytometry (Fig.III.4.2.), were selected for transmigration and flow perfusion assays using CCL5, its mutants and/or CXCL4 as stimuli.

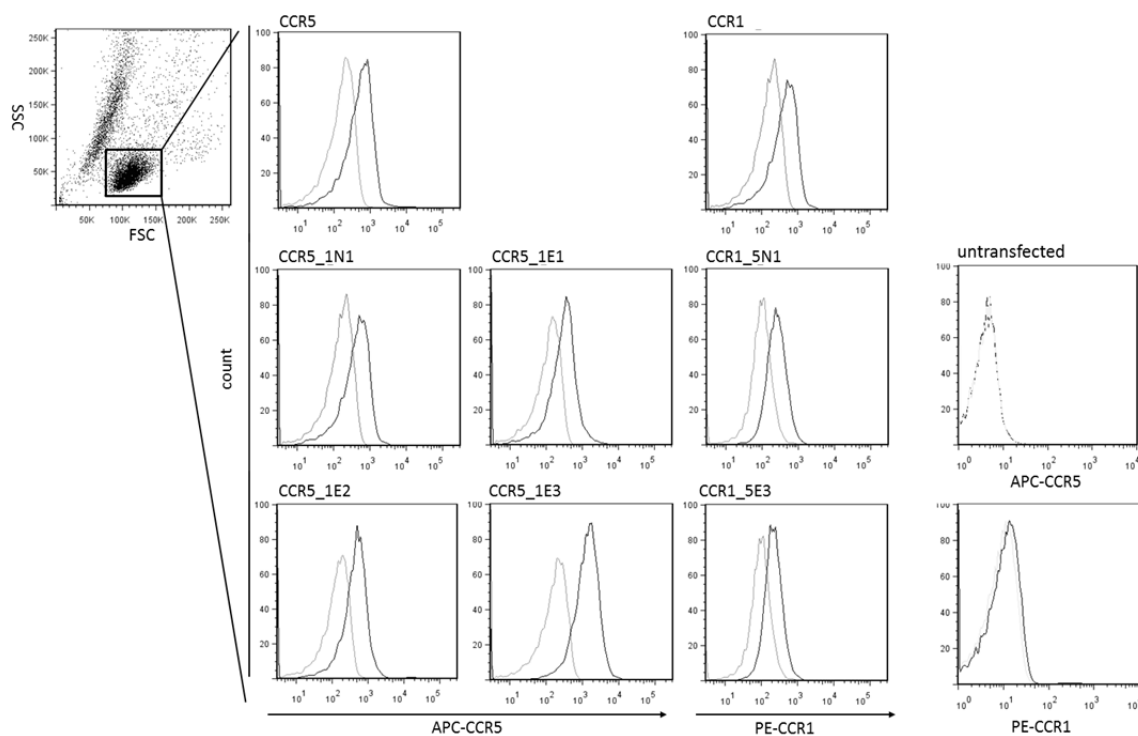


**Fig.III.4.2. Expression of CCR5, CCR1 and the related mutants on L1.2 pre-B lymphoma cells was analyzed by flow cytometry.** The black lines represent the specific mAb against CCR1 or CCR5 and the gray lines illustrate the isotype control.

CCL5 is known as a strong chemoattractant. Thus, to estimate the functionality of the CCR5, CCR1 and receptor chimera transfected cells, a Transwell<sup>TM</sup> chemotaxis assay was performed. CCR5-transfected cells robustly migrated towards wild-type CCL5 and (albeit less pronounced) to CCL5\_40s and CCL5\_50s, whereas CCR1-transfected cells migrated less efficiently towards CCL5 or its variants, which may be in line with previous data indicating a dominant role during cell arrest but a less important function during transmigration [155] (Fig.III.4.3.). All transfectants expressing chimeric CCR1/CCR5 receptors (Fig.III.4.3.C-F) transmigrated towards CCL5 to a similar extent as CCR5 transfectants, indicating that more than one extracellular loop has to be engaged in CCR5 activation. None of the transfectants responded fully to the 40s mutant (Fig.III.4.3. A-F). In contrast to the other chimeras, the chimeric CCR5 receptor carrying the CCR1-N-terminus (Fig.III.4.3.C) conferred comparable migration towards CCL5\_50s as wild-type CCR5 (Fig.III.4.3.B).

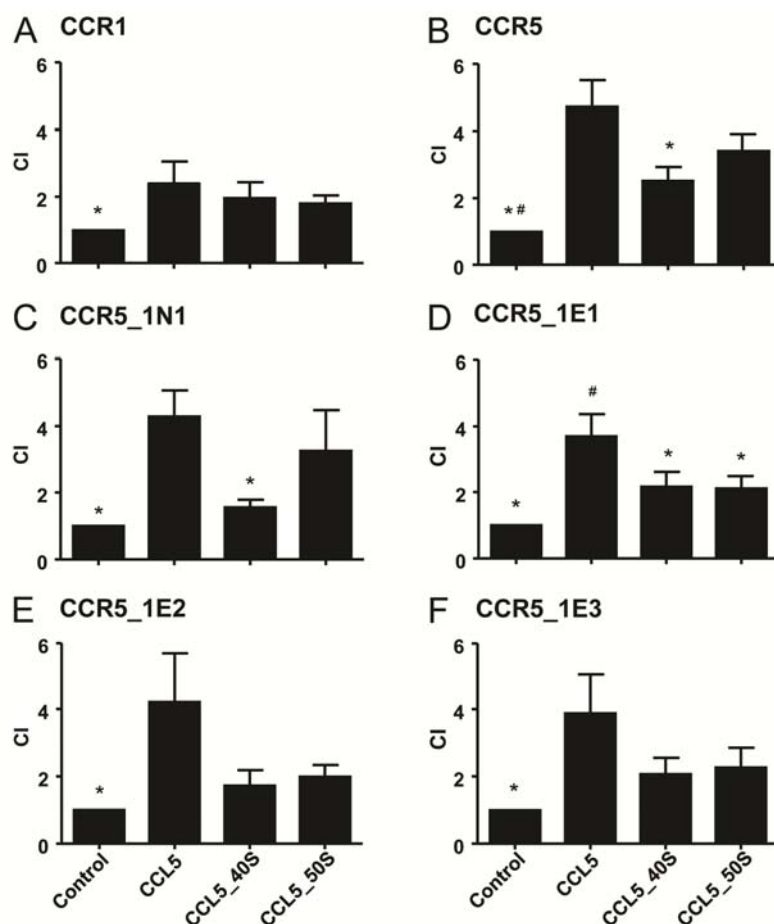


**Fig.III.4.3. Chemotaxis of receptor-transfectants towards CCL5 variants.**

Migratory response of *HEK293* cells transfected with CCR1 (A), CCR5 (B), CCR5\_1N1 (C), and CCR5\_1E1–3 (D, E) towards CCL5, CCL5\_50s, CCL5\_40s (each 100ng/ml) or negative control expressed as chemotactic index (CI = ratio to the control).

### III.4.2. FUNCTIONAL ROLE OF THE EXTRACELLULAR DOMAINS IN CCL5-INDUCED ARREST UNDER FLOW

To assess the differential roles of CCR1 and CCR5 in mediating stable leukocyte arrest induced by CCL5, we perfused L1.2 transfectants over TNF $\alpha$ -activated SVEC (simian virus-40 transformed endothelial cells). In response to wild-type CCL5, all receptor variants showed a comparable capacity to induce arrest (Fig.III.4.4. A-G). None of the transfectants responded to CCL5\_40s (Fig.III.4.4. A-G). It is conceivable that CCR1 transfectants could not be brought to arrest by CCL5\_40s, which lacks affinity for CCR1. The inability to induce significant arrest of CCR5 transfectants can be partially explained by the approximately 3-fold lower affinity of CCL5\_40s to CCR5 as compared to wild-type CCL5 [39] and because the 40s cluster supports GAG-dependent oligomerization [175].

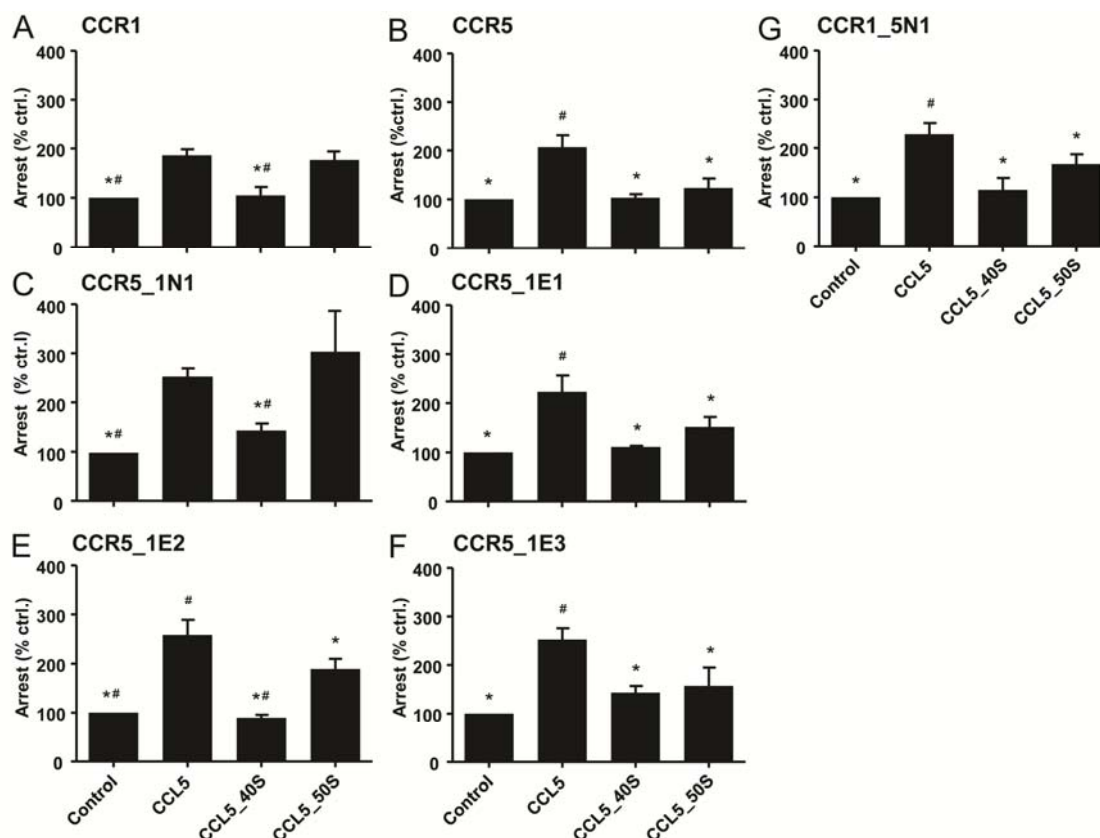


**Fig.III.4.4. Arrest of receptor-transfectants induced by CCL5 variants.**

Arrest of pre-B *LL1.2* cells transfected with CCR1 (A), CCR5 (B), CCR5-1N1 (C), CCR5-1E1–3 (D, E) and CCR1-5N1 (G) onto TNF $\alpha$ -activated SVEC cells under flow conditions in the absence or presence of CCL5, CCL5\_50s or CCL5\_40s (500 ng/ml).

The mutant CCL5\_50s, which has loss-of-function in a coordinative site for CCL5 surface presentation, behaved differently, as the CCR1 transfectants responded equally potent to CCL5\_50s and wild-type CCL5. This is in contrast to the CCR5, CCR5\_1E1, CCR5\_1E2 and CCR5\_1E3 transfectants, which only responded to wild-type CCL5 but not to CCL5\_50s (Fig.III.4.4. A-F). Interestingly, this effect could be reversed in transfectants expressing CCR5 containing the N-terminus of CCR1, which exhibited arrest comparable to CCR1, when stimulated with the CCL5\_50s variant (Fig.III.4.4. A, C). Thus, it could be reasoned that the basic amino acid residues in the 50s cluster are not important for the functionality of CCR1 in mediating cell arrest. This was in contrast to CCR5, which was only responsive to CCL5 with an intact 50s cluster. This was further confirmed by reverse transfer of the N-terminal region of CCR5 to CCR1, which resulted in a poorly responding variant that did not mediate cell arrest induced by CCL5\_50s under flow conditions (Fig.III.4.4. G). These results indicate that the 50s domain of CCL5 is not only involved in GAG binding and cell surface presentation but might also be involved in direct interactions with CCR5.

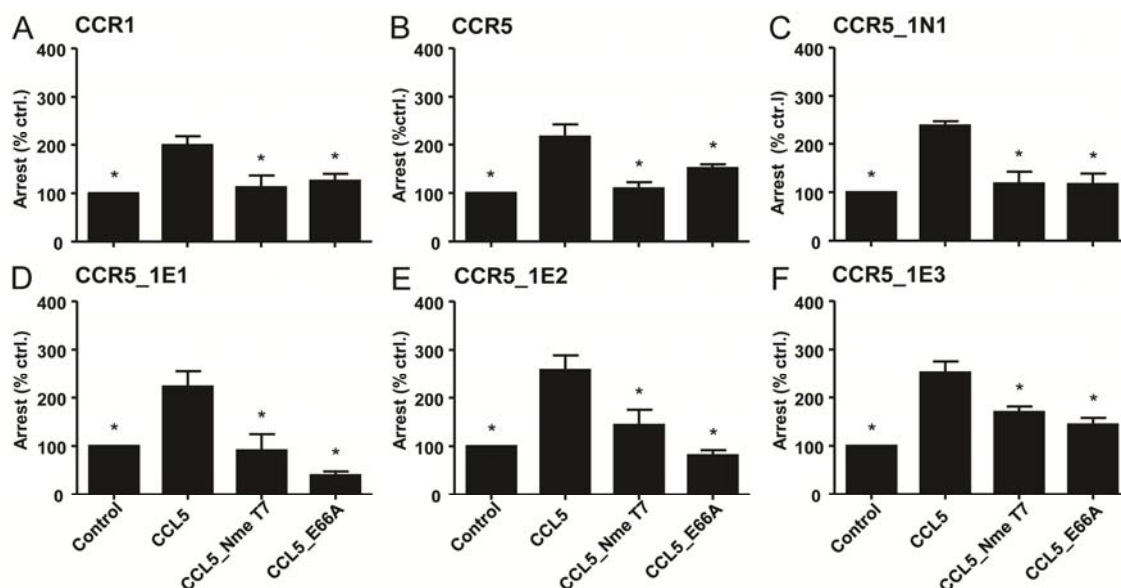


**Fig.III.4.5. Chemokine-induced arrest of chimeric receptor-transfected cells onto activated endothelial cells under flow conditions.** Arrest of pre-B *LI.2* cells transfected with CCR1 (A), CCR5 (B), CCR5-1N1 (C), CCR5-1E1-3 (D - F) onto TNF $\alpha$ -activated SVEC cells under flow conditions in the absence or presence of CCL5, CCL5\_NmeT7 or CCL5\_E66A (500ng/ml).

In addition, the oligomerization-deficient variants CCL5\_NmeT7 and CCL5\_E66A were inactive in promoting stable arrest under flow conditions. This highlights the important role of CCL5 oligomerization for efficient stimulation of leukocyte arrest on inflamed endothelium [137] and also demonstrates that oligomerization of CCL5 is a requirement of cell arrest in general, independent of its activation of CCR1 or CCR5 (Fig.III.4.5 A-F).

### III.4.3. CCR1 EXTRACELLULAR DOMAIN 3 IS INVOLVED IN ENHANCED ARREST INDUCED BY CCL5 AND CXCL4

Monocyte arrest induced by CCL5 is synergistically enhanced by CXCL4-CCL5 heterodimer formation, a mechanism that plays an important role in the development of atherosclerosis [18, 98] and acute lung injury [176]. To investigate a possible specialization of CCR1 and CCR5 in the synergistic action of CCL5 and CXCL4 and to identify the domain(s) involved, stable arrest was stimulated by CCL5 in the presence or absence of CXCL4.



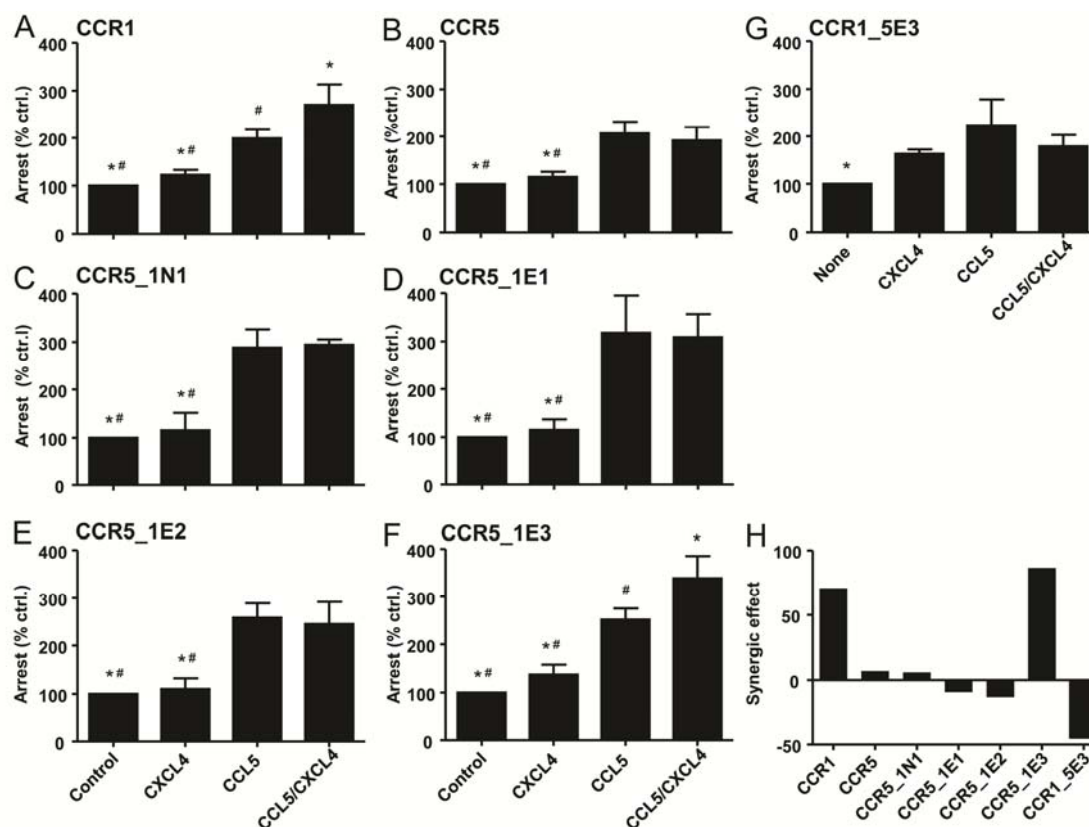


**Fig.III.4.6. Arrest of receptor-transfectants induced by CCL5/CXCL4.**

Arrest of pre-B *L1.2* cells transfected with CCR1 (A), CCR5 (B), CCR5-1N1 (C), CCR5-1E1-3 (D) and CCR1-5N1 (G) onto TNF $\alpha$ -activated SVEC cells under flow conditions in the absence or presence of CCL5, CXCL4 or CCL5 and CXCL4 (500ng/ml). (H) Synergistic effect of CCL5 and CXCL4 in the indicated transfectants.

All transfectants responded to stimulation with CCL5, whereas stimulation with CXCL4 alone did not result in significant arrest (Fig.III.4.6. A-G). Notably, the CCL5-induced arrest of CCR1-transfected *L1.2* cells was significantly enhanced by the presence of CXCL4 permissive to heteromer formation (Fig.III.4.6. A), whereas adhesion of CCR5-transfected *L1.2* cells was induced by CCL5 but not further increased by CXCL4 (Fig.III.4.6. B). Exchange of the N-terminus or the first or second extracellular loop in CCR5 for that of CCR1 did not confer a synergistic cell-recruiting activity (Fig.III.4.6. C-E). However, transposing the third extracellular loop of CCR1 into CCR5 resulted in a chimeric variant (CCR5\_1E3) that mimicked the response of CCR1 towards synergistic stimulation with CCL5 and CXCL4 (Fig.III.4.6. F, H). To verify a possible involvement of the third extracellular domain of CCR1 in the synergistic activity of CCL5 and CXCL4, the corresponding domain of CCR5 was transferred to CCR1. This particular chimeric CCR5 variant (CCR1\_5E3) did not mediate a specific enhancement of CCL5-induced cell arrest by CXCL4 and but rather appeared to result in a loss of activity (Fig.III.4.6. G, H).

### III.4.4. ROLE OF EXTRACELLULAR DOMAINS IN CCR1 AND CCR5 HETERODIMERIZATION

Monocytes and T cells have been shown to express both functional CCR1 and CCR5 [155]. Moreover, chemokine receptors were shown to heteromerize modulating their functional activity in various studies [177]. Thus, we hypothesized that in addition to the effects observed with single transfectants, CCR1-CCR5 dimerization, and especially the third extracellular loop of CCR1, might play a role in the synergistic activity of CCL5 and CXCL4. To demonstrate a physical interaction between CCR1 and CCR5, we performed co-immunoprecipitations (co-IP) of HEK293 cells double-transfected with wild type receptors and the chimeric variants (CCR1\_5E3 and CCR5\_1E3), cytoplasmatically Myc- (CCR1 and CCR1\_5E3) or HA-tagged (CCR5 and CCR5\_1E3) receptors.

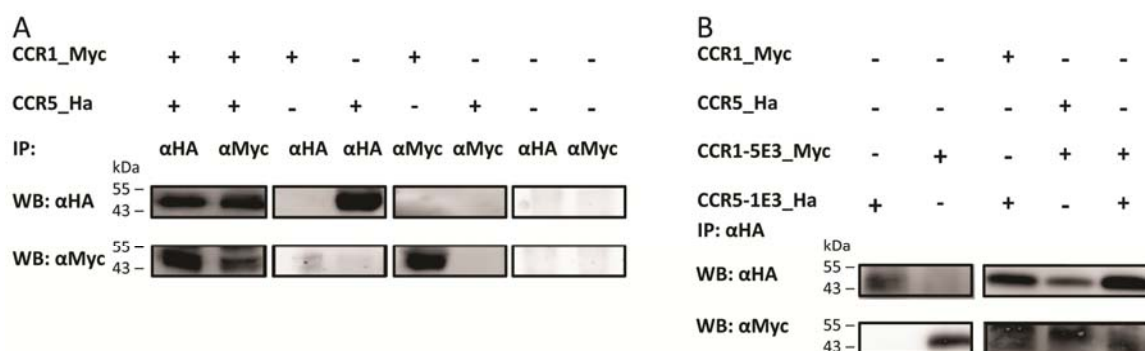


**Fig.III.4.7. CCR1 and CCR5 heterodimer formation.**

Co-immunoprecipitation (co-IP) of CCR1 with CCR5. Myc-tagged CCR1 was co-transfected with HA-tagged CCR5 into HEK293 cells. The lysate was subjected to co-IP with anti-HA or anti-Myc antibody and probed with anti-Myc antibody and anti-HA antibody. As a control, the same number of single transfected cells with either CCR5\_Myc or CCR1\_HA and untransfected HEK293 cells were treated in the exact same manner. (B) The chimeric receptors Myc-tagged CCR1\_5E3 and Ha-tagged CCR5\_1E3, single and double transfected or co-transfected with a wild-type receptor were subjected to co-IP with the anti-HA antibody and probed with antibodies against both tags.

Pull-down of CCR1\_Myc with an anti-Myc antibody resulted in the co-precipitation of CCR5\_HA, as detected by an anti-HA antibody and accordingly pull-down of CCR5\_HA resulted in co-precipitation of CCR1\_Myc (Fig.III.4.7. A). Co-expression and subsequent co-IP of CCR1-Myc with CCR5\_1E3-HA and of CCR5-HA with CCR1\_5E3-Myc still resulted in heterodimer formation, indicating that the third extracellular loop does not affect heterodimer formation (Fig.III.4.7. B). To investigate whether CCR1 and CCR5 are co-localized on the surface of cells, we co-expressed CCR1\_Myc and CCR5\_HA in HEK293 transfectants, which were subsequently visualized by two photon microscopy

(Fig.III.4.8. C-E). When expressed separately, the CCR1\_Myc and CCR5\_HA receptors appeared to be dispersed over the surface of the cells (Fig.III.4.8. E). When co-expressed, however, both receptors were clearly co-localized on the cell surface of HEK293 transfectants (Fig.III.4.8. C, D).

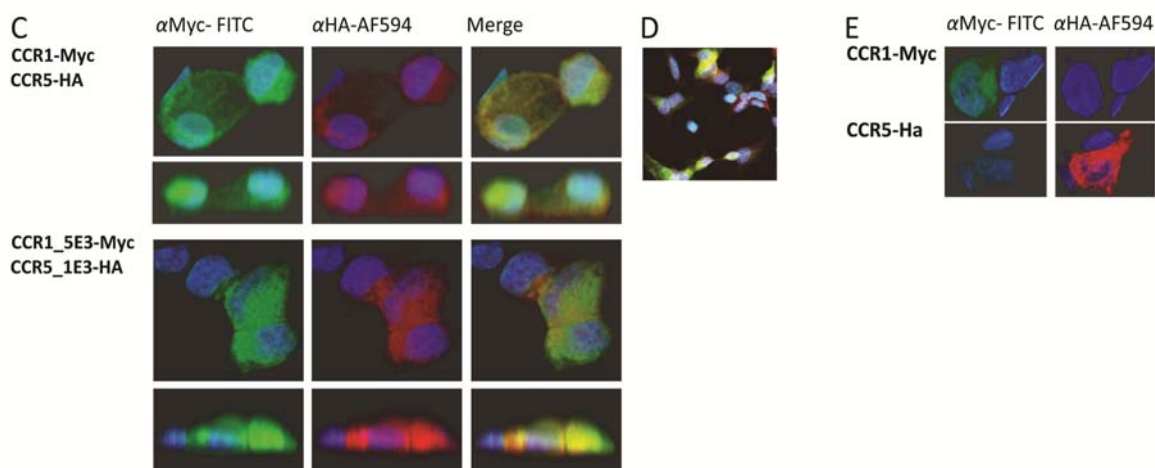


**Fig III.4.8. CCR1 and CCR5 co-localization**

The cellular distribution of the two chemokine receptors was analyzed by immunofluorescence. HEK293 cells transfected with either wild-type or chimeric receptors were stained against HA and Myc and visualized using two photon microscopy. The upper panel shows a 3D reconstruction (xy-view) of transfectants displaying co-localization of the wild-type receptors CCR1 (green) and CCR5 (red), and a transversal reconstruction of the same cells (yz-view, approximate cell volume  $1.7 \times 10^4 \mu\text{m}^3$ ). The lower panel shows that CCR1\_5E3 (green) and CCR5\_1E3 (red) expressed in HEK293 cells also co-localize (xy-view and corresponding transversal yz-view, approximate cell volume  $2.2 \times 10^4 \mu\text{m}^3$ ). (D) Representative section of double-transfected cells. (E) Control cells transfected with either CCR1\_Myc (green) or CCR5\_HA (red) alone were also subjected to immunofluorescence (approximate cell volume  $1.2 \times 10^4 \mu\text{m}^3$ ).

### III.4.5. MONOCYtic CCR1 IS REQUIRED TO MEDIATE CCL5-CXCL4-INDUCED ARREST

Synergistic arrest induced by CCL5 and enhanced by CXCL4, may be mediated by several mechanisms including the activation of chemokine receptor hetero(di)mers resulting in a switch from  $G_{\alpha i}$  to  $G_{\alpha q}$  signaling [62]. Since the arrest experiments described above permitted only the investigation of single receptor types, we used the monocytic THP-1 cell line expressing CCR1, CCR5 and CCR3 at levels comparable to primary monocytes [178] to study arrest under flow conditions on human aortic endothelial cells. The THP-1 cells were incubated with antagonists against  $G_{\alpha i}$  (pertussis toxin) and CCR1/3 (J113863), CCR3 (SB297006) and CCR5 (DAPTA) for 30 minutes prior to the experiment.

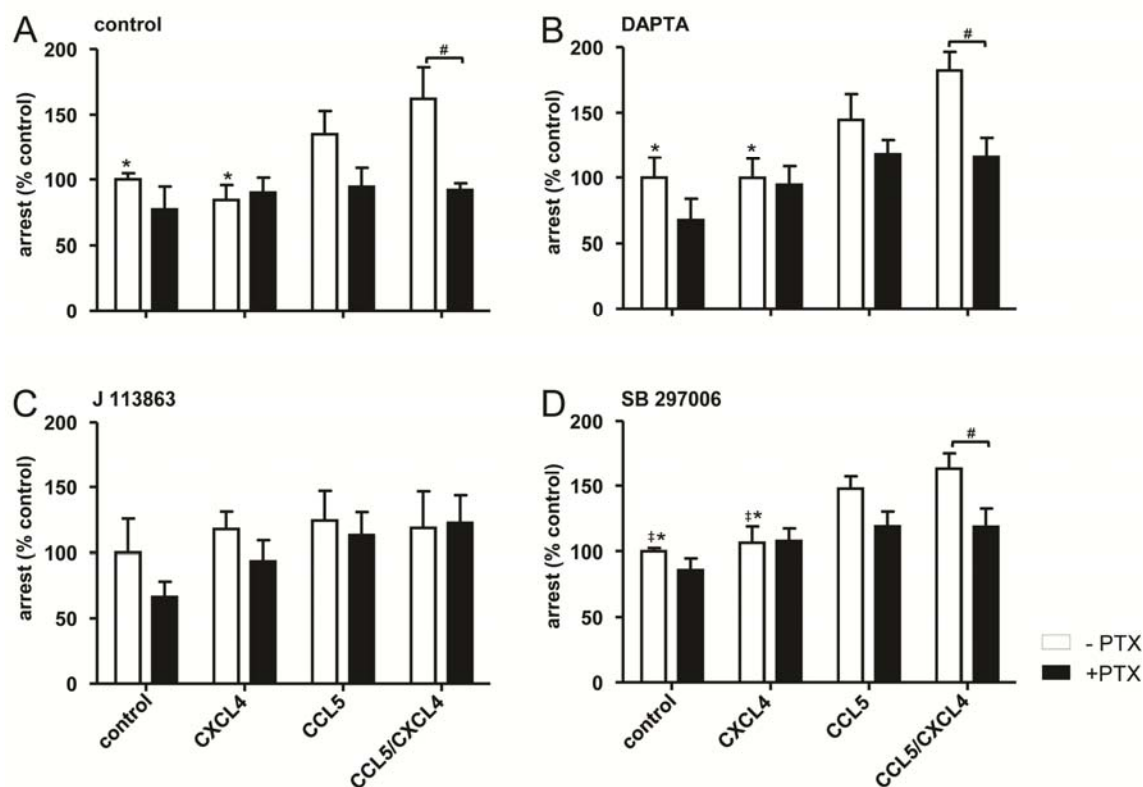


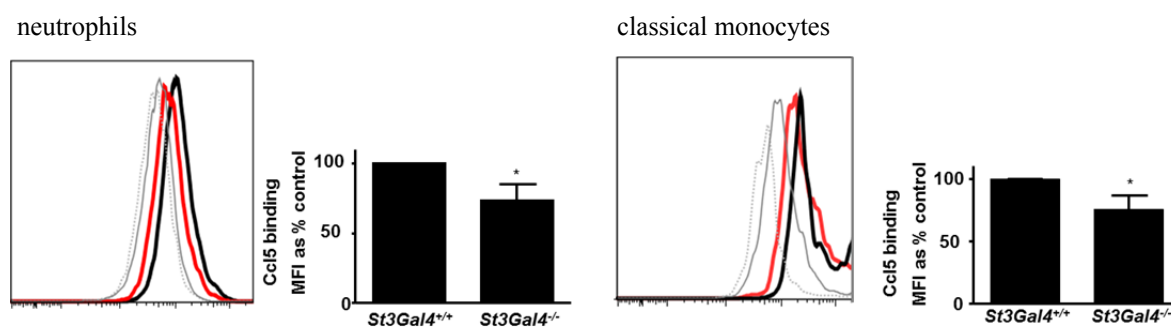
**Fig.III.4.9. Effect of antagonists on CCL5/CXCL4-induced arrest of THP-1 cells.**

Arrest of THP-1 cells on activated human aortic endothelial cells (HAoEC). THP-1 were stimulated with CCL5 (500 ng/ml) and/ or CXCL4 (500 ng/ml) with (solid bars) or without (empty bars) pertussis toxin (ptx), analyzed by 2-way-ANOVA (A-D) followed by Bonferroni pairwise analysis set to  $p < 0.05$ . Receptors were blocked by specific antagonists against CCR5 (B), CCR1 and CCR3 (C) or CCR3 (D, 80 nM SB297006) or left untreated (A). (Bonferroni, #  $P < 0.05$  +ptx vs -ptx; Newman-Keuls, ‡  $P < 0.05$  vs CCL5, \* $< 0.05$  vs CCL5-CXCL4;  $n \geq 4$ )

Without inhibitors a significant increase in cell adhesion was induced only by CCL5-CXCL4, which in turn was dependent on  $G_{\alpha i}$ -signaling (Fig.III.4.9. A). Selective inhibition of the receptors CCR3 (Fig.III.4.9. D) and CCR5 (Fig.III.4.9. B) did not significantly reduce the arrest response, although pertussis toxin again effectively diminished adhesion. Inhibition with J113863 however, which blocks CCR1 and CCR3, abolished the CCL5-CXCL4 effect consistent with a major role of CCR1 for leukocyte arrest (Fig.III.4.9. C). Thus, THP-1 cells activated by CCL5-CXCL4 require CCR1 signaling via  $G_{\alpha i}$  for an efficient arrest on human aortic endothelial cells, consistent with our findings in CCR1-transfected cells (Fig.III.4.9. A).

### III.5. FUNCTIONAL ROLE OF ST3GAL-IV IN CCL5 MEDIATED CELL RECRUITMENT

Sialylation was found to affect the ability of CXCR2 to mediate neutrophil adhesion and recruitment [91] and since *in vitro* data also suggested an important influence on CCR5 function [88], here we investigate the role of the  $\alpha$ 2-3 sialyltransferase ST3Gal-IV in CCL5 receptor activation and leukocyte trafficking. At first, we determined the ability of murine CCL5 to bind peripheral blood leukocytes isolated from either mice deficient for ST3Gal-IV or control mice. As reported earlier, ST3Gal-IV<sup>-/-</sup> mice appeared healthy and fertile and showed no difference in systemic leukocyte counts compared to control mice [179]. Bound CCL5 was detected by a fluorescence conjugated antibody and measured by FACS (II.10.6). Moreover a distinction was made between neutrophils and classical monocytes by incubation with a specific antibody cocktail (II.2.1 and II.10.6.). The CCL5 binding capacity to the ST3Gal-IV<sup>-/-</sup> leukocytes was reduced compared to the leukocytes isolated from the control animals. No significant difference could be observed between neutrophils and classical monocytes (Fig.III.5.1.), indicating that ST3Gal-IV is expressed in both cell types and that full binding capacity of CCL5 depends in part on the addition of negatively charged sialic acid residues to its corresponding receptors or in general to cell surface molecules.



*ST3Gal-IV*<sup>+/+</sup> control, *ST3GalIV*<sup>-/-</sup> control, *ST3GalIV*<sup>+/+</sup> Ccl5, *ST3GalIV*<sup>-/-</sup> Ccl5

#### Fig.III.5.1. ST3Gal-IV- deficiency reduces Ccl5 binding to neutrophils and monocytes.

Peripheral blood leukocytes were incubated with an antibody cocktail (anti-CD115,-Ly6G,-CD11b,-CD45) and murine Ccl5 (0.5  $\mu$ g/sample) followed by incubation with a fluorescently labeled anti-Ccl5 antibody. Fluorescence intensity was measured by FACS. Bar graphs depict mean binding capacity as MFI – MFI control calculated as % of control (n = 5 independent experiments).

Chemokine chemokine-receptor signaling has been shown to mediate the activation of integrins from low to high affinity state, triggering firm adhesion [180, 181] and CCL5 in particular mediates leukocyte adhesion. To reveal the impact of ST3Gal-IV on the CCL5-

mediated arrest, neutrophils and classical monocytes were perfused over TNF $\alpha$ -stimulated vascular endothelium in flow chamber adhesion assays (II.10.2.). The cells were either directly activated with CCL5 or CCL5 was allowed to deposit onto the activated monolayer. Arrest of ST3Gal-IV<sup>-/-</sup> monocytes and neutrophils was significantly reduced independent from the specific conditions. Together with the comparably low decrease of the CCL5 binding capacity (III.5.1.) the significant impaired adhesion may support the predominant role of ST3Gal-IV in the generation of functional selectins [179, 182-185]. Indicating a minor influence on the CCL5 chemokine receptor activation.

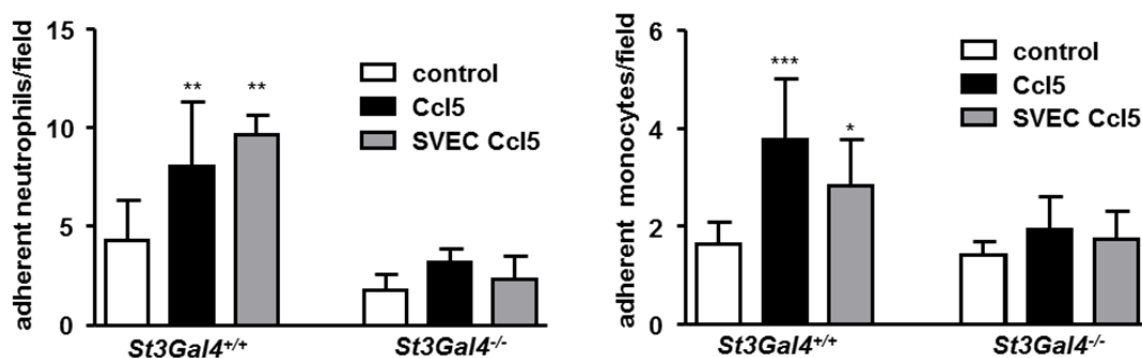
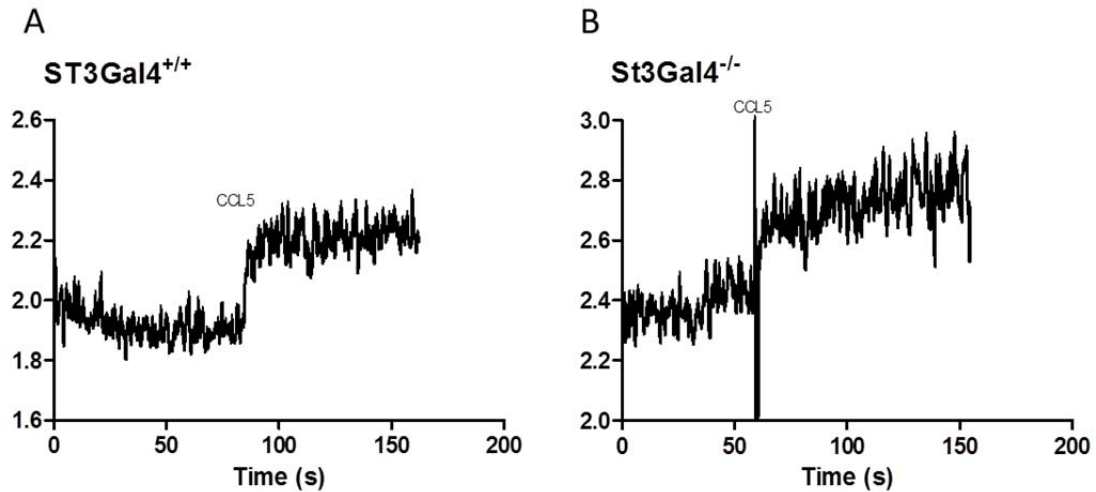


**Fig.III.5.2. ST3Gal-IV- deficiency reduces the CCL5 mediated adhesion of neutrophils and monocytes.**

Murine neutrophils (left) and monocytes (right) were perfused over TNF activated (20 ng, 4 h) mouse endothelial cells (SVEC) and the number of adherent cells was quantified. Ccl5 (5  $\mu$ g) was deposited 10 min prior to perfusion. Leukocytes were pre-treated with the murine Ccl5 (5  $\mu$ g, 10 min) where indicated (n = 5 independent experiments). \* p < 0.05, \*\* p < 0.01, \*\*\* p < 0.001; 1-way ANOVA with Tukey's Multiple Comparison test. Error bars represent mean  $\pm$  SD.

To further discriminate the influence of sialylation on the CCL5 receptor interaction and activation from the selectin functionality, we performed a calcium mobilization assay. Therefore neutrophils were isolated from mouse bone marrow cells employing FACS sorting. The cells were then loaded with the calcium indicator Fura-2 and the calcium burst was measured using a fluorescence spectrometer LS55 (PerkinElmer, USA) (II.10.5.).



**FigIII.5.3. CCL5 receptor activation is not ST3Gal-IV-dependent.**

Calcium mobilization upon stimulation of neutrophils isolated from (A) ST3Gal-IV<sup>-/-</sup> or (B) ST3Gal-IV<sup>+/+</sup> with CCL5. Calcium burst was visualized by using the calcium indicator Fura-2. Representative diagram of n=3 are shown.

Deviating to the slightly reduced CCL5 binding, in leukocytes regardless if isolated from ST3Gal-IV<sup>-/-</sup> (FigIII.5.3.-B) or from ST3Gal-IV<sup>+/+</sup> (FigIII.5.3.-A) mice similar calcium mobilization was measured upon stimulation with 100 ng/ml murine CCL5. This leads us to the conclusion that the extent in which the affinity of CCL5 is reduced might be rather due to “background binding”, to other molecules on the cell surface that are posttranslationally modified by ST3Gal-IV, than to the binding of CCL5 to the related receptors expressed by neutrophils and monocytes.



## IV. DISCUSSION

### IV.1. TWO DIFFERENT STRATEGIES TO PURIFY CCL5 AND THE CCL5 VARIANTS

CCL5 and the CCL5 variants Met-CCL5, CCL5-40s and CCL5-E66A were recombinantly expressed in *E. coli* (III.1.), depending on the subsequent use in either normal LB medium or in  $^{15}\text{N}$ -enriched medium, enabling selective and uniform isotopic labeling of CCL5 with  $^{15}\text{N}$  for NMR based studies (III.2.). Although posttranslational modifications, e.g. N-terminal truncation [81, 82] or glycosylation [76] have been reported, the functionally active form in humans (1-68) requires neither of these modifications. For this reason recombinant expression in a prokaryotic system, employing the Rosetta (DE3)-pLysS, is particularly suitable to obtain high amounts of pure and active CCL5. High-level expression of recombinant proteins in *E. coli* lead to the formation of highly aggregated proteins but since proteins folded from these inclusion bodies were shown to have the same structural and conformational integrity [186], the advantages, which were already mentioned in section II.6., can be taken into account. Like other CC chemokines, CCL5 is a small (8kDa) protein characterized by a superimposable monomeric fold with two cysteine bridges [132, 171], hence CCL5 was folded in reasonable yields from extracted inclusion bodies, as previously published [141, 187]. Following protocol B, where the solubilized protein was directly used in folding methodologies, it is essential to more extensively purify the inclusion bodies, as the bacterial contaminants may negatively influence protein folding [188]. This can be neglected if the protein is going to be partially purified by gel filtration (protocol A) prior to folding. Hence, for the second strategy B (II.6.3.) lysozyme and a DNase were added to reinforce cell lysis, followed by intensive washing with a detergent-containing buffer. Nevertheless, both protocols require a similar labor input to obtain the pre-cleaned inclusion bodies. However, folding CCL5 directly from the guanidine-HCl-solubilized pre-cleaned inclusion bodies and removing contaminants by dialyzing against 1% acetic acid, reduced the workload, since two chromatographic purification steps can be omitted [187]. It can be further expected that the losses of protein using the second strategy decrease because less chromatographic steps were necessary. Nevertheless this is just an assumption, since different constructs were used and the cells employing protocol A,



were grown in flasks on an orbital shaker, whereas later (when employing protocol B) it was possible to grow the cells in a fermenter, continuously vented and pH-adjusted. These optimized culture conditions alone lead to an highly increased yield [189]. Taken together, for the second purification strategy, compare flow scheme Fig.III.1.1.-B, the workload is reduced and it is less time consuming to obtain highly pure and active protein in comparison to the first purification strategy (Fig.III.1.1.-A). Nevertheless, purity and yield obtained with both protocols were satisfying, for the usage in *in vivo* and *in vitro* functional assays and it was further possible to produce  $^{15}\text{N}$ -enriched CCL5, which improved possibilities for the structural characterization of the heterodimerization of CCL5 and CXCL4 (III.2.)

### **IV.2. THE CXCL4/CCL5 HETERODIMER MEDIATES CELL RECRUITMENT FUNCTION VIA CCR1 AND/OR CCR5**

Initially it was observed that vascular deposition of CCL5 and CXCL4 could be associated with impaired atherosclerotic lesion formation after repeated injection of activated platelets into mice [190]. Atherosclerosis, is a chronic inflammatory disease of the arterial wall driven by chemokine mediated mononuclear cell recruitment to the lesion site, initiated by a local endothelial cell defect triggering intense immunological activity [191]. This is in line with the observation by *von Hundelshausen et. al.*, who demonstrated that CXCL4 enhances the primary function of CCL5 in promoting cell arrest [18, 64]. Moreover CXCL4 and CCL5 appear to play a crucial role in the progression of atherosclerosis [192]. In mice deficient for CXCL4, examination of lesions in the aortic roots of mice fed an atherogenic diet demonstrated a 20% reduction in atherosclerosis in CXCL4<sup>-/-</sup> compared to the wt mice [193]. The observations, that the deposition of CCL5 triggers shear-resistant monocyte arrest on inflamed or atherosclerotic endothelium [194] and that this could be amplified by a heterophilic interaction with CXCL4 [18], gave rise to the assumption that the reduced lesion size might be caused by the lack of synergy with CCL5. Further, molecular dynamics simulations (MD) revealed that a CXCL4/CCL5 heterodimer is highly thermodynamically favored [27]. In line with the previous observations, here heteronuclear single quantum coherence (HSQC) spectra of CCL5 and CXCL4 identified a decrease in CCL5 monomer signal intensities and chemical-shift changes that indicated a CC-type conformation, consistent with the predicted CCL5 and CXCL4 interaction

[98]. Accordingly, small peptide antagonists named MKEY (for the application into mouse) or CKEY2 (human), disrupted the heterocomplex formation and notably attenuated the accelerating effects of the CXCL4/CCL5 heteromer. The human orthologue CKEY2, was shown to compete with CXCL4 for binding to the N-terminus of CCL5 with high affinity ( $K_d = 100$  nM). Moreover the progression of atherosclerosis and the monocyte accumulation in the plaque were significantly reduced compared to a scrambled control peptide, sMKEY (data not shown). To further determine the pharmacological potential of MKEY, its inhibitory effect on monocyte recruitment *in vivo* was measured employing intravital microscopy, in comparison to the sMKEY control peptide and Met-CCL5. MKEY reduced the monocyte recruitment to the site of inflammation as effectively as Met-CCL5. Moreover, the comparable reduction of monocyte recruitment by MKEY and Met-CCL5, a strong antagonist of the CCL5 receptors CCR1 and CCR5, leads to the suggestion that CCL5 might depend on the auxiliary action of CXCL4 *in vivo*. Whether this effect occurs by activation of CCR1 or CCR5 is subject of this thesis (see below). In conclusion, disrupting the formation of CC-type CXCL4/CCL5 heteromers through the small peptide antagonist reduced inflammatory and atherogenic monocyte recruitment, pointing on the chemokine heterodimer formation as a promising therapeutic target.

#### **IV.3. EXCHANGE OF EXTRACELLULAR DOMAINS OF CCR1 AND CCR5 REVEALS CONFINED FUNCTIONS IN CCL5-MEDIATED CELL RECRUITMENT**

Even though CCR1 and CCR5 share various ligands, precisely CCL3, 5, 7, 8, 14 and 16, the response was shown to depend on the physiological context and the manner of presentation of the chemokine. For example, CCL5 induced flow-resistant arrest of CD4<sup>+</sup>CD45RO<sup>+</sup> T cells through CCR1, while subsequent transendothelial migration was triggered by CCR5 [137, 155]. This apparent specialization of CCR1 and CCR5 was facilitated by their specific requirements for the quaternary structure of CCL5, since the ability to form higher-order oligomers of CCL5 is important for the activation of CCR1 but not of CCR5 [137]. This structural requirement might be related to the mode of presentation of CCL5 on the endothelium. The immobilization of CCL5 on the vessel wall might increase the formation of large oligomers [45] that enhance the “visibility” of the chemokine stimulus to a rolling leukocyte. A stably adherent leukocyte however could subsequently migrate towards a soluble chemokine gradient that might be released

from the endothelium of the vessel wall, for which oligomerization is less important. For instance, CCL3/CCL4 (macrophage inflammatory protein-1 $\alpha$  and  $\beta$ ) can form a polydisperse distribution of rod-shaped double-helical polymers, which protects the chemokine from degradation by insulin-degrading enzymes, so that regulated polymerization for selective release and inactivation of monomers could aid in controlling the chemotactic gradient for migration *in vivo* [36]. Nevertheless, structural elements in the CCR1 and CCR5 receptors themselves might be responsible for their functional specialization and their preference for oligomeric forms of CCL5. Thus, we sought to identify specific roles of the extracellular domains of CCR1 and CCR5 in their specialization and preference. Our chimeric CCR1 and CCR5 mutants were all correctly expressed and functional as measured by chemotaxis assays. Consistent with previous reports, CCR1 less effectively mediated chemotaxis than CCR5 [155] and the 40s mutant of CCL5 induced only a weak response in our experimental setting. A somewhat different picture emerged under flow conditions. While neither CCR1 nor CCR5, nor any of the chimeric receptors, responded to stimulation with the variants of CCL5, which are restricted to a monomeric or dimeric state (NmeT7, E66A), all of the receptor variants reacted to wild-type CCL5. This reflects the importance of oligomerization of CCL5 as a major determinant for stable arrest onto endothelial cells.

The functional importance of the CCL5 oligomerization might be explained by a partial overlap of the GAG binding sites, such as the 40s cluster (RKNR), and the receptor binding or activation sites, preventing receptor binding when a CCL5 monomer is bound to a GAG. In the oligomeric state however, CCL5 might simultaneously bind to GAGs and to the receptor [38]. A model obtained from biophysical experiments provide a mechanism by which dual engagement could occur, supporting the concept that chemokines immobilized on the cell surfaces can simultaneously interact with receptors and GAGs [37]. In contrast to CCL5\_40s, the CCL5\_50s mutant is a CCL5 variant with a slightly reduced GAG-binding and substantial deficiency to bind endothelial cells, indicating a coordinative function in endothelial presentation [40]. In our experimental set up CCL5\_50s effectively induced flow-resistant adhesion of the CCR1 transfectants. A similar arrest was mediated via CCR5\_1N1, whereas CCR5\_1E1, CCR5\_1E2 and CCR5\_1E3 cells lost the full ability to adhere upon stimulation with CCL5\_50s. Accordingly, the reverse transfer of the N-terminal domain of CCR5 to CCR1 resulted in a CCR5 variant that responded well to wild-type CCL5 but poorly to CCL5\_50s,

suggesting that the 50s region directly interacts with the N-terminal region of CCR5 but not with CCR1. Previous studies have demonstrated that the 55KKWVR59 cluster determines the affinity to GAGs to a minor extent, compared with the 44RKNR47 cluster [39, 40]. However the 50s cluster was critical for the presentation of CCL5 on endothelial cells, to structures in histologic lymphatic or kidney specimen and was shown to be important for the leukocyte recruiting activity *in vivo* [40, 195]. Compared to the 50-100-fold reduced affinity of CCL5\_40s to CCR1, the CCL5\_50s mutant showed minimal alterations in CCR5 binding and activation, and had an approximately threefold reduced affinity (18 nM) for CCR1 [39]. This moderately reduced affinity was still sufficient to exert significant activity in our cell recruitment assays under flow conditions, particularly in combination with the CCR5\_1N1 chimeric receptor. Given the defined functional specialization of CCR1 and CCR5 that was observed in previous studies [137, 155], it is somewhat surprising that CCR5 was able to mediate CCL5-induced stable arrest on activated endothelial cells. CCR5 might be able to take over some of the arrest-promoting functions of CCR1, when expressed alone on the cell surface.

Nonetheless, since the leukocyte arrest-inducing function of CCL5 appears to be enhanced by the presence of CXCL4 *in vivo* [98, 173], our observations confirm that CCR1 might be the principal receptor promoting stable arrest. This is corroborated by the finding that it was possible to block the activity of the CCL5-CXCL4 heteromer by blocking CCR1 on THP-1 cells, known to express both CCR1 and CCR5. The structural requirement for this synergistic signal transduction appears to reside within the third extracellular domain of CCR1, since the chimeric CCR5\_1E3 but not the CCR1\_5E3 transfectants displayed essentially the same response towards CCL5/CXCL4 compared to those CCR1 transfected cells. These data indicate an involvement of the third extracellular loop of CCR1, because the transfer of this loop to CCR5 results in a chimera (CCR5\_1E3) able to mediate the synergy of CCL5 and CXCL4 confirmed by the reverse chimera CCR1\_5E3, which behaved like CCR5 in this respect. CCL5 may function as a “partial agonist” that mediates leukocyte arrest. In an environment rich in CCL5-CXCL4 heteromers, such as sites in the circulation where platelet activation takes place (e.g. plaque rupture, vessel injury), the heteromer may act as a “full agonist” accelerating the arrest response. The CCL5-CXCL4 complex can be regarded as a “full agonist” for CCR1. Different ligands can stabilize different active conformations of the same seven-transmembrane receptor. This ligand specific conformation may then lead to an altered

coupling to different cellular signaling molecules [56, 196] and it seems that the third extracellular loop of CCR1 is involved in the stabilization of the CCL5-CXCL4 specific active conformation of CCR1. The enhancing effect of CXCL4 on CCL5-mediated arrest was even higher in CCR5\_1E3 cells than in wild-type CCR1 cells. This chimera could reflect a CCR1/CCR5 heterodimer, which mediates the CCL5-CXCL4 signal under physiologic conditions where both receptors are expressed concomitantly.

Chemokine receptors readily form functional hetero- and homo-oligomers [51, 177] even if the mechanisms still need to be elucidated. The first crystal structure of a chemokine receptor highlighted the role of the extracellular part of the transmembrane domains V and VI in homodimerization of CXCR4 [51], which are in close proximity to the third extracellular loop. Indeed, we identified the dimerization and co-localization of CCR1 and CCR5 in double-transfectants, yet an exchange of the extracellular loop 3 did still allow the dimerization of CCR1 and CCR5. It is conceivable that a homodimerization of CCR1 could be as well involved in mediating the synergistic effects of CCL5 and CXCL4. Heteromerization of CCR2 and CCR5 has been shown to take place in recombinant cells and stimulation of CCR2-CCR5 co-transfectants with CCL2 and CCL5 resulted in a shift of pertussis toxin sensitive  $G\alpha_i$  to insensitive  $G\alpha_q$  cell arrest over chemotaxis [62]. The CCL5-CXCL4 mediated arrest of THP-1 cells could be blocked by a CCR1 antagonist or by pertussis toxin. In our experimental set up we neither found that receptor heterodimerization nor another ptx  $G\alpha_i$  independent signaling, were responsible for the additional effect through the CCL5-CXCL4 complex. CCR1 is sufficient in transmitting the arrest signal of the CCL5-CXCL4 heteromer via  $G\alpha_i$ .

In vivo, the ubiquitous inhibition of CCR1 did not necessarily result in a decreased monocyte or mononuclear cell recruitment as seen in increased arterial infiltration and atherosclerotic lesion development in CCR1-deficient mice which has been attributed to an altered immune response due to a change in the Th1/Th2 cytokine balance overriding the CCR1-mediated effects [157]. Likewise, CCR1 regulates inflammatory cell infiltration after renal ischemia-reperfusion injury without affecting tissue injury [197]. Moreover, a small molecule antagonist for CCR1 has been shown to prolong transplant rejection and to reduce progression of chronic renal allograft damage in models of heart and kidney transplantation, but developmental hurdles, such as lack of efficacy in clinical trials have not been resolved [198-200]. The important role of CCR1 and especially the

third extracellular loop in mediating the CCL5-CXCL4 effects may represent a new attractive target with a more selective structural site for designing future anti-inflammatory therapies.

#### **IV.4. ST3GAL-IV DEFICIENCY REDUCES CCL5 MEDIATED LEUKOCYTE TRANSMIGRATION**

Proinflammatory signaling results in the increased expression of adhesion molecules like selectins, which facilitates “capture” of the leukocytes to the vessel wall. Three different selectins have been identified: E-selectin (CD62E), P-selectin (CD62P), and L-selectin (CD62L). L-selectin is expressed on most types of leukocytes, E-selectin is expressed on activated endothelium, and P-selectin was first found in storage granules of platelets and is also expressed by endothelial cells [181]. During leukocyte recruitment, an essential role of posttranslational glycosylation has been identified for selectin ligand function. This became particularly apparent in mice with a genetic deletion in glycosyltransferases such as alpha(1,3)fucosyltransferase Fuc-TVII or the core 2 beta-1,6-N-acetylglucosaminyltransferase (C2 GlcNAcT) which led to a profound impairment of selectin-dependent leukocyte rolling *in vivo* [183, 184, 201]. While most glycosyltransferases involved in the generation of functional selectin ligands have not been reported to influence other steps of leukocyte trafficking, the  $\alpha$ 2-3 sialyltransferase (ST3Gal-IV) was suggested to influence the chemokine triggered arrest [202]. In 2002, mice deficient in the ST3Gal-IV were generated [203]. *In vivo* studies on P-, E-, and L-selectin-mediated leukocyte rolling in inflamed cremaster muscle venules of ST3Gal-IV<sup>-/-</sup> mice revealed a complete absence of L-selectin ligand function and a partial impairment in E-selectin dependent leukocyte rolling [179, 204]. In a recent publication, CXCR2 function was shown to be dependent on ST3Gal-IV-mediated sialylation, in ST3Gal-IV<sup>-/-</sup> mice leukocyte adhesion to inflamed microvessels was significantly reduced upon injection of the CXCR2 ligands CXCL1 or CXCL8. Additionally, *in vitro* assays indicated a reduced binding capacity of CXCL8 to ST3Gal-IV<sup>-/-</sup> neutrophils [91]. Another study provides evidence that ST3Gal-IV may also influence the CCR5-mediated cellular response, by using cells stably expressing CCR5 and CCR5 mutants where the serine and threonine residues, offering crucial O-glycosylation sites for sialylation (e.g. S6 and S7) were neutralized by exchange to alanine. These mutants were employed to estimate the binding of CCL3 and CCL4, showing that binding was strongly impaired to a CCR5\_S6A

mutant [88]. Since CCL5 binds and activates CCR5 and the CCL5/CCR5 axis is of great importance in many inflammatory diseases like atherosclerosis [157, 205] or rheumatoid arthritis [206, 207], we chose to investigate the role of ST3Gal-IV in CCL5-mediated leukocyte trafficking. Under steady state conditions, we could show here that the affinity of CCL5 to ST3Gal-IV<sup>-/-</sup> deficient neutrophils and monocytes was reduced in the same extent, indicating that in both cell types ST3Gal-IV is essential for the CCL5 receptor interaction or more generally for cell surface binding.

The chemokine-driven recruitment of specific leukocyte subsets to the site of inflammation is a hallmark in the pathogenesis of inflammatory diseases. Thus, to determine the influence of ST3Gal-IV deficiency on CCL5-mediated leukocyte recruitment, we perfused neutrophils and monocytes from ST3Gal-IV<sup>-/-</sup> or wt mice over TNF- $\alpha$ -stimulated mouse vascular endothelial cells. The lack of ST3Gal-IV in leukocytes severely impaired CCL5-mediated neutrophil and classical monocyte adhesion to activated SVEC in laminar flow chamber adhesion assays. These findings were supported by data obtained from intravital microscopy, where the adhesion of ST3Gal-IV<sup>-/-</sup> leukocytes was almost completely diminished (data not shown). CCL5 binding to neutrophils and also to classical monocytes isolated from ST3Gal-IV<sup>-/-</sup> mice was reduced but this reduction was less pronounced as that observed in the adhesion assays and intravital microscopy experiments, pointing towards a minor importance of ST3Gal-IV on the CCL5 receptor interaction. To further differentiate between the influence of ST3Gal-IV on the CCL5 receptor activation and selectin function, the calcium mobilization upon CCL5 stimulation was measured. Independent of the presence of ST3Gal-IV, CCL5 induced a calcium burst in the cytoplasm of wt or ST3Gal-IV<sup>-/-</sup> cells to a similar extent. Although, *in vitro* observations indicated a decline of CCL3 and CCL4 binding to a CCR5 receptor mutant lacking a putative sialylation site (CCR5\_S6A) [88], the latter results suggest that CCL5 binding and activation of its receptors *in vivo* is, if at all, only slightly reduced in the absence of ST3Gal-IV-mediated posttranslational modifications. We can not exclude the possibility that other CCL5 receptors expressed on neutrophils and monocytes [149], such as CCR1 and CCR3 compensate a reduced affinity to CCR5. However, the data so far do highlight the importance of ST3Gal-IV on the generation of functional selectins, supporting previous findings that describe a prominent role of sialyltransferases for selectin function [179, 183, 201, 203, 204].

## V SUMMARY

### V.1. SUMMARY

Chemokines are important mediators and regulators of leukocyte trafficking, therefore, they play a crucial role in the development of inflammatory diseases. CCL5 or RANTES (regulated upon activation, normal T cell expressed and secreted) is a chemokine of relevance to many diseases. Moreover, CCL5-induced monocyte adhesion to inflamed endothelium was shown to be improved in the presence of CXCL4 (Platelet Factor 4). Since this synergy could be attributed to heterodimer formation, the first section of the present study surveys the structural interaction of CCL5 with CXCL4. The interaction was monitored employing the  $^{15}\text{N}$ - $^1\text{H}$  heteronuclear single quantum coherence (HSQC) nuclear magnetic resonance (NMR) technique. For this purpose,  $^{15}\text{N}$ -enriched CCL5 was recombinantly expressed in *E. coli* and subsequently purified. In HSQC spectroscopy, chemical shift changes were mainly observed in the N-terminal residues, which pointed toward a CC-type rather than a CXC-type interaction. Furthermore, small peptide antagonists, inhibiting the CXCL4/CCL5 dimerization, were designed (CKEY2 and the mouse orthologue MKEY). To investigate their pharmacological potential, the influence of MKEY on leukocyte adhesion to activated endothelium was monitored using intravital microscopy. As a control Met-CCT5, a strong antagonist for CCR1 and CCR5, was cloned, expressed and purified employing FPLC and HPLC techniques. Leukocyte recruitment was severely impaired in the presence of MKEY, compared to a control peptide (sMKEY) and in a similar range of Met-CCL5 which encourages the assumption that the synergy is mediated via the receptors CCR1 and/or CCR5.

Despite all similarities, CCR1 and CCR5 were shown to mediate distinct functions when bound to CCL5, CCR1 rather mediates arrest and CCR5 appears to be more responsible for transendothelial migration. To establish which domains are important for this functional selectivity, we constructed different CCR5 variants with the distinct extracellular regions of CCR1. These chimeras were stably expressed in *LI.2* and *HEK293* cells and we investigated their function in response to CCL5, different CCL5 mutants, or together with CXCL4 using chemotaxis and cell arrest assays under laminar flow. First of all, CCL5, CCL5 40s and CCL5-E66A were recombinantly expressed and purified employing FPLC and HPLC techniques. By implementing CCL5 mutants (e.g. CCL5-E66A) with oligomerization defects in laminar flow assays, we were able to show



that all receptor variants require oligomerization of CCL5 in order to function properly. In addition, our results reveal that the 40S loop of CCL5 is important for both the CCR1- and CCR5-mediated cell arrest. The 50s loop of CCL5, however, appeared to have a strong preference for CCR5 in inducing cell arrest, since CCR1 responded normal towards CCL5 50s and CCR5 being non-responsive. When the N-terminal domain of CCR5 was exchanged for that of CCR1, the resulting chimera was fully responsive towards CCL5 50s, suggesting that the N-terminal region of CCR1 interacts with the 50s domain of CCR5. The synergistic effect of CXCL4 on CCL5 induced cell arrest was observed in cells exclusively expressing CCR1 when compared to cells expressing CCR5. When the third extracellular loop of CCR1 was engineered into CCR5, the resulting chimeric receptor showed a significant response to the CXCL4/CCL5 heterocomplex, compared to CCL5 alone. These results were confirmed by constructing CCR1-based reverse chimeras for the N-terminal domain and the third extracellular loop. Furthermore we could show the heterodimerization of CCR1 and CCR5 and the synergy of the CXCL4/CCL5 complex is in THP-1 cells mediated via  $G\alpha_i$ . In conclusion these results indicate that the extracellular regions of CCR1 and CCR5 have distinct and defined functions in leukocyte recruitment in response to CCL5.

In the third section of this thesis the role of the sialyltransferase ST3Gal-IV on CCL5 receptor interaction was investigated, by using neutrophils and monocytes isolated from ST3Gal-IV deficient and from control mice in functional assays *in vitro*. The results indicate that the addition of sialic acids to the terminal portions of the N- or O-linked sugar chains of the corresponding receptors of CCL5 is of a minor importance for receptor binding and activation, since the cells similarly mobilize calcium upon stimulation with CCL5. Whereas, the adhesion of neutrophils and monocytes from ST3Gal-IV<sup>-/-</sup> was significant diminished. Taken together the results obtained here rather support the importance of ST3Gal-IV on the generation of functional selectins, which is in line with previous publications.

## V.2. ZUSAMMENFASSUNG

Chemokine sind bedeutende Mediatoren und Regulatoren der Leukozyten Migration und spielen dadurch eine wichtige Rolle bei der Entstehung verschiedener entzündlicher Erkrankungen. Das proinflammatorische Chemokin CCL5 oder auch RANTES (regulated upon activation, normal T cell expressed and secreted) ist für die Entstehung zahlreicher Krankheiten von besonderer Relevanz. Es konnte gezeigt werden, dass die durch CCL5 vermittelte Adhäsion monozytärer Zellen auf entzündlichem Endothel durch das Zusammenwirken mit CXCL4 verstärkt wurde. Da dieser Synergismus der Dimerisierung von CXCL4 mit CCL5 zugeschrieben werden konnte, wurden im ersten Teil der vorliegenden Arbeit die strukturellen Grundlagen der Heterodimer Bildung untersucht. Diese Interaktion wurde mit Hilfe der  $^{15}\text{N}$ - $^1\text{H}$  HSQC (von „heteronuclear single quantum coherence“) Kernspinresonanzspektroskopie untersucht. Dazu wurde  $^{15}\text{N}$  angereichertes CCL5 rekombinant in *E. coli* exprimiert und anschließend aufgereinigt. Die HSQC Spektren zeigten chemische Verschiebungen insbesondere in den N-terminalen Aminosäuren von CCL5, was eher auf eine CC denn auf eine CXC typische Interaktion hindeutet. Im Rahmen dieser Studie wurden kleine antagonistische Peptide entwickelt und synthetisiert, CKEY2 und dessen Maus Ortholog MKEY, welche die Heterodimer Bildung von CXCL4 und CCL5 unterbinden. Um Ihre pharmakologische Wirksamkeit zu ermitteln wurde der Einfluss von MKEY auf die Leukozyten Adhäsion an entzündlichem Endothel untersucht. Zum Vergleich und als Kontrolle wurde Met-CCL5, ein Rezeptor Antagonist für CCR1 und CCR5, eingesetzt. Met-CCL5 wurde dazu kloniert, rekombinant exprimiert und mit Hilfe von FPLC und HPLC Methoden aufgereinigt. Dabei zeigte sich in Gegenwart von MKEY eine deutlich verminderte Adhäsion von Leukozyten. Darüber hinaus legte der Vergleich mit Met-CCL5, die Vermutung nahe, dass es sich bei CCR1 und/oder CCR5 um den Rezeptor für das CXCL4/CCL5 Heteromer handelt. Die Chemokin Rezeptoren CCR1 und CCR5 sind sich in Struktur und auch Aminosäuresequenz sehr ähnlich. Abgesehen von dieser ausgeprägten Homologie konnte gezeigt werden, dass sie, durch CCL5 induziert, distinkte Funktionen vermitteln. CCR1 vermittelt verstärkt Arrest und CCR5 scheint in höherem Maße für die transendotheliale Migration verantwortlich. Um untersuchen zu können welche Rezeptor Domänen für diese funktionelle Selektivität von Bedeutung sind, wurden CCR5 Varianten mit bestimmten extrazellulären Domänen von CCR1 konstruiert, *LI.2* und *HEK-293* Zellen stabil transfiziert und ihre Funktion nach Stimulation mit CCL5,

verschiedenen CCL5 Mutanten oder zusammen mit CXCL4 in Chemotaxis und Zell Arrest Experimenten untersucht. Dazu wurden zunächst CCL5, CCL5-40s und CCL5-E66A rekombinant exprimiert und aufgereinigt. Wir konnten zeigen dass, die Oligomer Bildung für alle Rezeptor Varianten zur Vermittlung der Zelladhäsion unter laminaren Flussbedingungen von Bedeutung ist. CCL5 Mutanten mit Defekten bei der Oligomerisierung (z.B. CCL5-E66A) waren nicht in der Lage einen sichtbaren Arrest zu induzieren. Darüber hinaus konnten wir feststellen, dass die 40s Domäne für den CCL5 vermittelten Zellarrest sowohl für CCR1 als auch CCR5 von Bedeutung ist. Die 50s Domäne von CCL5 hingegen scheint nur von größerer Relevanz für den CCR5 vermittelten Zellarrest zu sein, da CCR1 normal auf CCL5 mit einem mutierten 50s Motiv reagiert, wohingegen CCR5 exprimierende Zellen keine Adhäsion zeigen. Wenn allerdings die N-terminale Domäne von CCR5 gegen die von CCR1 ausgetauscht wurde, zeigte die daraus resultierende Chimäre ein mit CCR1 vergleichbares Verhalten. Dies ließ uns vermuten, dass der N-terminus von CCR5 mit 50s Motiv von CCL5 zu interagieren scheint. Der synergistische Einfluss von CXCL4 auf den CCL5 vermittelten Zellarrest wurde nur bei Zellen, die ausschließlich CCR1 exprimierten beobachtet. Eine Chimäre, bei der die dritte extrazelluläre Domäne von CCR5 durch die von CCR1 ersetzt wurde, reagierte wiederum signifikant auf den CXCL4/CCL5 Hetero-Komplex im Vergleich zu CCL5. Diese Ergebnisse konnten in Kontrollexperimenten mit entsprechenden Umkehrmutanten weiter verifiziert werden. Darüber hinaus konnten wir die Heteromerisierung von CCR1 und CCR5 zeigen, und dass sowohl das CCL5 Signal als auch das Signal des CXCL4/CCL5 Komplexes durch  $G\alpha_i$  in THP Zellen vermittelt wird. Zusammenfassend lassen diese Ergebnisse vermuten, dass die extrazellulären Regionen der Rezeptoren CCR1 und CCR5 distinkte und definierte Funktionen bei der Interaktion mit und der Aktivierung durch CCL5 haben. Im dritten Abschnitt der vorliegenden Arbeit wurde der Einfluss der Sialyltransferase ST3Gal-IV auf die Interaktion von CCL5 mit seinen Rezeptoren untersucht. Dazu wurden Neutrophile und Monozyten aus ST3Gal-IV defizienten und Kontroll Mäusen isoliert und in funktionellen Experimenten verglichen. Die Ergebnisse lassen vermuten, dass eine fehlende Sialylierung die CCL5-Rezeptor-Aktivierung nicht beeinträchtigt, da CCL5 in ST3Gal-IV defizienten und wt Zellen gleichermaßen Calcium mobilisieren konnte. Wohingegen die Adhäsion von ST3Gal-IV<sup>-/-</sup> Zellen deutlich beeinträchtigt war. Unsere Ergebnisse stützen frühere Veröffentlichungen die eine besondere Bedeutung von ST3Gal-IV bei der Generierung funktioneller Selektine gezeigt haben.

## VI ACKNOWLEDGEMENT

Hiermit möchte ich mich bei allen Personen bedanken, die zum Gelingen meiner Doktorarbeit beigetragen haben.

Mein Dank gilt Herrn Prof. Dr. Christian Weber für die Ermöglichung dieser Doktorarbeit, die hervorragenden Arbeitsbedingungen und die wissenschaftliche Betreuung.

Herrn Priv.-Doz. Dr. Rory R. Koenen für die Betreuung meiner Doktorarbeit, den wissenschaftlichen Austausch und für die Möglichkeit, auch eigene Ideen verwirklichen zu können.

Herrn Dr. Philipp von Hundelshausen für viele aufschlussreiche und hilfreiche Diskussionen und die Unterstützung dieser Arbeit.

Prof. Dr. Jürgen Bernhagen danke ich an dieser Stelle für die Übernahme der Zweitkorrektur dieser Arbeit.

Ich danke meinen Arbeitskollegen des IMCAR für ihre fachliche Unterstützung und die schöne Zeit in Aachen. Danke außerdem für die vielen schönen Unternehmungen und geselligen Runden außerhalb des Labors. Danke Ake, Delia, Dirk, Heidi, Helene, Holger, Isabella, Jean-Eric, Jürgen, Klaus, Kiril, Leon, Martin H., Martin S., Michael, Norbert, Remco, Sakine, Santosh, Silvia und Yvonne J und Wendy. Besonderer Dank gilt Ali und Xavier für Ihre Unterstützung, den wissenschaftliche Diskurs und auch so manche weniger ernste Diskussion.

Außerdem den neuen Kollegen des IPEK für einen guten Start in München. Danke Almudena, Diana, Ela, Gitte, Janina, Jasmin, Larissa, Manuela, Marcella, Nada, Sascha, Steven, Suman und Veit.

An dieser Stelle möchte ich mich bei den TAs Barbara, Lusi und Sabine bedanken, ohne Eure Hilfe wäre diese Arbeit nicht zustande gekommen.

Ganz herzlich bedanken möchte ich mich bei Yvonne D. für das Korrektur lesen meiner Arbeit und den sehr hilfreichen wissenschaftlichen Diskurs. Auch für unseren vielen amüsanten und interessanten Gespräche, so manche notwendige und lieb gemeinte Ansprache und Deine Freundschaft. Großen Dank auch bei Maik und Oli für Ihre Geduld,

Aufmunterung und Hilfe in schwierigen Momenten (Stichwort Spaghetti) tolle Koch- und Spieleabende und die anderen erinnerungswürdigen Unternehmungen. Vielen Dank Euch Dreien.

Zum Schluss möchte ich mich ganz besonders herzlich bei meiner Familie und meinen Freunden für alles bedanken, für Ihren Rückhalt und für die oft so notwendige Ablenkung, insbesondere bei meinen Eltern, die immer ein offenes Ohr für mich hatten, mich immer unterstützt und an mich geglaubt haben.

## V.II. REFERENCES

1. Newton, K. and V.M. Dixit, *Signaling in innate immunity and inflammation*. Cold Spring Harb Perspect Biol, 2012. **4**(3).
2. Janeway, C.A., Jr. and R. Medzhitov, *Introduction: the role of innate immunity in the adaptive immune response*. Semin Immunol, 1998. **10**(5): p. 349-50.
3. Zlotnik, A., A.M. Burkhardt, and B. Homey, *Homeostatic chemokine receptors and organ-specific metastasis*. Nat Rev Immunol, 2011. **11**(9): p. 597-606.
4. Rossi, D. and A. Zlotnik, *The biology of chemokines and their receptors*. Annu Rev Immunol, 2000. **18**: p. 217-42.
5. Schall, T.J. and A.E. Proudfoot, *Overcoming hurdles in developing successful drugs targeting chemokine receptors*. Nat Rev Immunol, 2011. **11**(5): p. 355-63.
6. Keeley, E.C., B. Mehrad, and R.M. Strieter, *Chemokines as mediators of tumor angiogenesis and neovascularization*. Exp Cell Res, 2011. **317**(5): p. 685-90.
7. Raman, D., T. Sobolik-Delmaire, and A. Richmond, *Chemokines in health and disease*. Exp Cell Res, 2011. **317**(5): p. 575-89.
8. Zlotnik, A. and O. Yoshie, *Chemokines: a new classification system and their role in immunity*. Immunity, 2000. **12**(2): p. 121-7.
9. Oppenheim, J.J., et al., *Properties of the novel proinflammatory supergene "intercrine" cytokine family*. Annu Rev Immunol, 1991. **9**: p. 617-48.
10. Rollins, B.J., *Chemokines*. Blood, 1997. **90**(3): p. 909-28.
11. Blanchet, X., et al., *Touch of chemokines*. Front Immunol, 2012. **3**: p. 175.
12. Schober, A., *Chemokines in vascular dysfunction and remodeling*. Arterioscler Thromb Vasc Biol, 2008. **28**(11): p. 1950-9.
13. Weber, C. and R.R. Koenen, *Fine-tuning leukocyte responses: towards a chemokine 'interactome'*. Trends Immunol, 2006. **27**(6): p. 268-73.
14. Guan, E., J. Wang, and M.A. Norcross, *Identification of human macrophage inflammatory proteins 1alpha and 1beta as a native secreted heterodimer*. J Biol Chem, 2001. **276**(15): p. 12404-9.
15. Strieter, R.M., et al., *The functional role of the ELR motif in CXC chemokine-mediated angiogenesis*. J Biol Chem, 1995. **270**(45): p. 27348-57.
16. Belperio, J.A., et al., *CXC chemokines in angiogenesis*. J Leukoc Biol, 2000. **68**(1): p. 1-8.
17. Balestrieri, M.L., et al., *Understanding the immunoangiostatic CXC chemokine network*. Cardiovasc Res, 2008. **78**(2): p. 250-6.

## References

---

18. von Hundelshausen, P., et al., *Heterophilic interactions of platelet factor 4 and RANTES promote monocyte arrest on endothelium*. *Blood*, 2005. **105**(3): p. 924-30.
19. Sticht, H., et al., *Solution structure of the human CC chemokine 2: A monomeric representative of the CC chemokine subtype*. *Biochemistry*, 1999. **38**(19): p. 5995-6002.
20. Seizer, P., et al., *CXCL16 is a novel scavenger receptor on platelets and is associated with acute coronary syndrome*. *Thromb Haemost*, 2011. **105**(6): p. 1112-4.
21. Murphy, P.M., et al., *International union of pharmacology. XXII. Nomenclature for chemokine receptors*. *Pharmacol Rev*, 2000. **52**(1): p. 145-76.
22. Proudfoot, A.E., *The biological relevance of chemokine-proteoglycan interactions*. *Biochem Soc Trans*, 2006. **34**(Pt 3): p. 422-6.
23. Gerard, C. and B.J. Rollins, *Chemokines and disease*. *Nat Immunol*, 2001. **2**(2): p. 108-15.
24. Nomiyama, H., N. Osada, and O. Yoshie, *The evolution of mammalian chemokine genes*. *Cytokine Growth Factor Rev*, 2010. **21**(4): p. 253-62.
25. Murdoch, C. and A. Finn, *Chemokine receptors and their role in inflammation and infectious diseases*. *Blood*, 2000. **95**(10): p. 3032-43.
26. Czaplewski, L.G., et al., *Identification of amino acid residues critical for aggregation of human CC chemokines macrophage inflammatory protein (MIP)-1alpha, MIP-1beta, and RANTES. Characterization of active disaggregated chemokine variants*. *J Biol Chem*, 1999. **274**(23): p. 16077-84.
27. Nesmelova, I.V., et al., *CXC and CC chemokines form mixed heterodimers: association free energies from molecular dynamics simulations and experimental correlations*. *J Biol Chem*, 2008. **283**(35): p. 24155-66.
28. Rajarathnam, K., et al., *Neutrophil activation by monomeric interleukin-8*. *Science*, 1994. **264**(5155): p. 90-2.
29. Laurence, J.S., et al., *CC chemokine MIP-1 beta can function as a monomer and depends on Phe13 for receptor binding*. *Biochemistry*, 2000. **39**(12): p. 3401-9.
30. Paavola, C.D., et al., *Monomeric monocyte chemoattractant protein-1 (MCP-1) binds and activates the MCP-1 receptor CCR2B*. *J Biol Chem*, 1998. **273**(50): p. 33157-65.
31. Paoletti, S., et al., *A rich chemokine environment strongly enhances leukocyte migration and activities*. *Blood*, 2005. **105**(9): p. 3405-12.
32. Roscic-Mrkic, B., et al., *RANTES (CCL5) uses the proteoglycan CD44 as an auxiliary receptor to mediate cellular activation signals and HIV-1 enhancement*. *Blood*, 2003. **102**(4): p. 1169-77.

33. Lau, E.K., et al., *Identification of the glycosaminoglycan binding site of the CC chemokine, MCP-1: implications for structure and function in vivo*. J Biol Chem, 2004. **279**(21): p. 22294-305.
34. Swaminathan, G.J., et al., *Crystal structures of oligomeric forms of the IP-10/CXCL10 chemokine*. Structure, 2003. **11**(5): p. 521-32.
35. Murphy, J.W., et al., *Heterologous quaternary structure of CXCL12 and its relationship to the CC chemokine family*. Proteins, 2010. **78**(5): p. 1331-7.
36. Ren, M., et al., *Polymerization of MIP-1 chemokine (CCL3 and CCL4) and clearance of MIP-1 by insulin-degrading enzyme*. EMBO J, 2010. **29**(23): p. 3952-66.
37. Wang, X., et al., *Oligomeric structure of the chemokine CCL5/RANTES from NMR, MS, and SAXS data*. Structure, 2011. **19**(8): p. 1138-48.
38. Proudfoot, A.E., et al., *Glycosaminoglycan binding and oligomerization are essential for the in vivo activity of certain chemokines*. Proc Natl Acad Sci U S A, 2003. **100**(4): p. 1885-90.
39. Proudfoot, A.E., et al., *The BBXB motif of RANTES is the principal site for heparin binding and controls receptor selectivity*. J Biol Chem, 2001. **276**(14): p. 10620-6.
40. Segerer, S., et al., *The basic residue cluster (55)KKWVR(59) in CCL5 is required for in vivo biologic function*. Mol Immunol, 2009. **46**(13): p. 2533-8.
41. Salanga, C.L. and T.M. Handel, *Chemokine oligomerization and interactions with receptors and glycosaminoglycans: the role of structural dynamics in function*. Exp Cell Res, 2011. **317**(5): p. 590-601.
42. Witt, D.P. and A.D. Lander, *Differential binding of chemokines to glycosaminoglycan subpopulations*. Curr Biol, 1994. **4**(5): p. 394-400.
43. Kuschert, G.S., et al., *Glycosaminoglycans interact selectively with chemokines and modulate receptor binding and cellular responses*. Biochemistry, 1999. **38**(39): p. 12959-68.
44. Severin, I.C., et al., *Characterization of the chemokine CXCL11-heparin interaction suggests two different affinities for glycosaminoglycans*. J Biol Chem, 2010. **285**(23): p. 17713-24.
45. Hoogewerf, A.J., et al., *Glycosaminoglycans mediate cell surface oligomerization of chemokines*. Biochemistry, 1997. **36**(44): p. 13570-8.
46. Rosenbaum, D.M., S.G. Rasmussen, and B.K. Kobilka, *The structure and function of G-protein-coupled receptors*. Nature, 2009. **459**(7245): p. 356-63.
47. Pease, J.E. and T.J. Williams, *The attraction of chemokines as a target for specific anti-inflammatory therapy*. Br J Pharmacol, 2006. **147 Suppl 1**: p. S212-21.



## References

---

48. Nomiya, H., N. Osada, and O. Yoshie, *A family tree of vertebrate chemokine receptors for a unified nomenclature*. Dev Comp Immunol, 2011. **35**(7): p. 705-15.
49. Graham, G.J., et al., *The biochemistry and biology of the atypical chemokine receptors*. Immunol Lett, 2012. **145**(1-2): p. 30-8.
50. Pruenster, M., et al., *The Duffy antigen receptor for chemokines transports chemokines and supports their promigratory activity*. Nat Immunol, 2009. **10**(1): p. 101-8.
51. Wu, B., et al., *Structures of the CXCR4 chemokine GPCR with small-molecule and cyclic peptide antagonists*. Science, 2010. **330**(6007): p. 1066-71.
52. Katritch, V., V. Cherezov, and R.C. Stevens, *Diversity and modularity of G protein-coupled receptor structures*. Trends Pharmacol Sci, 2012. **33**(1): p. 17-27.
53. Park, S.H., et al., *Structure of the chemokine receptor CXCR1 in phospholipid bilayers*. Nature, 2012. **491**(7426): p. 779-83.
54. Crump, M.P., et al., *Solution structure and basis for functional activity of stromal cell-derived factor-1; dissociation of CXCR4 activation from binding and inhibition of HIV-1*. EMBO J, 1997. **16**(23): p. 6996-7007.
55. Monteclaro, F.S. and I.F. Charo, *The amino-terminal extracellular domain of the MCP-1 receptor, but not the RANTES/MIP-1alpha receptor, confers chemokine selectivity. Evidence for a two-step mechanism for MCP-1 receptor activation*. J Biol Chem, 1996. **271**(32): p. 19084-92.
56. Kahsai, A.W., et al., *Multiple ligand-specific conformations of the beta2-adrenergic receptor*. Nat Chem Biol, 2011. **7**(10): p. 692-700.
57. Gupta, S.K., et al., *Pharmacological evidence for complex and multiple site interaction of CXCR4 with SDF-1alpha: implications for development of selective CXCR4 antagonists*. Immunol Lett, 2001. **78**(1): p. 29-34.
58. Rajagopalan, L. and K. Rajarathnam, *Structural basis of chemokine receptor function--a model for binding affinity and ligand selectivity*. Biosci Rep, 2006. **26**(5): p. 325-39.
59. Joseph, P.R., et al., *Probing the role of CXC motif in chemokine CXCL8 for high affinity binding and activation of CXCR1 and CXCR2 receptors*. J Biol Chem, 2010. **285**(38): p. 29262-9.
60. Hepler, J.R. and A.G. Gilman, *G proteins*. Trends Biochem Sci, 1992. **17**(10): p. 383-7.
61. Rot, A. and U.H. von Andrian, *Chemokines in innate and adaptive host defense: basic chemokines grammar for immune cells*. Annu Rev Immunol, 2004. **22**: p. 891-928.

62. Mellado, M., et al., *Chemokine receptor homo- or heterodimerization activates distinct signaling pathways*. *Embo J*, 2001. **20**(10): p. 2497-507.
63. Ley, K., et al., *Getting to the site of inflammation: the leukocyte adhesion cascade updated*. *Nat Rev Immunol*, 2007. **7**(9): p. 678-89.
64. Weber, C. and H. Noels, *Atherosclerosis: current pathogenesis and therapeutic options*. *Nat Med*, 2011. **17**(11): p. 1410-22.
65. Nourshargh, S., P.L. Hordijk, and M. Sixt, *Breaching multiple barriers: leukocyte motility through venular walls and the interstitium*. *Nat Rev Mol Cell Biol*, 2010. **11**(5): p. 366-78.
66. Hellberg, C., et al., *Ca<sup>2+</sup> signalling mechanisms of the beta 2 integrin on neutrophils: involvement of phospholipase C gamma 2 and Ins(1,4,5)P<sub>3</sub>*. *Biochem J*, 1996. **317** ( Pt 2): p. 403-9.
67. Kinashi, T., *Intracellular signalling controlling integrin activation in lymphocytes*. *Nat Rev Immunol*, 2005. **5**(7): p. 546-59.
68. Afonso, P.V. and C.A. Parent, *PI3K and chemotaxis: a priming issue?* *Sci Signal*, 2011. **4**(170): p. pe22.
69. Kolsch, V., P.G. Charest, and R.A. Firtel, *The regulation of cell motility and chemotaxis by phospholipid signaling*. *J Cell Sci*, 2008. **121**(Pt 5): p. 551-9.
70. Arai, H. and I.F. Charo, *Differential regulation of G-protein-mediated signaling by chemokine receptors*. *J Biol Chem*, 1996. **271**(36): p. 21814-9.
71. Gouwy, M., et al., *Synergy between coproduced CC and CXC chemokines in monocyte chemotaxis through receptor-mediated events*. *Mol Pharmacol*, 2008. **74**(2): p. 485-95.
72. Molon, B., et al., *T cell costimulation by chemokine receptors*. *Nat Immunol*, 2005. **6**(5): p. 465-71.
73. Shi, G., et al., *Identification of an alternative G $\alpha$ q-dependent chemokine receptor signal transduction pathway in dendritic cells and granulocytes*. *J Exp Med*, 2007. **204**(11): p. 2705-18.
74. Pitsilos, S., et al., *Platelet factor 4 localization in carotid atherosclerotic plaques: correlation with clinical parameters*. *Thromb Haemost*, 2003. **90**(6): p. 1112-20.
75. Mortier, A., J. Van Damme, and P. Proost, *Overview of the mechanisms regulating chemokine activity and availability*. *Immunol Lett*, 2012. **145**(1-2): p. 2-9.
76. Mortier, A., et al., *Effect of posttranslational processing on the in vitro and in vivo activity of chemokines*. *Exp Cell Res*, 2011. **317**(5): p. 642-54.
77. Proost, P., S. Struyf, and J. Van Damme, *Natural post-translational modifications of chemokines*. *Biochem Soc Trans*, 2006. **34**(Pt 6): p. 997-1001.

78. Reinhold, D., et al., *DP IV/CD26, APN/CD13 and related enzymes as regulators of T cell immunity: implications for experimental encephalomyelitis and multiple sclerosis*. Front Biosci, 2008. **13**: p. 2356-63.
79. Mortier, A., J. Van Damme, and P. Proost, *Regulation of chemokine activity by posttranslational modification*. Pharmacol Ther, 2008. **120**(2): p. 197-217.
80. Kruidenier, L., et al., *Myofibroblast matrix metalloproteinases activate the neutrophil chemoattractant CXCL7 from intestinal epithelial cells*. Gastroenterology, 2006. **130**(1): p. 127-36.
81. Proost, P., et al., *Amino-terminal truncation of chemokines by CD26/dipeptidyl-peptidase IV. Conversion of RANTES into a potent inhibitor of monocyte chemotaxis and HIV-1-infection*. J Biol Chem, 1998. **273**(13): p. 7222-7.
82. Struyf, S., et al., *Natural truncation of RANTES abolishes signaling through the CC chemokine receptors CCR1 and CCR3, impairs its chemotactic potency and generates a CC chemokine inhibitor*. Eur J Immunol, 1998. **28**(4): p. 1262-71.
83. Preobrazhensky, A.A., et al., *Monocyte chemotactic protein-1 receptor CCR2B is a glycoprotein that has tyrosine sulfation in a conserved extracellular N-terminal region*. J Immunol, 2000. **165**(9): p. 5295-303.
84. Choe, H., et al., *Sulphated tyrosines mediate association of chemokines and Plasmodium vivax Duffy binding protein with the Duffy antigen/receptor for chemokines (DARC)*. Mol Microbiol, 2005. **55**(5): p. 1413-22.
85. Grodecka, M., et al., *Analysis of recombinant Duffy protein-linked N-glycans using lectins and glycosidases*. Acta Biochim Pol, 2010. **57**(1): p. 49-53.
86. Czerwinski, M., et al., *Mutational analysis of the N-glycosylation sites of Duffy antigen/receptor for chemokines*. Biochem Biophys Res Commun, 2007. **356**(3): p. 816-21.
87. Ludwig, A., et al., *Identification of distinct surface-expressed and intracellular CXC-chemokine receptor 2 glycoforms in neutrophils: N-glycosylation is essential for maintenance of receptor surface expression*. J Immunol, 2000. **165**(2): p. 1044-52.
88. Bannert, N., et al., *Sialylated O-glycans and sulfated tyrosines in the NH<sub>2</sub>-terminal domain of CC chemokine receptor 5 contribute to high affinity binding of chemokines*. J Exp Med, 2001. **194**(11): p. 1661-73.
89. Li, Y. and X. Chen, *Sialic acid metabolism and sialyltransferases: natural functions and applications*. Appl Microbiol Biotechnol, 2012. **94**(4): p. 887-905.
90. Rifat, S., et al., *Expression of sialyltransferase activity on intact human neutrophils*. J Leukoc Biol, 2008. **84**(4): p. 1075-81.
91. Frommhold, D., et al., *Sialyltransferase ST3Gal-IV controls CXCR2-mediated firm leukocyte arrest during inflammation*. J Exp Med, 2008. **205**(6): p. 1435-46.

92. Gouwy, M., et al., *Synergy between proinflammatory ligands of G protein-coupled receptors in neutrophil activation and migration*. J Leukoc Biol, 2004. **76**(1): p. 185-94.
93. Struyf, S., et al., *Chemokines synergize in the recruitment of circulating neutrophils into inflamed tissue*. Eur J Immunol, 2005. **35**(5): p. 1583-91.
94. Gouwy, M., et al., *CXCR4 and CCR5 ligands cooperate in monocyte and lymphocyte migration and in inhibition of dual-tropic (R5/X4) HIV-1 infection*. Eur J Immunol, 2011. **41**(4): p. 963-73.
95. Crown, S.E., et al., *Heterodimerization of CCR2 chemokines and regulation by glycosaminoglycan binding*. J Biol Chem, 2006. **281**(35): p. 25438-46.
96. Sambrook, J. and D. Russell, *Molecular cloning*. 2001.
97. Nesmelova, I.V., et al., *Platelet factor 4 and interleukin-8 CXC chemokine heterodimer formation modulates function at the quaternary structural level*. J Biol Chem, 2005. **280**(6): p. 4948-58.
98. Koenen, R.R., et al., *Disrupting functional interactions between platelet chemokines inhibits atherosclerosis in hyperlipidemic mice*. Nat Med, 2009. **15**(1): p. 97-103.
99. Sebastiani, S., et al., *CCL22-induced responses are powerfully enhanced by synergy inducing chemokines via CCR4: evidence for the involvement of first beta-strand of chemokine*. Eur J Immunol, 2005. **35**(3): p. 746-56.
100. Venetz, D., et al., *Perivascular expression of CXCL9 and CXCL12 in primary central nervous system lymphoma: T-cell infiltration and positioning of malignant B cells*. Int J Cancer, 2010. **127**(10): p. 2300-12.
101. Kuscher, K., et al., *Synergy-inducing chemokines enhance CCR2 ligand activities on monocytes*. Eur J Immunol, 2009. **39**(4): p. 1118-28.
102. Dudek, A.Z., et al., *Platelet factor 4 promotes adhesion of hematopoietic progenitor cells and binds IL-8: novel mechanisms for modulation of hematopoiesis*. Blood, 2003. **101**(12): p. 4687-94.
103. White, J.H., et al., *Heterodimerization is required for the formation of a functional GABA(B) receptor*. Nature, 1998. **396**(6712): p. 679-82.
104. Fotiadis, D., et al., *Atomic-force microscopy: Rhodopsin dimers in native disc membranes*. Nature, 2003. **421**(6919): p. 127-8.
105. Liang, Y., et al., *Organization of the G protein-coupled receptors rhodopsin and opsin in native membranes*. J Biol Chem, 2003. **278**(24): p. 21655-62.
106. Das, S.T., et al., *Monomeric and dimeric CXCL8 are both essential for in vivo neutrophil recruitment*. PLoS One, 2010. **5**(7): p. e11754.

## References

---

107. Veldkamp, C.T., et al., *Structural basis of CXCR4 sulfotyrosine recognition by the chemokine SDF-1/CXCL12*. *Sci Signal*, 2008. **1**(37): p. ra4.
108. Parenty, G., S. Appelbe, and G. Milligan, *CXCR2 chemokine receptor antagonism enhances DOP opioid receptor function via allosteric regulation of the CXCR2-DOP receptor heterodimer*. *Biochem J*, 2008. **412**(2): p. 245-56.
109. Chen, C., et al., *Heterodimerization and cross-desensitization between the mu-opioid receptor and the chemokine CCR5 receptor*. *Eur J Pharmacol*, 2004. **483**(2-3): p. 175-86.
110. Suzuki, S., et al., *Interactions of opioid and chemokine receptors: oligomerization of mu, kappa, and delta with CCR5 on immune cells*. *Exp Cell Res*, 2002. **280**(2): p. 192-200.
111. Liu, R., et al., *Homozygous defect in HIV-1 coreceptor accounts for resistance of some multiply-exposed individuals to HIV-1 infection*. *Cell*, 1996. **86**(3): p. 367-77.
112. Benkirane, M., et al., *Mechanism of transdominant inhibition of CCR5-mediated HIV-1 infection by ccr5delta32*. *J Biol Chem*, 1997. **272**(49): p. 30603-6.
113. Contento, R.L., et al., *CXCR4-CCR5: a couple modulating T cell functions*. *Proc Natl Acad Sci U S A*, 2008. **105**(29): p. 10101-6.
114. El-Asmar, L., et al., *Evidence for negative binding cooperativity within CCR5-CCR2b heterodimers*. *Mol Pharmacol*, 2005. **67**(2): p. 460-9.
115. Wilson, S., G. Wilkinson, and G. Milligan, *The CXCR1 and CXCR2 receptors form constitutive homo- and heterodimers selectively and with equal apparent affinities*. *J Biol Chem*, 2005. **280**(31): p. 28663-74.
116. Naumann, U., et al., *CXCR7 functions as a scavenger for CXCL12 and CXCL11*. *PLoS One*, 2010. **5**(2): p. e9175.
117. Sierro, F., et al., *Disrupted cardiac development but normal hematopoiesis in mice deficient in the second CXCL12/SDF-1 receptor, CXCR7*. *Proc Natl Acad Sci U S A*, 2007. **104**(37): p. 14759-64.
118. Sohy, D., et al., *Hetero-oligomerization of CCR2, CCR5, and CXCR4 and the protean effects of "selective" antagonists*. *J Biol Chem*, 2009. **284**(45): p. 31270-9.
119. Szabo, I., et al., *Heterologous desensitization of opioid receptors by chemokines inhibits chemotaxis and enhances the perception of pain*. *Proc Natl Acad Sci U S A*, 2002. **99**(16): p. 10276-81.
120. Szabo, I., et al., *Selective inactivation of CCR5 and decreased infectivity of R5 HIV-1 strains mediated by opioid-induced heterologous desensitization*. *J Leukoc Biol*, 2003. **74**(6): p. 1074-82.

121. Pello, O.M., et al., *Ligand stabilization of CXCR4/delta-opioid receptor heterodimers reveals a mechanism for immune response regulation*. Eur J Immunol, 2008. **38**(2): p. 537-49.
122. Fiore, M.M. and V.V. Kakkar, *Platelet factor 4 neutralizes heparan sulfate-enhanced antithrombin inactivation of factor Xa by preventing interaction(s) of enzyme with polysaccharide*. Biochem Biophys Res Commun, 2003. **311**(1): p. 71-6.
123. Loscalzo, J., B. Melnick, and R.I. Handin, *The interaction of platelet factor four and glycosaminoglycans*. Arch Biochem Biophys, 1985. **240**(1): p. 446-55.
124. Brandt, E., et al., *Platelet-derived CXC chemokines: old players in new games*. Immunol Rev, 2000. **177**: p. 204-16.
125. Lasagni, L., et al., *An alternatively spliced variant of CXCR3 mediates the inhibition of endothelial cell growth induced by IP-10, Mig, and I-TAC, and acts as functional receptor for platelet factor 4*. J Exp Med, 2003. **197**(11): p. 1537-49.
126. Mueller, A., et al., *CXCL4-induced migration of activated T lymphocytes is mediated by the chemokine receptor CXCR3*. J Leukoc Biol, 2008. **83**(4): p. 875-82.
127. Struyf, S., et al., *Angiostatic and chemotactic activities of the CXC chemokine CXCL4L1 (platelet factor-4 variant) are mediated by CXCR3*. Blood, 2011. **117**(2): p. 480-8.
128. Campanella, G.S., R.A. Colvin, and A.D. Luster, *CXCL10 can inhibit endothelial cell proliferation independently of CXCR3*. PLoS One, 2010. **5**(9): p. e12700.
129. Dudek, A.Z., et al., *Platelet factor 4 binds to glycanated forms of thrombomodulin and to protein C. A potential mechanism for enhancing generation of activated protein C*. J Biol Chem, 1997. **272**(50): p. 31785-92.
130. Petersen, F., et al., *A chondroitin sulfate proteoglycan on human neutrophils specifically binds platelet factor 4 and is involved in cell activation*. J Immunol, 1998. **161**(8): p. 4347-55.
131. Mayo, K.H., et al., *Heparin binding to platelet factor-4. An NMR and site-directed mutagenesis study: arginine residues are crucial for binding*. Biochem J, 1995. **312** ( Pt 2): p. 357-65.
132. Schall, T.J., et al., *Selective attraction of monocytes and T lymphocytes of the memory phenotype by cytokine RANTES*. Nature, 1990. **347**(6294): p. 669-71.
133. Schall, T.J., et al., *A human T cell-specific molecule is a member of a new gene family*. J Immunol, 1988. **141**(3): p. 1018-25.
134. Kameyoshi, Y., et al., *Cytokine RANTES released by thrombin-stimulated platelets is a potent attractant for human eosinophils*. J Exp Med, 1992. **176**(2): p. 587-92.

135. Klinger, M.H., et al., *Immunocytochemical localization of the chemokines RANTES and MIP-1 alpha within human platelets and their release during storage*. *Int Arch Allergy Immunol*, 1995. **107**(4): p. 541-6.
136. Martin, L., et al., *Structural and functional analysis of the RANTES-glycosaminoglycans interactions*. *Biochemistry*, 2001. **40**(21): p. 6303-18.
137. Baltus, T., et al., *Oligomerization of RANTES is required for CCR1-mediated arrest but not CCR5-mediated transmigration of leukocytes on inflamed endothelium*. *Blood*, 2003. **102**(6): p. 1985-8.
138. Szczucinski, A. and J. Losy, *CCL5, CXCL10 and CXCL11 chemokines in patients with active and stable relapsing-remitting multiple sclerosis*. *Neuroimmunomodulation*, 2011. **18**(1): p. 67-72.
139. Proudfoot, A.E., A.L. de Souza, and V. Muzio, *The use of chemokine antagonists in EAE models*. *J Neuroimmunol*, 2008. **198**(1-2): p. 27-30.
140. Szczucinski, A. and J. Losy, *Chemokines and chemokine receptors in multiple sclerosis. Potential targets for new therapies*. *Acta Neurol Scand*, 2007. **115**(3): p. 137-46.
141. Proudfoot, A.E., et al., *Extension of recombinant human RANTES by the retention of the initiating methionine produces a potent antagonist*. *J Biol Chem*, 1996. **271**(5): p. 2599-603.
142. Yang, Y.F., et al., *A non-peptide CCR5 antagonist inhibits collagen-induced arthritis by modulating T cell migration without affecting anti-collagen T cell responses*. *Eur J Immunol*, 2002. **32**(8): p. 2124-32.
143. Shahrara, S., et al., *Amelioration of rat adjuvant-induced arthritis by Met-RANTES*. *Arthritis Rheum*, 2005. **52**(6): p. 1907-19.
144. Vierboom, M.P., et al., *Inhibition of the development of collagen-induced arthritis in rhesus monkeys by a small molecular weight antagonist of CCR5*. *Arthritis Rheum*, 2005. **52**(2): p. 627-36.
145. Amat, M., et al., *Pharmacological blockade of CCR1 ameliorates murine arthritis and alters cytokine networks in vivo*. *Br J Pharmacol*, 2006. **149**(6): p. 666-75.
146. Veillard, N.R., et al., *Differential influence of chemokine receptors CCR2 and CXCR3 in development of atherosclerosis in vivo*. *Circulation*, 2005. **112**(6): p. 870-8.
147. Berres, M.L., et al., *Antagonism of the chemokine Ccl5 ameliorates experimental liver fibrosis in mice*. *J Clin Invest*, 2010. **120**(11): p. 4129-40.
148. Neote, K., et al., *Molecular cloning, functional expression, and signaling characteristics of a C-C chemokine receptor*. *Cell*, 1993. **72**(3): p. 415-25.
149. Koelink, P.J., et al., *Targeting chemokine receptors in chronic inflammatory diseases: an extensive review*. *Pharmacol Ther*, 2012. **133**(1): p. 1-18.

150. Viola, A. and A.D. Luster, *Chemokines and their receptors: drug targets in immunity and inflammation*. *Annu Rev Pharmacol Toxicol*, 2008. **48**: p. 171-97.
151. Blanpain, C., et al., *CCR5 binds multiple CC-chemokines: MCP-3 acts as a natural antagonist*. *Blood*, 1999. **94**(6): p. 1899-905.
152. Issafras, H., et al., *Constitutive agonist-independent CCR5 oligomerization and antibody-mediated clustering occurring at physiological levels of receptors*. *J Biol Chem*, 2002. **277**(38): p. 34666-73.
153. Hernanz-Falcon, P., et al., *Identification of amino acid residues crucial for chemokine receptor dimerization*. *Nat Immunol*, 2004. **5**(2): p. 216-23.
154. Paterlini, M.G., *Structure modeling of the chemokine receptor CCR5: implications for ligand binding and selectivity*. *Biophys J*, 2002. **83**(6): p. 3012-31.
155. Weber, C., et al., *Specialized roles of the chemokine receptors CCR1 and CCR5 in the recruitment of monocytes and T(H)1-like/CD45RO(+) T cells*. *Blood*, 2001. **97**(4): p. 1144-6.
156. Potteaux, S., et al., *Role of bone marrow-derived CC-chemokine receptor 5 in the development of atherosclerosis of low-density lipoprotein receptor knockout mice*. *Arterioscler Thromb Vasc Biol*, 2006. **26**(8): p. 1858-63.
157. Braunersreuther, V., et al., *Ccr5 but not Ccr1 deficiency reduces development of diet-induced atherosclerosis in mice*. *Arterioscler Thromb Vasc Biol*, 2007. **27**(2): p. 373-9.
158. Braunersreuther, V., F. Mach, and S. Steffens, *The specific role of chemokines in atherosclerosis*. *Thromb Haemost*, 2007. **97**(5): p. 714-21.
159. van Wanrooij, E.J., et al., *HIV entry inhibitor TAK-779 attenuates atherogenesis in low-density lipoprotein receptor-deficient mice*. *Arterioscler Thromb Vasc Biol*, 2005. **25**(12): p. 2642-7.
160. Mack, M., et al., *Aminoxy-pentane-RANTES induces CCR5 internalization but inhibits recycling: a novel inhibitory mechanism of HIV infectivity*. *J Exp Med*, 1998. **187**(8): p. 1215-24.
161. Elsner, J., et al., *Aminoxy-pentane-RANTES induces CCR3 activation and internalization of CCR3 from the surface of human eosinophils*. *Int Arch Allergy Immunol*, 2001. **124**(1-3): p. 227-9.
162. Baltus, T., et al., *Differential and additive effects of platelet-derived chemokines on monocyte arrest on inflamed endothelium under flow conditions*. *J Leukoc Biol*, 2005. **78**(2): p. 435-41.
163. Thiele, S., et al., *Allosteric and orthosteric sites in CC chemokine receptor (CCR5), a chimeric receptor approach*. *J Biol Chem*, 2011. **286**(43): p. 37543-54.
164. Saiki, R.K., et al., *Primer-directed enzymatic amplification of DNA with a thermostable DNA polymerase*. *Science*, 1988. **239**(4839): p. 487-91.



165. Magrane, M. and U. Consortium, *UniProt Knowledgebase: a hub of integrated protein data*. Database (Oxford), 2011. **2011**: p. bar009.
166. Thompson, J.D., D.G. Higgins, and T.J. Gibson, *CLUSTAL W: improving the sensitivity of progressive multiple sequence alignment through sequence weighting, position-specific gap penalties and weight matrix choice*. Nucleic acids research, 1994. **22**(22): p. 4673-80.
167. Lowry, O.H., et al., *Protein measurement with the Folin phenol reagent*. J Biol Chem, 1951. **193**(1): p. 265-75.
168. Laemmli, U.K., *Cleavage of structural proteins during the assembly of the head of bacteriophage T4*. Nature, 1970. **227**(5259): p. 680-5.
169. Blum, H., H. Beier, and H. Gross, *Improved silverstaining of plant proteins, RNA and DNA in polyacrylamide gels*. Electrophoresis, 1987. **8**: p. 93-99.
170. LaVallie, E.R., et al., *A thioredoxin gene fusion expression system that circumvents inclusion body formation in the E. coli cytoplasm*. Biotechnology (N Y), 1993. **11**(2): p. 187-93.
171. Chung, C.W., et al., *The three-dimensional solution structure of RANTES*. Biochemistry, 1995. **34**(29): p. 9307-14.
172. Duma, L., et al., *Recognition of RANTES by extracellular parts of the CCR5 receptor*. J Mol Biol, 2007. **365**(4): p. 1063-75.
173. Sarabi, A., et al., *CXCL4L1 inhibits angiogenesis and induces undirected endothelial cell migration without affecting endothelial cell proliferation and monocyte recruitment*. Journal of thrombosis and haemostasis : JTH, 2011. **9**(1): p. 209-19.
174. Vasina, E.M., et al., *Microparticles from apoptotic platelets promote resident macrophage differentiation*. Cell Death Dis, 2011. **2**: p. e211.
175. Johnson, Z., et al., *Interference with heparin binding and oligomerization creates a novel anti-inflammatory strategy targeting the chemokine system*. Journal of immunology, 2004. **173**(9): p. 5776-85.
176. Grommes, J., et al., *Disruption of platelet-derived chemokine heteromers prevents neutrophil extravasation in acute lung injury*. American journal of respiratory and critical care medicine, 2012. **185**(6): p. 628-36.
177. Kramp, B.K., et al., *Heterophilic chemokine receptor interactions in chemokine signaling and biology*. Exp Cell Res, 2011. **317**(5): p. 655-63.
178. Wright, W.R., et al., *Inflammatory transcriptome profiling of human monocytes exposed acutely to cigarette smoke*. PloS one, 2012. **7**(2): p. e30120.
179. Sperandio, M., et al., *Alpha 2,3-sialyltransferase-IV is essential for L-selectin ligand function in inflammation*. Eur J Immunol, 2006. **36**(12): p. 3207-15.

180. Springer, T.A., *Traffic signals on endothelium for lymphocyte recirculation and leukocyte emigration*. *Annu Rev Physiol*, 1995. **57**: p. 827-72.
181. Vestweber, D. and J.E. Blanks, *Mechanisms that regulate the function of the selectins and their ligands*. *Physiol Rev*, 1999. **79**(1): p. 181-213.
182. Tenno, M., et al., *Initiation of protein O glycosylation by the polypeptide GalNAcT-1 in vascular biology and humoral immunity*. *Mol Cell Biol*, 2007. **27**(24): p. 8783-96.
183. Ellies, L.G., et al., *Core 2 oligosaccharide biosynthesis distinguishes between selectin ligands essential for leukocyte homing and inflammation*. *Immunity*, 1998. **9**(6): p. 881-90.
184. Sperandio, M., et al., *Severe impairment of leukocyte rolling in venules of core 2 glucosaminyltransferase-deficient mice*. *Blood*, 2001. **97**(12): p. 3812-9.
185. Weninger, W., et al., *Specialized contributions by alpha(1,3)-fucosyltransferase-IV and FucT-VII during leukocyte rolling in dermal microvessels*. *Immunity*, 2000. **12**(6): p. 665-76.
186. Tsumoto, K., et al., *Role of arginine in protein refolding, solubilization, and purification*. *Biotechnol Prog*, 2004. **20**(5): p. 1301-8.
187. Rek, A., et al., *A biophysical insight into the RANTES-glycosaminoglycan interaction*. *Biochim Biophys Acta*, 2009. **1794**(4): p. 577-82.
188. Maachupalli-Reddy, J., B.D. Kelley, and E. De Bernardez Clark, *Effect of inclusion body contaminants on the oxidative renaturation of hen egg white lysozyme*. *Biotechnol Prog*, 1997. **13**(2): p. 144-50.
189. Bird, P.I., et al., *Production of recombinant serpins in Escherichia coli*. *Methods*, 2004. **32**(2): p. 169-76.
190. Huo, Y., et al., *Circulating activated platelets exacerbate atherosclerosis in mice deficient in apolipoprotein E*. *Nat Med*, 2003. **9**(1): p. 61-7.
191. Galkina, E. and K. Ley, *Immune and inflammatory mechanisms of atherosclerosis (\*)*. *Annu Rev Immunol*, 2009. **27**: p. 165-97.
192. Weber, C., A. Zernecke, and P. Libby, *The multifaceted contributions of leukocyte subsets to atherosclerosis: lessons from mouse models*. *Nat Rev Immunol*, 2008. **8**(10): p. 802-15.
193. Sachais, B.S., et al., *Elimination of platelet factor 4 (PF4) from platelets reduces atherosclerosis in C57Bl/6 and apoE-/- mice*. *Thromb Haemost*, 2007. **98**(5): p. 1108-13.
194. von Hundelshausen, P., et al., *RANTES deposition by platelets triggers monocyte arrest on inflamed and atherosclerotic endothelium*. *Circulation*, 2001. **103**(13): p. 1772-7.

## References

---

195. Segerer, S., et al., *Selective binding and presentation of CCL5 by discrete tissue microenvironments during renal inflammation*. J Am Soc Nephrol, 2007. **18**(6): p. 1835-44.
196. Kenakin, T., *Functional selectivity and biased receptor signaling*. J Pharmacol Exp Ther, 2011. **336**(2): p. 296-302.
197. Furuichi, K., et al., *Chemokine receptor CCR1 regulates inflammatory cell infiltration after renal ischemia-reperfusion injury*. Journal of immunology, 2008. **181**(12): p. 8670-6.
198. Horuk, R., et al., *CCR1-specific non-peptide antagonist: efficacy in a rabbit allograft rejection model*. Immunol Lett, 2001. **76**(3): p. 193-201.
199. Horuk, R., *Chemokine receptor antagonists: overcoming developmental hurdles*. Nat Rev Drug Discov, 2009. **8**(1): p. 23-33.
200. Bedke, J., et al., *Beneficial effects of CCR1 blockade on the progression of chronic renal allograft damage*. Am J Transplant, 2007. **7**(3): p. 527-37.
201. Maly, P., et al., *The alpha(1,3)fucosyltransferase Fuc-TVII controls leukocyte trafficking through an essential role in L-, E-, and P-selectin ligand biosynthesis*. Cell, 1996. **86**(4): p. 643-53.
202. Lowe, J.B. and J.D. Marth, *A genetic approach to Mammalian glycan function*. Annu Rev Biochem, 2003. **72**: p. 643-91.
203. Ellies, L.G., et al., *Sialyltransferase ST3Gal-IV operates as a dominant modifier of hemostasis by concealing asialoglycoprotein receptor ligands*. Proc Natl Acad Sci U S A, 2002. **99**(15): p. 10042-7.
204. Ellies, L.G., et al., *Sialyltransferase specificity in selectin ligand formation*. Blood, 2002. **100**(10): p. 3618-25.
205. Drechsler, M., et al., *Hyperlipidemia-triggered neutrophilia promotes early atherosclerosis*. Circulation, 2010. **122**(18): p. 1837-45.
206. Haringman, J.J., et al., *Chemokine and chemokine receptor expression in paired peripheral blood mononuclear cells and synovial tissue of patients with rheumatoid arthritis, osteoarthritis, and reactive arthritis*. Ann Rheum Dis, 2006. **65**(3): p. 294-300.
207. Zapico, I., et al., *CCR5 (chemokine receptor-5) DNA-polymorphism influences the severity of rheumatoid arthritis*. Genes Immun, 2000. **1**(4): p. 288-9.

## VIII. SUPPLEMENT

N-terminus TM-1  
 CCR5 M D Y Q V S S P I Y D I N - - - Y Y T S E P C Q K I N V K Q I A A R L L P P L Y S L V F I F G F V G N  
 CCR5\_1N1 M E T P N T T E D Y D T T T E F D Y G D A T P C Q K V N E R A F G A Q L L P P L Y S L V F I F G F V G N  
 CCR5\_1E1 M D Y Q V S S P I Y D I N - - - Y Y T S E P C Q K I N V K Q I A A R L L P P L Y S L V F I F G F V G N  
 CCR5\_1E2 M D Y Q V S S P I Y D I N - - - Y Y T S E P C Q K I N V K Q I A A R L L P P L Y S L V F I F G F V G N  
 CCR5\_1E3 M D Y Q V S S P I Y D I N - - - Y Y T S E P C Q K I N V K Q I A A R L L P P L Y S L V F I F G F V G N  
 TM-1 ICL-1 TM-2 ECL-1  
 CCR5 M L V I L I L I N C K R L K S M T D I Y L L N L A I S D L F F L L T V P F W A H Y - A A A Q W D F G N T  
 CCR5\_1N1 M L V I L I L I N C K R L K S M T D I Y L L N L A I S D L F F L L T V P F W A H Y - A A A Q W D F G N T  
 CCR5\_1E1 M L V I L I L I N C K R L K S M T D I Y L L N L A I S D L F F L L T V P F W A H Y K L K D D W V F G D A  
 CCR5\_1E2 M L V I L I L I N C K R L K S M T D I Y L L N L A I S D L F F L L T V P F W A H Y - A A A Q W D F G N T  
 CCR5\_1E3 M L V I L I L I N C K R L K S M T D I Y L L N L A I S D L F F L L T V P F W A H Y - A A A Q W D F G N T  
 ECL-1 TM-3 ICL-2 TM-4  
 CCR5 M C Q L L T G L Y F I G F F S G I F F I I L L T I D R Y L A V V H A V F A L K A R T V T F G V V T S V I  
 CCR5\_1N1 M C Q L L T G L Y F I G F F S G I F F I I L L T I D R Y L A V V H A V F A L K A R T V T F G V V T S V I  
 CCR5\_1E1 M C K L L T G L Y F I G F F S G I F F I I L L T I D R Y L A V V H A V F A L K A R T V T F G V V T S V I  
 CCR5\_1E2 M C Q L L T G L Y F I G F F S G I F F I I L L T I D R Y L A V V H A V F A L K A R T V T F G V V T S V I  
 CCR5\_1E3 M C Q L L T G L Y F I G F F S G I F F I I L L T I D R Y L A V V H A V F A L K A R T V T F G V V T S V I  
 TM-4 ECL-2 TM-5  
 CCR5 T W V V A V F A S L P G I I F T R S Q K E G L H Y T C S S H F P Y S Q Y Q F W K N F Q T L K I V I L G L  
 CCR5\_1N1 T W V V A V F A S L P G I I F T R S Q K E G L H Y T C S S H F P Y S Q Y Q F W K N F Q T L K I V I L G L  
 CCR5\_1E1 T W V V A V F A S L P G I I F T R S Q K E G L H Y T C S S H F P Y S Q Y Q F W K N F Q T L K I V I L G L  
 CCR5\_1E2 T W V V A V F A S L P G I I F S K T Q W E F T H H T C S L H F P H E S L R E W K L F Q A L K L V I L G L  
 CCR5\_1E3 T W V V A V F A S L P G I I F T R S Q K E G L H Y T C S S H F P Y S Q Y Q F W K N F Q T L K I V I L G L  
 TM-5 ICL-3 TM-6  
 CCR5 V L P L L V M V I C Y S G I L K T L L R C R N E K K R H R A V R L I F T I M I V Y F L F W A P Y N I V L  
 CCR5\_1N1 V L P L L V M V I C Y S G I L K T L L R C R N E K K R H R A V R L I F T I M I V Y F L F W A P Y N I V L  
 CCR5\_1E1 V L P L L V M V I C Y S G I L K T L L R C R N E K K R H R A V R L I F T I M I V Y F L F W A P Y N I V L  
 CCR5\_1E2 V L P L L V M V I C Y S G I L K T L L R C R N E K K R H R A V R L I F T I M I V Y F L F W A P Y N I V L  
 CCR5\_1E3 V L P L L V M V I C Y S G I L K T L L R C R N E K K R H R A V R L I F T I M I V Y F L F W A P Y N I V L  
 TM-6 ECL-3 TM-7 C-terminus  
 CCR5 L L N T F Q E F F G L N N C S S S N R L D Q A M Q V T E T L G M T H C C I N P I I Y A F V G E K F R N Y  
 CCR5\_1N1 L L N T F Q E F F G L N N C S S S N R L D Q A M Q V T E T L G M T H C C I N P I I Y A F V G E K F R N Y  
 CCR5\_1E1 L L N T F Q E F F G L N N C S S S N R L D Q A M Q V T E T L G M T H C C I N P I I Y A F V G E K F R N Y  
 CCR5\_1E2 L L N T F Q E F F G L N N C S S S N R L D Q A M Q V T E T L G M T H C C I N P I I Y A F V G E K F R N Y  
 CCR5\_1E3 L L N T F Q D F L F T H E C E Q S R H L D L A V Q V T E T L G M T H C C I N P I I Y A F V G E K F R N Y  
 C-terminus  
 CCR5 L L V F F Q K H I A K R F C K C C S I F Q Q E A P E R A S S V Y T R S T G E Q E I S V G L S T P  
 CCR5\_1N1 L L V F F Q K H I A K R F C K C C S I F Q Q E A P E R A S S V Y T R S T G E Q E I S V G L S T P  
 CCR5\_1E1 L L V F F Q K H I A K R F C K C C S I F Q Q E A P E R A S S V Y T R S T G E Q E I S V G L S T P  
 CCR5\_1E2 L L V F F Q K H I A K R F C K C C S I F Q Q E A P E R A S S V Y T R S T G E Q E I S V G L S T P  
 CCR5\_1E3 L L V F F Q K H I A K R F C K C C S I F Q Q E A P E R A S S V Y T R S T G E Q E I S V G L S T P  
 N-terminus TM-1  
 hccr1 M E T P N T T E D Y D T T T E F D Y G D A T P C Q K V N E R A F G A Q L L P P L Y S L V F V I G L V G N  
 CCR1\_5N1 M D Y Q V S S P I Y D I N - - - Y Y T S E P C Q K I N V K Q I A A R L L P P L Y S L V F I F G F V G N  
 CCR1\_5E3 M E T P N T T E D Y D T T T E F D Y G D A T P C Q K V N E R A F G A Q L L P P L Y S L V F V I G L V G N  
 TM-1 ICL-1 TM-2 ECL-1  
 hccr1 I L V V L V L V Q Y K R L K N M T S I Y L L N L A I S D L L F L F T L P F W I D Y K L K D D W V F G D A  
 CCR1\_5N1 I L V V L V L V Q Y K R L K N M T S I Y L L N L A I S D L L F L F T L P F W I D Y K L K D D W V F G D A  
 CCR1\_5E3 I L V V L V L V Q Y K R L K N M T S I Y L L N L A I S D L L F L F T L P F W I D Y K L K D D W V F G D A  
 ECL-1 TM-3 ICL-2 TM-4  
 hccr1 M C K I L S G F Y Y T G L Y S E I F F I I L L T I D R Y L A I V H A V F A L R A R T V T F G V I T S I I  
 CCR1\_5N1 M C K I L S G F Y Y T G L Y S E I F F I I L L T I D R Y L A I V H A V F A L R A R T V T F G V I T S I I  
 CCR1\_5E3 M C K I L S G F Y Y T G L Y S E I F F I I L L T I D R Y L A I V H A V F A L R A R T V T F G V I T S I I  
 TM-4 ECL-2 TM-5  
 hccr1 I W A L A I L A S M P G L Y F S K T Q W E F T H H T C S L H F P H E S L R E W K L F Q A L K L N L F G L  
 CCR1\_5N1 I W A L A I L A S M P G L Y F S K T Q W E F T H H T C S L H F P H E S L R E W K L F Q A L K L N L F G L  
 CCR1\_5E3 I W A L A I L A S M P G L Y F S K T Q W E F T H H T C S L H F P H E S L R E W K L F Q A L K L N L F G L  
 TM-5 ICL-3 TM-6  
 hccr1 V L P L L V M I I C Y T G I I K I L L R R P N E K K S K A V R L I F V I M I I F F L F W T P Y N L T I L  
 CCR1\_5N1 V L P L L V M I I C Y T G I I K I L L R R P N E K K S K A V R L I F V I M I I F F L F W T P Y N L T I L  
 CCR1\_5E3 V L P L L V M I I C Y T G I I K I L L R R P N E K K S K A V R L I F V I M I I F F L F W T P Y N L T I L  
 TM-6 ECL-3 TM-7 C-terminus  
 hccr1\_ I S V F Q D F L F T H E C E Q S R H L D L A V Q V T E V I A Y T H C C V N P V I Y A F V G E R F R K Y L  
 CCR1\_5N1 I S V F Q D F L F T H E C E Q S R H L D L A V Q V T E V I A Y T H C C V N P V I Y A F V G E R F R K Y L  
 CCR1\_5E3 I S V F Q E F F G L N N C S S S N R L D Q A M Q V T E V I A Y T H C C V N P V I Y A F V G E R F R K Y L  
 C-terminus  
 hccr1 R Q L F H R R V A V H L V K W L P P L S V D R L E R V S S T S P S T G E H E L S A G F S T P  
 CCR1\_5N1 R Q L F H R R V A V H L V K W L P P L S V D R L E R V S S T S P S T G E H E L S A G F S T P  
 CCR1\_5E3 R Q L F H R R V A V H L V K W L P P L S V D R L E R V S S T S P S T G E H E L S A G F S T P

## IX. CURRICULUM VITAE

### Persönliche Daten:

Name: Birgit Kramp  
Geburtsdatum: 15.07.1978  
Geburtsort: Eschweiler in Nordrhein-Westfalen  
Nationalität: Deutsch

### Bildungsweg:

August 1988 - Juni 1997      Besuch des Mädchengymnasium Jülich  
St. Josef-Schule  
Abschluss: Allgemeine Hochschulreife

Oktober 1997 - März 2001      Diplomstudium Biologie an der Gesamthochschule  
Kassel, Universität

Oktober 2000      Abschluss: Vordiplom

Oktober 2000 - März 2001      Großpraktika in den Fachbereichen Zoologie und  
Humanbiologie als Teil des Hauptstudiums.

März 2001- August 2006      Wechsel an die Rheinisch-Westfälische Technische  
Hochschule Aachen zur Fortsetzung des  
Diplomstudiums Biologie.  
Schwerpunkte: Molekulare Genetik und Mikrobiologie  
Abschluss: Diplom-Biologin

Juli 2005 - Juli 2006      Diplomandin am Institut für Angewandte  
Mikrobiologie  
Bei Herrn Prof. Dr. Bernd Schäfer.

Mai 2007 – Februar 2010      Doktorandin am Institut für Molekulare Herz-  
Kreislaufforschung (IMCAR) unter der Leitung von  
Univ.-Prof. Dr. med. Christian Weber, Aachen

Februar 2010 bis heute      Institut für Prophylaxe und Epidemiologie der  
Kreislaufkrankheiten (IPEK) unter der Leitung von  
Univ.-Prof. Dr. med. Christian Weber an der  
Ludwig-Maximilian Universität München

**Publications:**

1. Rory R. Koenen, Philipp von Hundelshausen, Irina V. Nesmelova, Alma Zerneck, Elisa A. Liehn, Alisina Sarabi, **Birgit K. Kramp**, Anna M. Piccinini, Søren R. Paludan, M. Anna Kowalska, Andreas J. Kungl, Tilman M. Hackeng, Kevin H. Mayo, Christian Weber (2009). Disrupting functional interactions between platelet chemokines inhibits atherosclerosis in hyperlipidemic mice. *Nat. Med.* **15**(1): 97-103.
2. Alisina Sarabi, **Birgit K. Kramp**, Maik Drechsler, Tilman M. Hackeng, Oliver Soehnlein, Christian Weber, Rory R. Koenen, Philipp von Hundelshausen (2011). CXCL4L1 inhibits angiogenesis and induces undirected endothelial cell migration without affecting endothelial cell proliferation and monocyte recruitment. *J. Thromb. Haemost.* **9**(1):209-19.
3. **Birgit K. Kramp**, Alisina Sarabi, Rory R. Koenen, Christian Weber (2011). Heterophilic chemokine receptor interactions in chemokine signaling and biology. *Exp. Cell Res.* **317**(5):655-63.
4. Otilia Postea., Elena M. Vasina, Sandra Cauwenberghs, Delia Projahn, Elisa A. Liehn, Dirk Lievens, Wendy Theelen, **Birgit K. Kramp**, Elena Butoi Dragomir, Oliver Soehnlein, Johan W.M. Heemskerk, Andreas Ludwig, Christian Weber, Rory R. Koenen (2012). CX<sub>3</sub>CR1 expression on platelets is increased during hyperlipidemia and contributes to platelet-monocyte complex formation and vascular recruitment. *Arterioscler. Thromb. Vasc. Biol.* **32**(5):1186-93.
5. **Birgit K. Kramp**, Remco T.A. Megens, Alisina Sarabi, Sabine Winkler, Delia Projahn, Christian Weber, Rory R. Koenen, Philipp von Hundelshausen (2013). Exchange of extracellular domains of CCR1 and CCR5 reveals confined functions in CCL5-mediated cell recruitment. *Thromb. Haemost.* **110**(4):795-806.
6. Helene Hartwig, Maik Drechsler, Dirk Lievens, **Birgit K. Kramp**, Philipp von Hundelshausen, Esther Lutgens, Christian Weber, Yvonne Döring, Oliver Soehnlein (2014). Platelet-derived PF4 reduces neutrophil apoptosis following arterial occlusion. *Thromb Haemost.*, in press.
7. Delia Projahn, Sakine Simsekyilmaz, Smriti Singh, Isabella Kanzler, **Birgit K. Kramp**, Marcella Langer, Alexandrina Burlacu, Jürgen Bernhagen, Doris Klee, Alma Zerneck, Tilman M. Hackeng, Jürgen Groll, Christian Weber, Elisa A. Liehn, Rory R. Koenen (2014). Controlled intramyocardial release of engineered

- chemokines by biodegradable hydrogels as a treatment approach of myocardial infarction. J. Cell. Mol. Med., in press.
8. Yvonne Döring, Heidi Noels, **Birgit K. Kramp**, Manuela Mandl, Dirk Lievens, Maik Drechsler, Pathricia Tilstam, Marcella Langer, Helene Hartwig, Markus Sperandio, Oliver Soehnlein, Christian Weber (2014). Sialyltransferase ST3Gal-IV deficiency reduces Ccl5-mediated phagocyte accumulation in atherosclerosis. Circ. Res., in press.
  9. Ilze Bot, Isabelle T.M.N. Daissormont, Alma Zerneck, **Birgit K. Kramp**, Saskia C.A. de Jager, Marijke M. Westra, Martine Bot, Peter J. van Santbrink, Theo J.C. van Berkel, Pal Aukrust, Rory R. Koenen, Christian Weber, Erik A.L. Biessen. CXCR4 blockade induces atherosclerosis by perturbing neutrophil apoptosis and senescence. Cardiovasc. Res., in revision.